AD NUMBER

AD849147

LIMITATION CHANGES

TO:

Approved for public release; distribution is unlimited.

FROM:

Distribution authorized to U.S. Gov't. agencies and their contractors; Critical Technology; SEP 1968. Other requests shall be referred to Air Force Armament Laboratory, ATZV, Eglin AFB, FL 32542. This document contains export-controlled technical data.

AUTHORITY

afatl ltr, 25 feb 1977

AFATL-TR-68-113

BALLUTE STABILIZATION SYSTEM FOR M-118 BOMB

J. J. Graham
Goodyear Aerospace Corporation

Technical Report AFATL-TR-68-113

SEPTEMBER 1968

AIR FORCE ARMAMENT LABORATORY
AIR FORCE SYSTEMS COMMAND
EGLIN AIR FORCE BASE, FLORIDA

BALLUTE STABILIZATION SYSTEM FOR M-118 BOMB

J. J. Graham

FOREWORD

This final technical report was prepared by Goodyear Aerospace Corporation, Akron, Ohio, under Project 1263, Task 1263-01, entitled "BALLUTE Stabilization System for the M-118 Bomb," and Air Force Contract No. FO8635-68-C-0147. The report covers the period from 1 July 1968 through 31 December 1968. Mr. Earl S. Suters, Jr., of the Air Force Armament Laboratory (ATZV) served as contract monitor. The contractor's report number is GER-13967.

Contributing personnel from Goodyear Aerospace were A. C. Aebischer, section head in the Recovery Systems Engineering Department; J. J. Graham, project engineer; T. W. Brunner, aerodynamic analysis; J. F. Houmard, structural analysis; E. L. Fargo, test operations; and R. R. Barton, documentation.

Information in this report is embargoed under the Department of State International Traffic In Arms Regulations. This report may be released to foreign governments by departments or agencies of the U. S. Government subject to approval of the Air Force Armament Laboratory (ATZV), Eglin AFB, Florida 32542, or higher authority within the Department of the Air Force. Private individuals or firms require a Department of State export license.

This technical report has been reviewed and is approved.

ROY C. COMPTON
Acting Chief, Engineering Division

ABSTRACT

A drag-stabilization system utilizing a ram-air inflatable BALLUTE was considered for compatible application to the operational M-118 bomb where use of the conventional M-135 fin assembly is physically prohibitive. Wind-tunnel tests of 1/10-scale models were conducted and the results were analyzed to determine a stable BALLUTE size and configuration. A positive operating mechanism was designed to ensure consistent deployment of ram-air scoops for initiating the BALLUTE inflation. Stress and reliability analyses were performed to support the design effort, and the first prototype was vibration tested to prepare the system hardware for Air Force flight testing. Several fabricated units were recommended for intended bomb drops to enable evaluation of the concept.

(The reverse of this page is blank)

TABLE OF CONTENTS

LIST OF FIGURES

LIST OF TABLES

(The reverse of this page is blank)

SECTION I

INTRODUCTION

Potential operations of the M-118 bomb are limited with use of the conventional M-135 fin assembly. In lieu of the fins, a drag-stabilization system utilizing a packageable, ram-air-inflatable BALLUTE[a] was designed and developed. Prototypes were fabricated for flight testing to determine the feasibility of the concept.

The development of the system was based on meeting the contractual conditions of operational compatibility, including the several requirements for service, environment, physical limitations, and performance. Efforts substantiating the design documentation to which the prototype system was produced were the aerodynamic analysis, stress analysis, reliability estimate, and the vibration test.

[a]TM, Goodyear Aerospace Corporation, Akron, Ohio.

SECTION II

DESIGN REQUIREMENTS

1. GENERAL

The contractor was to use current aerospace BALLUTE technology to design an inflatable and deployable stabilization system. The system was to be assembled in an aerodynamic container and attached to the baseplate of the M-118 bomb body through an adapter-spacer ring. The undeployed system package could not exceed 24 in. in diameter or 29 in. in length. Release and inflation of the BALLUTE stabilizing decelerator from the resulting canister housing was not to take place until the weapon is a minimum of 10 ft from the aircraft, and the method of inflation was to be designed to provide consistent deployment at any aircraft angle of release.

In the interest of production, the canister was to have access openings for conventional provisioning and servicing of the M-118 bomb. Also, design of the system was to provide for specific environmental tests and to be readily maintainable.

2. CONDITIONS

Design conditions for service required that the BALLUTE system stabilize the bomb when released at level and dive modes from external carriage at all speeds to 600 knots and altitudes from 5,000 ft to 28,000 ft above sea level. Also, the production system is to function when used in any temperature from -65 to +160 F and after prolonged storage within this same temperature range.

3. PERFORMANCE

The performance parameters evaluated were carriage stability, separation from the aircraft, and low dispersion of the bomb/BALLUTE ballistic trajectory in comparison with attainments of the conventional M-118 bomb equipped with the M-135 fins. Background efforts toward preparing the design to meet performance requirements are contained in the aerodynamic analysis and report of the 1/10-scale model wind-tunnel test and the structural analysis.

A 98-percent reliability expected for production models based on the prototype design is found in the reliability estimate included in this report. The fabricated prototype was subjected to a specified vibration test, and the description and results also are included.

SECTION III

AERODYNAMIC ANALYSIS

1. PROGRAM TASKS

The aerodynamic requirements for the M-118 bomb stabilization system program consisted of the following tasks.

1. A BALLUTE configuration was to be selected to act as a stabilizer on the bomb to provide nearly the same stabilization characteristics as the present standard M-118 bomb with fins. This selection would be made on the basis of a 1/10-scale subsonic wind tunnel test program considering only dynamic and static stability characteristics.

2. An estimate of the new M-118 bomb configuration characteristics (C_L, C_M, and C_D) was to be made using standard aerodynamic, theoretical, and empirical techniques. This estimate was required in support of a structural load analysis.

3. A brief trajectory analysis of the new M-118 bomb configuration separation characteristics from the pertinent aircraft was required.

4. An aerodynamic analysis of the BALLUTE inflation characteristics was required.

Each task listed above was investigated within limits set by the complexity of the problem and the time allowed for a solution.

The results of Task 4 were incorporated in the section covering structural analysis.

2. WIND-TUNNEL TEST PROGRAM

a. Preliminary Considerations

A subsonic wind-tunnel test program was conducted by the contractor on several bomb/BALLUTE configurations. The purpose of this program was to determine the static and dynamic stability characteristics of each configuration and to choose a BALLUTE that would serve as a stabilizer on the M-118 bomb and have nearly the same stability characteristics as the present M-118 bomb. The BALLUTE first selected was not required to have an optimum shape in regards to performance, but only to have a shape satisfactory for a feasibility demonstration. Because of the short duration available in which to select a BALLUTE configuration, only a dynamic stability test program was made. From the data collected, only the relative dynamic and static stability characteristics were obtained. A qualitative analysis of the data indicated that a 30-in.-diameter BALLUTE with a 5-percent burble fence would approach the required stability criteria.

b. Description of Subsonic Wind Tunnel

The Goodyear Aerospace subsonic wind tunnel is of the horizontal, closed-return type. The tunnel is 64 ft long, 25 ft wide, and 11 ft high. The tunnel test section is 66 in. long, 61 in. wide, and 43 in. high. Tunnel speed is controlled by propeller pitch through an electric propeller hub. The velocity capability of the tunnel is in excess of 200 fps. Other related characteristics of the tunnel are its turbulence factor of approximately 1.8 and its contraction ratio of 5.

Basic instrumentation of the tunnel includes a motor-driven beam-type balance system capable of measuring three aerodynamic components simultaneously and manometer banks for monitoring tunnel conditions and taking pressure readings for a model when desired. The balance system can be used to obtain all six force and moment components with three different setups required. Further details of this facility are provided in Reference 1.

c. Test Models

In selecting a BALLUTE configuration, it was necessary to build eight test models for stability evaluation. Although a BALLUTE is a stabilizing device, its stability effectiveness when used as an attached stabilizer is generally not known. For this reason, it was necessary to study several candidate BALLUTE sizes and configurations to ascertain the relative effectiveness of each. All models were constructed to a 1/10 scale. Table I lists the BALLUTE and non-BALLUTE configurations tested during the wind-tunnel program; included are appropriate dimensional characteristics of the BALLUTEs.

TABLE I. TEST MODEL CONFIGURATIONS

Model	Designation
A	Standard M-118 bomb + fin assembly
B	Standard M-118 bomb + canister section
C	Model B + 28-in.-diameter BALLUTE
D	Model B + 34-in.-diameter BALLUTE
E	Model B + 40-in.-diameter BALLUTE
F	Model B + 34-in.-diameter tucked-back BALLUTE
G	Model B + 33-in.-diameter BALLUTE + 6-in. burble fence
H	Model B + 30-in.-diameter BALLUTE

d. Test Setup and Procedure

The general arrangement of the wind-tunnel test apparatus used during the wind-tunnel test program is shown in Figure 1. All test models were

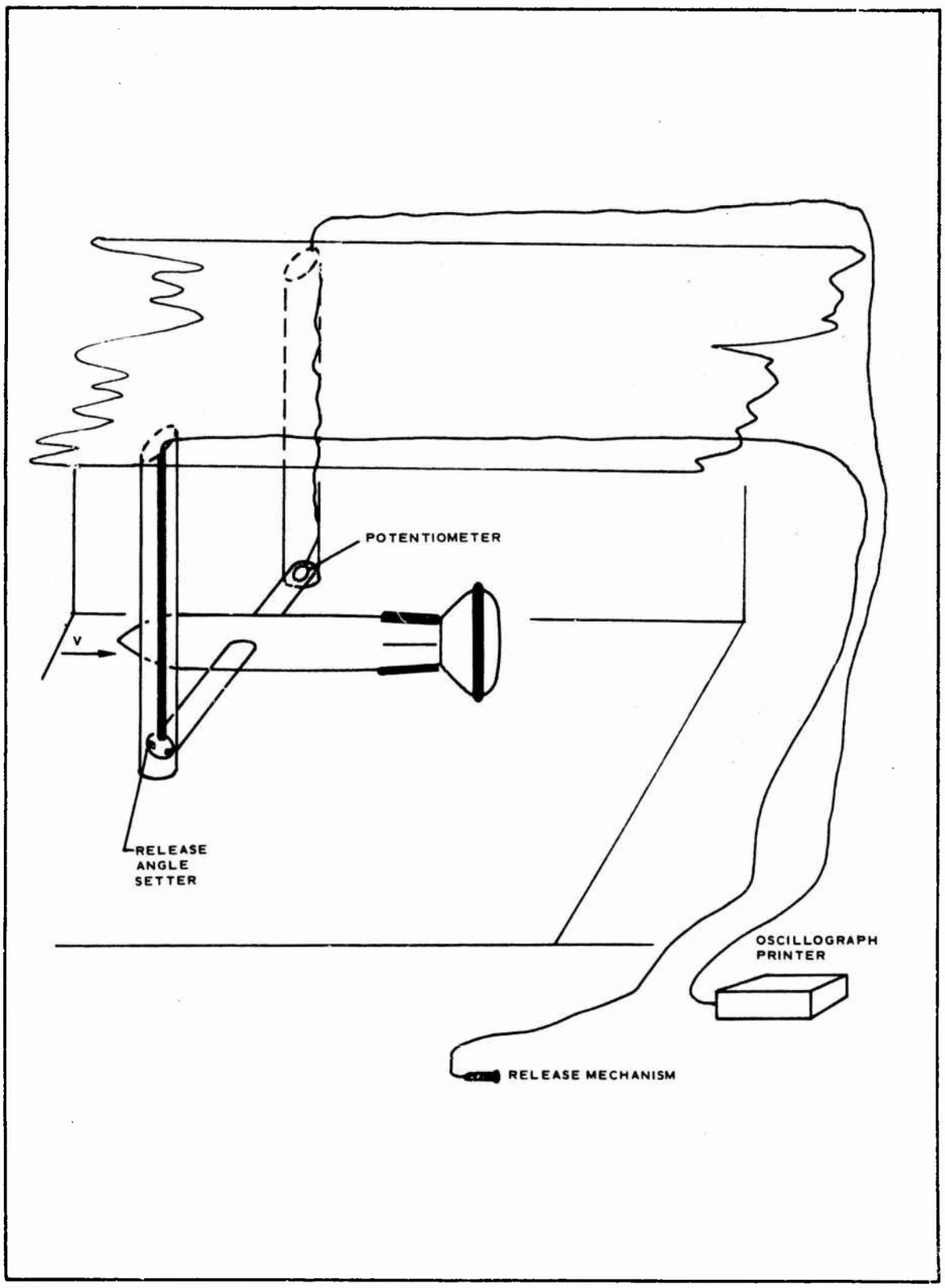

Figure 1. Wind-Tunnel Test Setup

rigidly mounted on a circular shaft that passed through the model cg. This shaft was supported from the tunnel ceiling by two rigid support legs and rotated freely. This arrangement allowed the model to respond dynamically to the tunnel flow when released from an initial angle-of-attack. A small pod was mounted on one side of the circular shaft and tied in with an oscillograph printer. By rigidly attaching this pod to the shaft, it was possible to record the dynamic response of each model as a function of time.

All tests were conducted at a tunnel dynamic pressure of 30 psf. The following procedure was followed during the test program.

1. Mount the model and ballast accordingly until the cg lies at the point where the shaft intersects the model body.
2. Obtain a zero angle-of-attack pod setting.
3. Set the model at a given release angle of attack.
4. Run tunnel up to desired conditions.
5. Start oscillograph printer and release the model.
6. Repeat same run for repeatability.

e. Test Results

The results of this test program are generally qualitative since the amount of time and effort required to perform a thorough analysis at this time was prohibitive. The results of this test program are listed in Table II. Only a representative sampling of the data obtained is presented here. Figure I-1 in Appendix I shows the oscillograph traces obtained from the test program. These traces are intended to show stability comparisons between various model configurations.

In a few instances, an attempt was made to determine the aerodynamic characteristics $C_{M_{\dot{\theta}}}$ and $C_{M_{\alpha}}$. The method of reducing the data was taken from Reference 2. Briefly this method involves the summing of moments in the form of a second order differential equation of motion:

$$I\ddot{\alpha} + P_o\dot{\alpha} + K_o\alpha = 0 \qquad (1)$$

where $I\ddot{\alpha}$ is the pitching moment of the bomb mass due to angular acceleration. The second term describes the moment due to aerodynamic damping while the third term is the restoring moment for unit angle of attack. The general solution to this differential equation of motion is of the form:

$$\alpha = \alpha_{trace}$$

$$= \alpha_o e^{-(P_o/2I)t}\left[\cos(\omega t) + \frac{P_o}{2I\omega}\sin\omega t\right]. \qquad (2)$$

TABLE II. WIND-TUNNEL TEST RESULTS

Test no.	Model	Stability	Comments
1	Standard bomb	Stable	Excellent stability; fins in +-orientation
2	Standard bomb	Stable	Excellent stability; fins in X-orientation
4	Standard bomb	Stable	Excellent stability; fins in +-orientation
7	28-in. -diameter BALLUTE	Unstable	Model trimmed at α = 30 deg following a release at α = 45 deg
10	28-in. -diameter BALLUTE + 6-in. burble fence	Unstable	Model trimmed at α = 30 deg following a release at α = 70 deg
14	34-in. -diameter BALLUTE	Stable	Damping occurs after a long time interval
16	34-in. -diameter BALLUTE + 6-in. burble fence	Stable	Damping occurs after a long time interval
17	40-in. -diameter BALLUTE	Stable	Damping occurs after a long time interval
21	40-in. -diameter BALLUTE + 6-in. burble fence	Dynamically unstable	No damping characteristics evident
27	28-in. -diameter BALLUTE + 6-in. burble fence	Stable	Trip wire on model nose (nonrepeatable)
34	40-in. -diameter BALLUTE	Stable	Use of strakes as flow separation devices demonstrated (repeatable)
35	Bomb with canister section	Unstable	Trims at α = ±65 deg
36	34-in. -diameter conical tucked-back BALLUTE	Stable	Four longitudinal strakes mounted on canister section
39	38.5-in. -diameter BALLUTE	Stable	Four strakes used; long damping period
41	28-in. -diameter BALLUTE	Stable	Good stability with four strakes
45	28-in. -diameter BALLUTE	Unstable	Same as Run 45; indicates marginal static stability
46	28-in. -diameter BALLUTE	Stable	Good stability with four strakes
48	34-in. -diameter BALLUTE	Stable	Good stability but longer damping period than 28-in. -diameter BALLUTE; four strakes
49	34-in. -diameter BALLUTE	Dynamically unstable	Change from X-orientation to +-orientation of four strakes on canister section
51	40-in. -diameter BALLUTE	Dynamically unstable	Strakes in X-orientation
53	28-in. -diameter BALLUTE	Stable	Eight strakes; excellent stability
56	30-in. -diameter BALLUTE	Stable	Eight strakes; excellent stability
58	30-in. -diameter BALLUTE + 2-percent burble fence	Stable	Eight strakes; slight loss in stability
61	30-in. -diameter BALLUTE + 6-percent burble fence	Stable	Eight strakes; slight loss in stability

The envelope of oscillation is described by the relation

$$\alpha = \alpha_o e_o e^{-(P_o/2I)t}$$

$$= \alpha_{envelope} \cdot \qquad (3)$$

This type of solution is illustrated in Figure 2.

The frequency of the damped oscillations is given by the expression

$$\omega = \sqrt{\left(\frac{K_o}{I}\right) - \left(\frac{P_o}{2I}\right)^2} \text{ (rad/sec)} , \qquad (4)$$

where ω is taken directly off the oscillograph trace. Equation 3 can be rewritten in the form

$$P_o = \frac{2I}{\Delta t} \ell n \, (\alpha_o/\alpha) \qquad (5)$$

Having determined the constant P_o, it is possible to evaluate the constant K_o

$$K_o = \left[\omega^2 + (P_o/2I)^2\right] I \qquad (6)$$

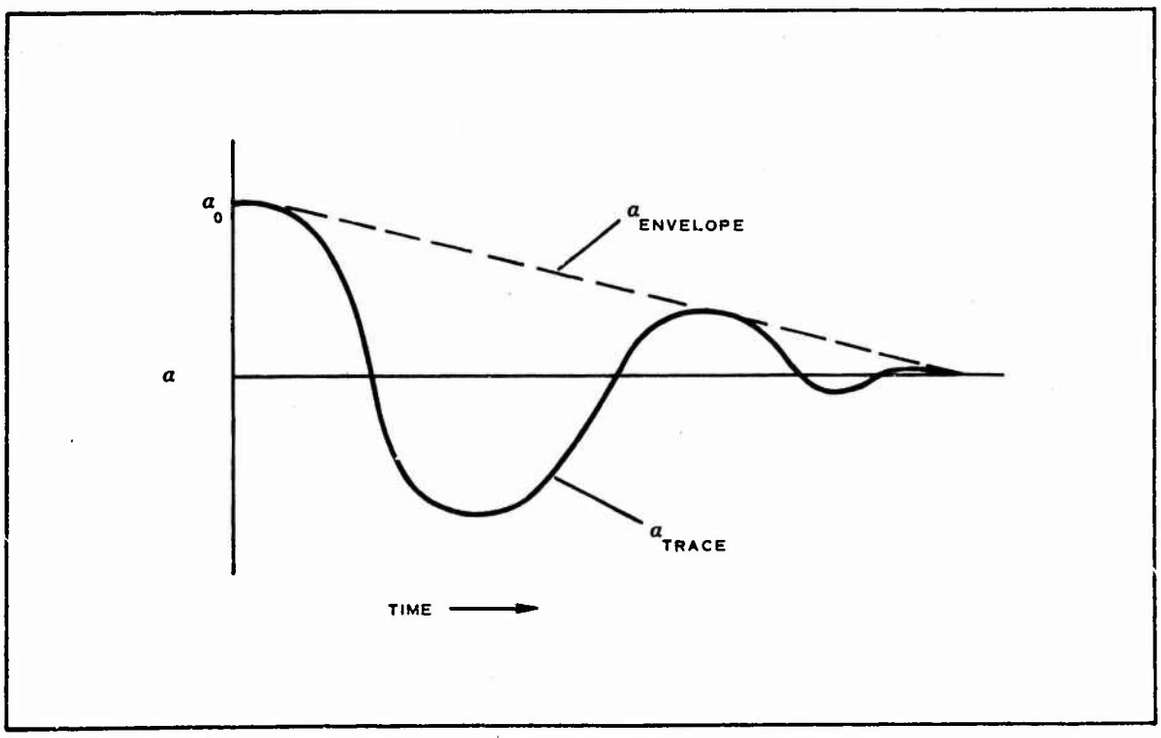

Figure 2. Envelope of Oscillation

If it is assumed that the damping term above is small compared to ω^2, then the aerodynamic characteristics, $C_{M_{\dot{\theta}}}$ and $C_{M_{\alpha}}$ can be obtained through the following equations:

$$C_{M_{\dot{\theta}}} = -\frac{4P_o}{\rho V S \bar{c}^2} \tag{7}$$

$$C_{M_{\alpha}} = \frac{-2K_o}{\rho V^2 S \bar{c}} \tag{8}$$

Note that the pitch moment of inertia, I, must be determined by analytical or experimental techniques. For this analysis, I was obtained experimentally. These results are tabulated in Table III, which is located below in Item f.

f. Discussion of Test Results

The five series of test runs included the following five configurations at 1/10 scale:

1. M-118 bomb with a standard tail
2. M-118 bomb with a canister end piece
3. M-118 bomb with a 28-in. attached BALLUTE
4. M-118 bomb with a 34-in. attached BALLUTE
5. M-118 bomb with a 40-in. attached BALLUTE

Burble fences were added to the BALLUTEs during the first series of tests as part of the test procedure. The basic bomb was tested at various release angles up to 70 deg for both the plus and cruciform orientations. In each of the test runs, the static and dynamic characteristics were excellent and repeatable. Removal of the tail section results in a statically unstable configuration as expected. This static instability was a result of the extreme forward location of the bomb cp with respect to its center of gravity.

Following these tests, the three candidate BALLUTEs were each in turn attached to the basic bomb and tested. The major portion of the tests were initiated at a release angle of 70 deg. The 2.8-in.-diameter BALLUTE was tested and found to be both statically and dynamically unstable. For various release angles, this configuration trimmed out at several angles of attack, indicating neutral stability. It is highly likely that the aerodynamic center is extremely close to the cg for this configuration. The addition of a burble fence to this configuration did not improve the stability characteristics. This implied that the center of pressure location is unaffected by the burble fence addition. Tests on the 3.4-in.-diameter BALLUTE showed that this configuration was statically stable, but had long damping periods. Upon adding a 10-percent burble fence to this configuration, it was possible to obtain a configuration that was both

dynamically and statically stable, but the damping period was not reduced significantly. Subsequent tests on the 4.0-in.-diameter BALLUTE without a burble fence gave the same results as obtained for the 3.4-in.-diameter BALLUTE. The addition of a burble fence made the 4.0-in.-diameter BALLUTE dynamically unstable.

Close examination of the oscillograph traces at this point revealed extremely long damping periods in comparison to those of the standard bomb for the larger sized BALLUTEs. It was noted however, that the 2.8-in.-diameter BALLUTEs did exhibit good damping characteristics in one test where the flow was tripped ahead of the wind-tunnel model normal separation point, however, repeatability was not achieved. This approach is standard in wind-tunnel testing procedures as a means of simulating true flow separation characteristics. Additional testing of the 2.8-in.-diameter BALLUTE with various tripping procedures failed to produce stability. Techniques of inducing flow separation were attempted on the larger sized BALLUTEs with only marginal success being attained. At this point, it was decided that a set of longitudinal strakes mounted on the canister section would likely produce a realistic separated flow. A new series of tests were conducted with four longitudinal strakes mounted on the canister section of the bomb. The BALLUTEs were all retested along with two new BALLUTE configurations, which included a 3.4-in.-diameter conical tucked back BALLUTE and a 3.9-in.-diameter standard BALLUTE, including a 0.6-in.-diameter burble fence. All models tested exhibited both dynamic and static stability except for one test on the 2.8-in.-diameter BALLUTE. Based on the results of these tests, the following two general conclusions were obtained.

1. Increasing the size of the BALLUTE decreases the dynamic stability.

2. Decreasing the size of the BALLUTE decreases the static stability.

Based on the results of these tests, a candidate BALLUTE with 30-in. body diameter was selected for additional testing. This configuration was chosen over the 28-in. diameter BALLUTE because of the smaller BALLUTE's questionable static stability characteristics. Several dynamic tests were run on this configuration with and without burble fences. In addition, eight strakes were mounted on the canister section to ensure static stability and a true separated flow condition. In all tests, there was excellent static and dynamic stability characteristics. It was noted that the addition of a burble fence would decrease stability slightly.

Table III presents a comparison of the static and dynamic stability of several configurations tested. The data reduction method was described previously.

From these tests, it was concluded that the 3.0-in.-diameter BALLUTE would be a satisfactory BALLUTE to mount on the M-118 bomb. In addition, it was decided that a five-percent burble fence would be mounted on the BALLUTE even though the data showed degraded performance. The use of a burble fence was dictated by previous experience with BALLUTEs that normally required its use. The use of eight small strakes or fins

TABLE III. COMPARISON OF STATIC AND DYNAMIC STABILITY

Model	$C_{M_{\dot{\theta}}}$	$C_{M_{\alpha}}$	$\bar{r}_{yy}$ (slug-ft^2)
Standard bomb	-1170/rad	-33.4 /rad	0.0114
28-in. BALLUTE	-195/rad	- 3.31/rad	0.00686
30-in. BALLUTE	-236/rad	- 3.84/rad	0.00829
30-in. BALLUTE + burble fence	-193/rad	- 2.96/rad	0.00904
38.5-in. BALLUTE + burble fence	-188.5/rad	- 4.98/rad	0.01255

also was carried over into the final configuration although their requirement as part of the flight configuration has not been demonstrated, since flow separation is expected to be satisfactory on the full-scale configuration.

3. AERODYNAMIC CHARACTERISTICS

Aerodynamic characteristics were developed for two aerodynamic configurations in support of the M-118 bomb design load analysis:

1. M-118 bomb and canister section
2. M-118 bomb with deployed 30-in.-diameter BALLUTE

The method used to determine the aerodynamic characteristics is to assume that the BALLUTE can be approximated as four thick fins, each having the two-dimensional geometrical details of the BALLUTE. This approach is based on the assumption that an attached BALLUTE is similar geometrically to that of a flared body and that the static aerodynamics, C_L and C_M, are equivalent to those of four thick fins. These assumptions are not unrealistic as evidenced from the literature that shows similar aerodynamic characteristics between flared and blunt-fin vehicles.

The aerodynamic characteristics were generated from a computer program developed at the David Taylor Model Basin for the calculation of the static aerodynamic characteristics of low-aspect-ratio, wing-body-tail combinations. This program had been obtained by the contractor and adapted to its IBM 360 digital computer (Reference 3).

The aerodynamic coefficients are determined by the theoretical methods of potential theory, line-vortex theory, second-order shock expansion, and viscous cross-flow theory. Empirical data from various sources also are included. In general, the program selects linear and nonlinear

coefficients for the wing, body, and tail; the combination effects of the body on the wing, the body on the tail; and the various drag contributions of a given configuration.

All individual lift, drag, and moment contributions are summed up and printed as computer output. The program is considered valid only for angles of attack up to 20 deg. To use this program, the first configuration was treated as a tail-body combination, while the second configuration was treated as a wing-body-tail configuration. The results of this program were used to estimate the aerodynamic loads on each configuration. The aerodynamic coefficients that were calculated at a Mach number of 0.95 are presented in Figure 3. The drag coefficient of the attached BALLUTE configuration has been calculated using the recent wind-tunnel results obtained at AEDC. The results showed that an attached BALLUTE had a drag coefficient of 1.03 referenced to body maximum cross-sectional area, including that of a BALLUTE.

The aerodynamic coefficients (C_L, C_D, and C_M) were transferred from a wind-axis system to a body-axis system for a load analysis in accordance with MIL-A-8591D for a wing-mounted store. The resultant loads and moments acting on the bomb in its wing mounted location are shown in Tables IV and V. These results are considered approximate as nonlinear theory is not accurate at high angles of attack. The coefficients used in calculating the forces and moments were extrapolated to what is thought to be conservative values.

TABLE IV. AERODYNAMIC LOADS WITH BOMB MOUNTED AT 0-DEG INCIDENCE*

Load diagram point	α (deg)	β (deg)	N (lb)	M (ft-lb)	Y (lb)	η (ft-lb)	A (lb)
1, 2	36.2	± 2.86	25,000	0.0	± 330	± 700	866
3, 4	-21.7	± 2.86	-6,100	-3600	± 330	± 700	866
5	-17.6	±12.4	-4,000	-3550	±2300	±2950	866
6	32.0	±12.4	14,200	1000	±2300	±2950	866

*Loads for q = 1050 psf.

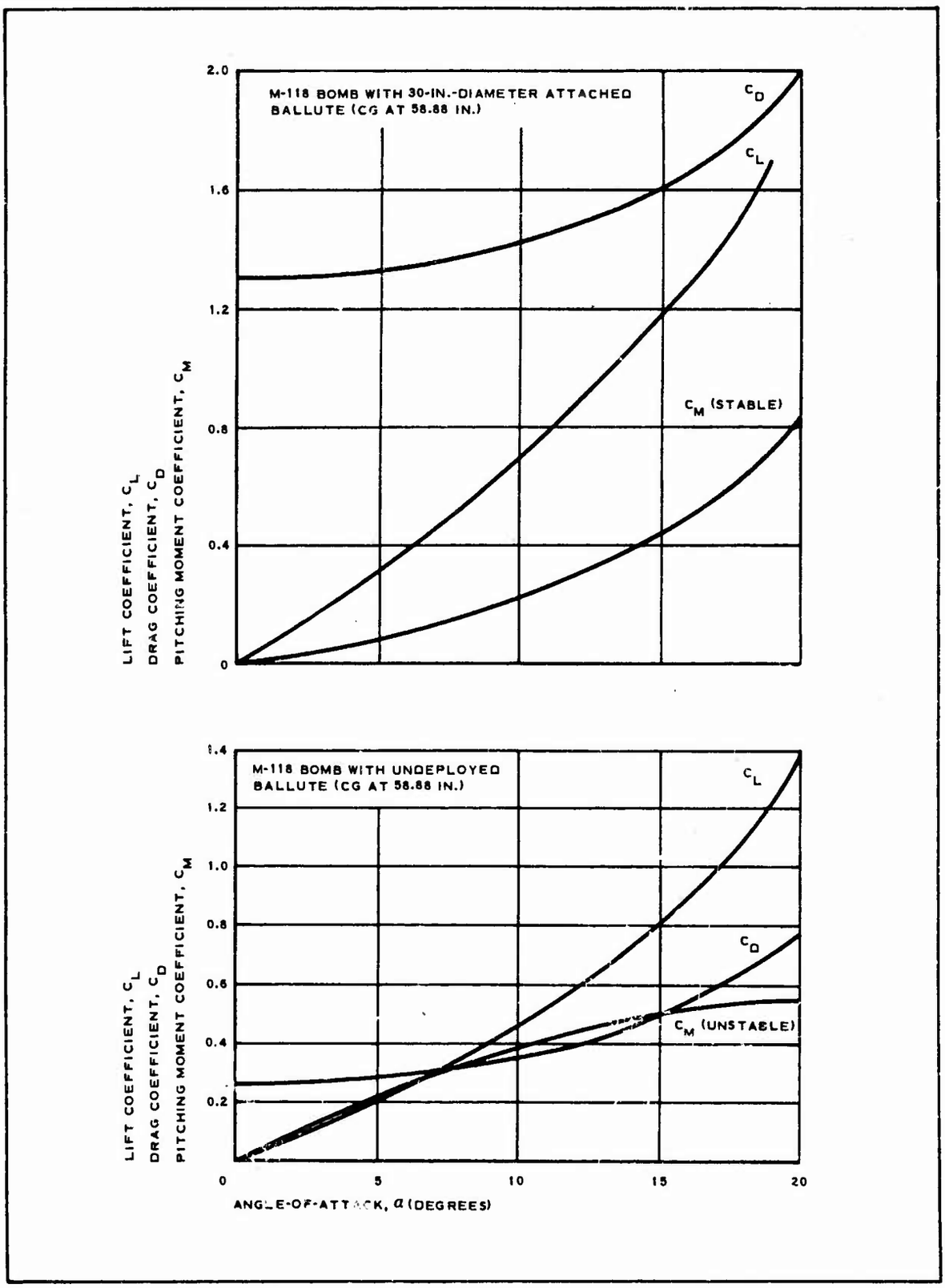

Figure 3. Aerodynamic Characteristics of Two Bomb/BALLUTE Configurations

TABLE V. AERODYNAMIC LOADS WITH BOMB MOUNTED AT -3.0-DEG INCIDENCE*

Load diagram point	α (deg)	β (deg)	N (lb)	M (ft-lb)	Y (lb)	(ft-lb)	A (lb)
1, 2	33.2	± 2.86	16,000	500	± 330	± 700	866
3, 4	-18.7	± 2.86	-4,500	-3600	± 330	± 700	866
5	-20.6	±12.4	-5,500	-3650	±2300	±2950	866
6	39.0	±12.4	11,300	2500	±2300	±2950	866

*Loads for q = 1050 psf.

4. STORE SEPARATION ANALYSIS

A brief analysis of the M-118 bomb separation characteristics from pertinent aircraft was conducted using a three-degree-of-freedom computer program. No attempt was made to define the complete mechanics of the separation process due to a lack of flow field data on the aircraft and accurate aerodynamic data on the M-118 bomb. The lack of these data is not expected to significantly alter the present findings. Briefly, the mechanics of separation include the ejection of the M-118 bomb from the aircraft while maintaining a straight and level flight attitude, the resultant motion developed by the bomb during the first 10 ft of absolute travel, and finally the mechanics of BALLUTE deployment and its subsequent dynamic behavior.

The flight condition investigated was a straight and level attitude release at Mach 0.95 and 5000-ft altitude. Separation is accomplished by two 9450-lb kickers, each located 15 in. fore and aft of the bomb mounting lugs. These kickers initially impart to the M-118 bomb a vertical velocity component of -17.4 fps. The bomb aerodynamic characteristics that were estimated for the M-118 bomb are listed as follows:

$$C_{D_o} = 0.27$$

$$C_{N_\alpha} = 3.14/\text{radian}$$

$$C_{M_\alpha} = 2.06/\text{radian (unstable)}$$

$$C_{M_q} = 0.0/\text{radian}$$

These aerodynamic characteristics are considered valid only in the linear angle-of-attack range, -10 deg = α = 10 deg, but were assumed to be valid at higher angles of attack. Two significant effects are expected to occur at higher angles of attack that were not considered here; namely, the lift force on the bomb is expected to exceed that specified from the linear coefficients and, secondly, the unstable pitching moment is expected to decrease at higher angles of attack with the result that the bomb has a stable trim point at an angle of attack near 60 deg.

The consequences of ignoring these higher angles of attack effects and their resultant impact on the dynamic motion of the bomb were not ascertained at this time.

Initial separation characteristics (orientation and velocity) were chosen for extreme conditions where applicable. No aircraft flow field effects were included. Aircraft motion following bomb release was ignored, and finally the bomb was assumed to have an unstable noseup pitching rate of -23.4 deg/sec as a result of the bomb cg being forward of the midpoint of the mounting lugs.

A separation trajectory (Reference 4) was generated for the conditions stated with the result that a 10-ft separation distance would be obtained in 0.45 sec. The bomb angle of attack was near 30 deg and was pitching nose up at a rate of 135 deg/sec as a result of the bomb instability.

At a separation distance of 10 ft, the BALLUTE deployment sequence was initiated with the result that the bomb pitching motion was damped out successfully. The BALLUTE deployment was assumed to occur in 0.5 sec with all BALLUTE aerodynamic characteristics being linearly attained over this prescribed time interval. The separation time history obtained from this computer simulation is shown in Figure 4. The conclusion reached from this short analysis was that the M-118 bomb separation should pose no significant problem for the aircraft when flying in a straight and level attitude for Mach numbers up to 0.95.

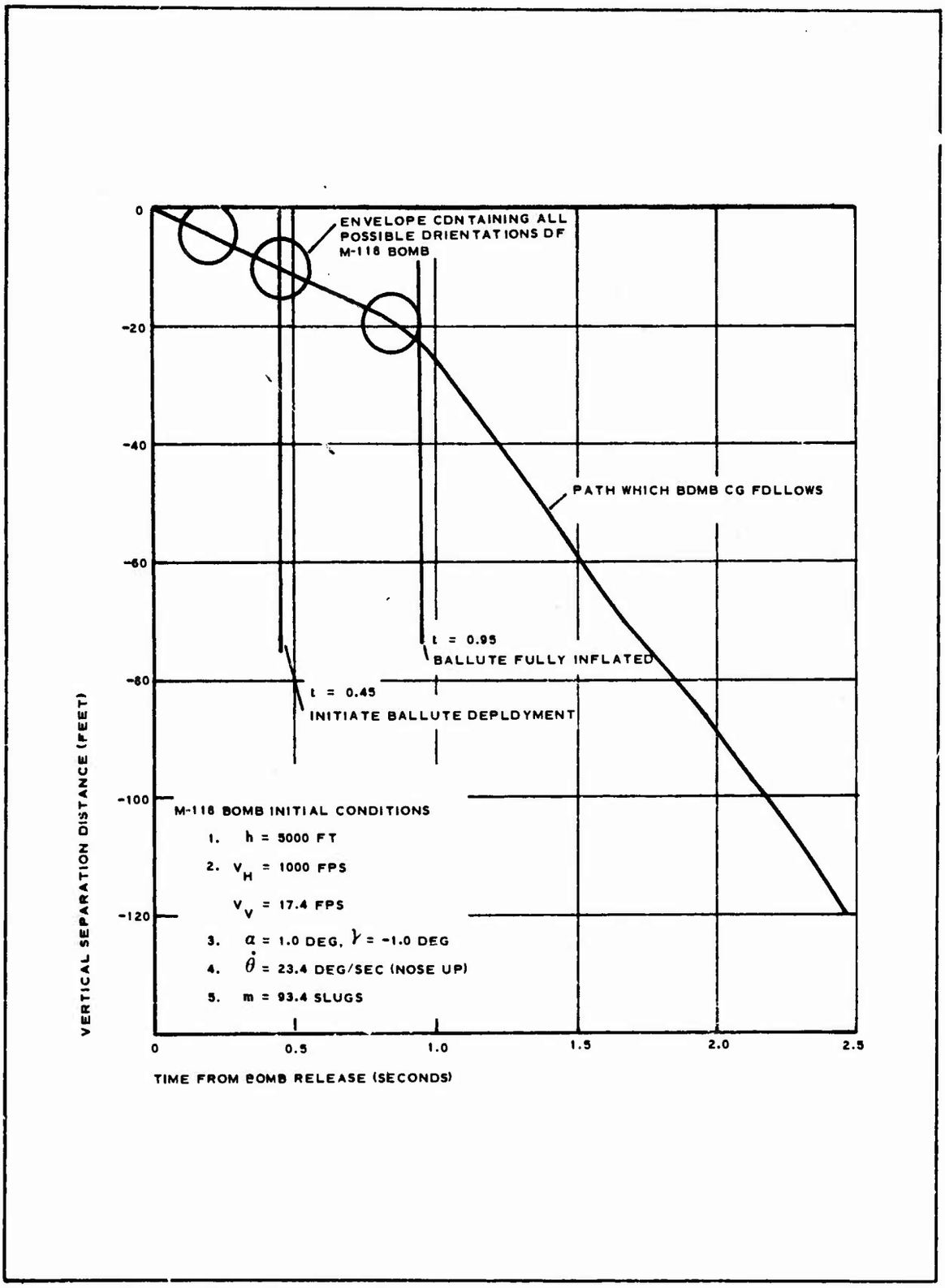

Figure 4. Separation Time and Trajectory of M-118 Bomb

SECTION IV

STRUCTURAL ANALYSIS

1. OBJECTIVE

The objective of this section is to show the ability of the BALLUTE stabilization system to withstand the loads imposed during flight conditions of feasibility testing. In general, the approach pursued in the structural analysis is considered to be conservative. Margins of safety have been based upon ultimate factors of safety of 2 and 3 for the metal and fabric components, respectively. The components analyzed are considered to be critical. All other items not analyzed were considered not critical by comparison. Results of this structural analysis are summarized in Table VI.

2. DISCUSSION

Adaptation of the stabilization BALLUTE to the 3000-lb M-118 bomb entails replacement of the tail cone/fin assembly with a canister that contains the packaged BALLUTE and the mechanical components required to deploy and inflate it.

The bomb is ejected downward from the wing of the aircraft by two kickers that are centered with respect to cg of the original configuration. Since the cg of the BALLUTE configuration is about 1.62 in. forward, a nose-up pitching moment of 2550 ft-lb is applied for the specified ejection load of 9450 lb by each kicker. Deployment of the BALLUTE is initiated by a 10-ft-long static line of 3/32-in. steel cable that is connected to the wing with a 150 lb (minimum) to 215 lb (maximum) breakaway fitting. Although this cable remains with the bomb, it does shear two (1/16-in. diameter) soft aluminum rivets that release the ram-air inlets and the BALLUTE deployment mechanism. These are detailed in Appendix II (see Figures II-2 and II-3) and are stress analyzed for the deployment loads in the body of this report.

The fabric BALLUTE and its connections must not only exhibit adequate strength to withstand the deployment and the aerodynamic forces, but it also must maintain an inflated shape that reasonably approximates the fabricated design shape This latter condition depends upon the relationship between the internal pressure of the BALLUTE due to ram air and the external pressure distribution over the surface of the BALLUTE. The stability of the design shape is indicated in this section by showing that tensile stresses exist over the entire surface of the BALLUTE.

The following four loading conditions were considered:

1. Inertia and aerodynamic loads during carriage
2. Ejection loads
3. BALLUTE deployment loads
4. BALLUTE shape with the aerodynamic drag forces

TABLE VI. SUMMARY OF STRUCTURAL ANALYSIS RESULTS

Item	Loading condition	Type of stress	Minimum margin of safety	Comments
Canister	Carriage and ejection forces	. . .	High	Estimated by comparison with the existing bomb
Steel static line	Ejection force	Tensile	+1.7	. . .
Release bar	BALLUTE deployment	Flexural	+0.11	. . .
Door release ring	BALLUTE deployment	. . .	High	Estimated by inspection
Ram-air inlets	Inlet deployment	Flexural	Adequate	The spring retention tabs could take a permanent deflection of 0.2 in.
Back assembly (AN-3 bolts)	BALLUTE deployment	Single shear	. . .	Adequacy of the bolts cannot be verified analytically due to the dependency upon an unpredictable frictional force
BALLUTE fabric	Aerodynamic drag	Tensile	+0.13	Conservative
BALLUTE meridian straps	Aerodynamic drag	Tensile	+0.17	Conservative
BALLUTE burble fence	Aerodynamic drag	Peel of the cement	Adequate	Verified by pressure test

Of these conditions, only the last two were considered sufficiently critical to warrant the limited stress analysis that possibly may be conducted within the scope of this accelerated program. The primary justification for ruling out the carriage and the ejection loads is based on a comparison of the operational configuration of the conventional M-118 bomb with that of this program. In both cases, the resultant inertia, aerodynamic, and ejection forces act near the cg. Since the length of the tail of the operational configurations is 3.5 times that of the BALLUTE canister and since the BALLUTE canister is essentially a conical frustrum of 3/16-in.-thick steel as compared to 0.093-in.-thick steel for the existing configuration, the BALLUTE canister will exhibit higher margins of safety. For example, consider flexural stresses at the BALLUTE canister to bomb interface. The critical buckling stress is conservatively given by $F_{bcr} = 0.09E/(r/t)$ (Reference 5).

For $E = 30 \times 10^6$ psi, $r = 11$ in., and $t = 0.188$ in.,

$$F_{bcr} = \frac{(0.09)(30)(10)^6}{\frac{11}{0.188}}$$

$$= 46,200 \text{ psi} ;$$

or the critical bending moment is

$$M_{cr} = F_{bcr}\pi r^2 t$$

$$= 46,200\pi(121)(0.188)$$

$$= 3.3 \times 10^6 \text{ in.-lb} .$$

The allowable moment for a factor of safety of 2 is thus, 1.65×10^6 in.-lb.

Consider the ejection loads at the interface (Section A-A in Figure 5):

$$\text{Shear, } S = 163.8\,g$$

and

$$\text{Moment, } M = (107.54 - 92.47)(163.8)g = 2470\,g .$$

When given an ejection force = 18.9 kips (resultant of two kickers),

$$g = \frac{18,900}{3,010} = 6.3 .$$

Then

$$S = (163.8)(6.3) = 1030\text{-lb limit} ,$$

and

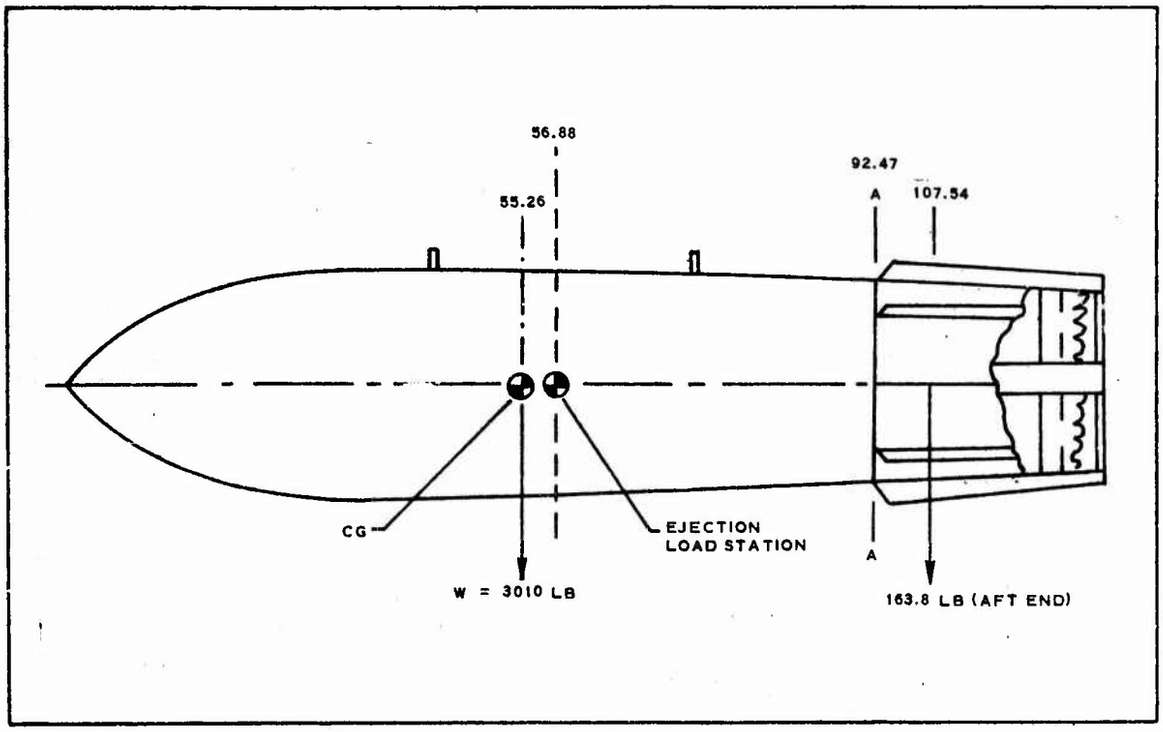

Figure 5. Ejection Loads

$$M = (2470)(6.3) = 15,600\text{-in.-lb limit}.$$

Therefore, the critical moment at the canister to bomb interface from buckling is two orders of magnitude more than the moment due to the ejection force and 58 times the moment due to 11.5 g's as specified in Figure 8 of Reference 6. Of course, aerodynamic forces must be superimposed with these inertia load levels, but these cannot possibly be high enough to yield a marginal stress condition.

The canister, the BALLUTE, and the deployment mechanisms are analyzed in Item 3 below for the deployment and the aerodynamic forces.

3. ANALYSIS

a. Steel Cable Static Line

The components of the bomb/BALLUTE configuration are considered in the order by which they are loaded, starting with the static line pull that initiates the deployment sequence.

The steel cable static line has a 3/32-in. diameter and an ultimate strength, F_{tu} = 1200 lb (Reference 7). The minimum and maximum strengths of the breakaway fitting are 150 lb and 215 lb, respectively. The load required to shear the two 1/16-in. soft aluminum rivets (1100-0) is as follows:

$$F_{su} = 8000 \text{ psi (Reference 8, p 41)},$$

and

$$T_{su} = 2\left(\frac{\pi}{4}\right)d^2F_{su} = \left(\frac{\pi}{2}\right)\left(\frac{1}{256}\right)(8000) = 49.2 \text{ lb}.$$

Therefore,

$$\text{M.S.} = \frac{F_{tu}}{(\text{F.S.})(T)} - 1 = \frac{1200}{(2)(215)} - 1 = +1.7 .$$

b. Release Bar

The release bar (see Figure II-4, Part -33, in Appendix II) is a torsion bar that is unloaded upon shearing of the rivets. The bar rotates and disengages from a slot in the door release ring (see Figure II-7, Part -101). This ring then rotates, releasing the four ram-air inlets as well as the tube (Part -13) and its backplate assembly (Part -103) as shown in Figure II-7.

The bar resists the load from two 25-lb tension springs located on the door release ring at a radius of 4.313 in. The tab on the end of the bar is at a radius of 4.625 in. so that the applied load as shown by Figure 6 is:

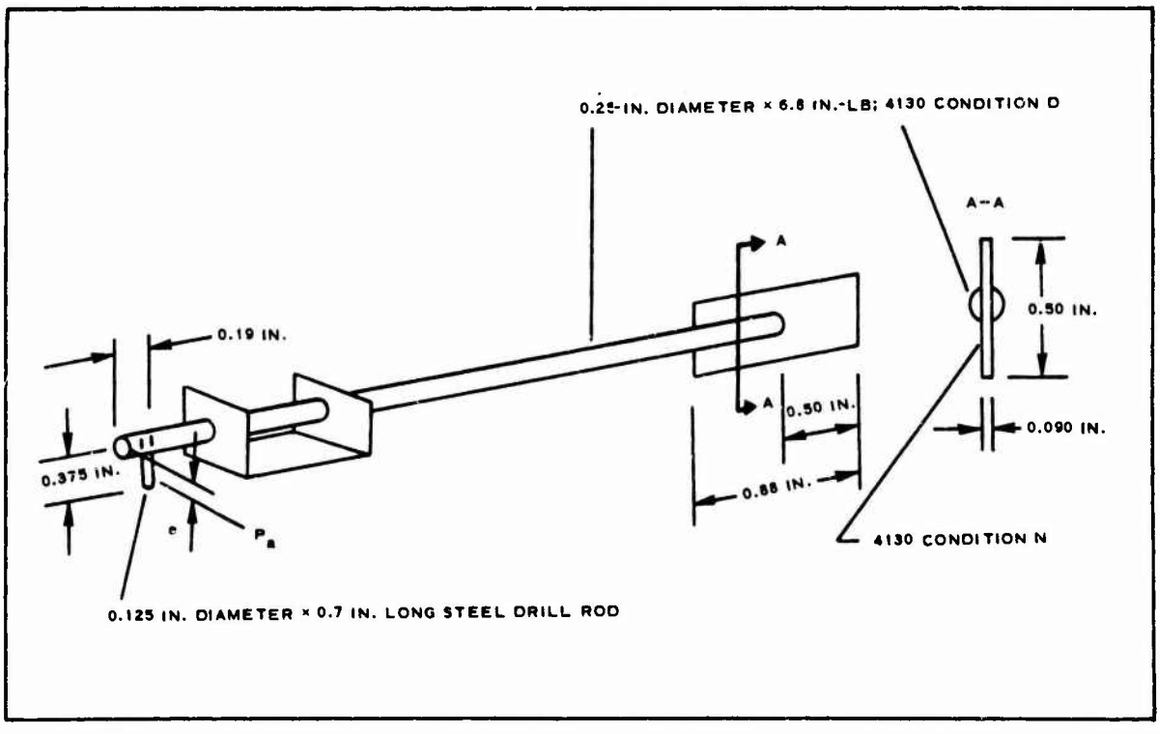

Figure 6. Release Bar

$$P_a = (50)\left(\frac{4.313}{4.625}\right) = 46.6 \text{ lb} .$$

Conservatively take the torque arm, e, as e = 0.375 in. The torque on the bar and the maximum bending moment on the cantilevered drill rod tab are, respectively,

$$T = eP_a = (0.375)(46.6) = 17.6 \text{ in.-lb} ,$$

and

$$M_{max} = (0.375 - 0.125)(46.6) = 11.7 \text{ in.-lb} .$$

The shear and the flexural stresses in the tab are:

$$f_s = \frac{4P_a}{\pi d^2} = \frac{(4)(46.6)}{\frac{\pi}{64}} = 3800 \text{ psi} ,$$

and

$$f_b = \frac{M_c}{I} = \frac{32\,M}{\pi d^3} = \frac{(32)(11.7)}{\frac{\pi}{512}} = 61,000 \text{ psi} .$$

Considering the common tool steel alloys such as AISI 4140 or 4340 indicates minimum ultimate tensile and yield strengths of 135 ksi and 125 ksi, respectively. Hence, for a factor of safety of 2 on ultimate, the minimum margin is at least

$$\text{M.S.} = \frac{F_{tu}}{(\text{F.S.})(f_b)} - 1 = \frac{135}{(2)(61)} - 1 = +0.11 .$$

The basic torsional shear stress in the bar is

$$f_s = \frac{Tr}{J} = \frac{Td}{4I} = \frac{16T}{\pi D^3} = \frac{(16)(17.6)}{\frac{\pi}{64}} = 5750 \text{ psi} .$$

However, much higher stresses occur near each end of the bar where the slot and the drill rod hole reduce the section and cause stress concentrations. Of these two sections, the drill rod end is critical. Although stress concentration factors for a torsion shaft with a transverse hole are given in Reference 9, the hole to shaft diameter ratio of d/D = 0.5 is beyond the range of data. In fact, the values of Reference 9 terminate at d/D = 0.25, where the concentration factor is 2.16 and appears to be asymptotically increasing to ∞ at a value that is significantly less than d/D = 0.5. The following alternate approach will be pursued.

Consider the net cross section of the bar at the centerline of the transverse hole. A load distribution that balances the applied torque and shear is assumed as shown in Figure 7A.

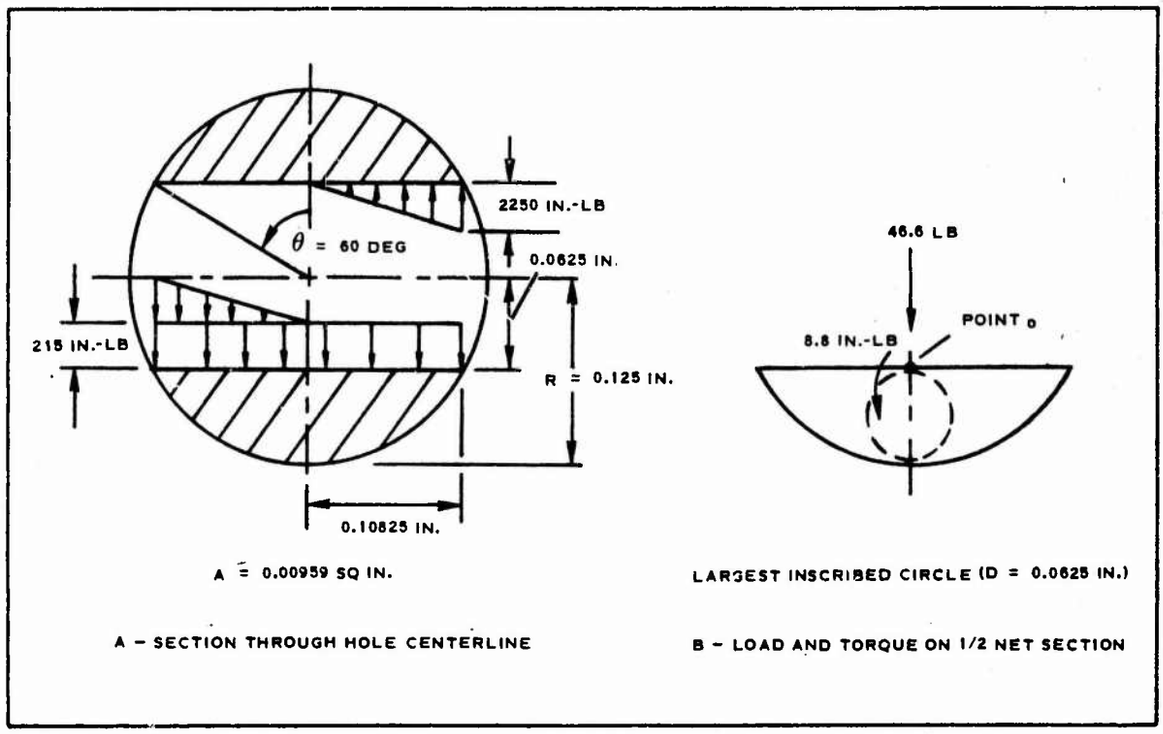

Figure 7. Cross Section of Release Bar at Drill Rod

The shear stress due to the load is taken as being distributed over half the net area:

$$f_{sv} = \frac{46.6}{0.00959} = 4870 \text{ psi} .$$

The maximum torsional shear stress that occurs at the center of the flat boundary (Point 0, Figure 4B) is approximated by considering the maximum inscribed circle and following the method of Case 15, p 177, of Reference 10:

$$s = \frac{Tc}{K} ,$$

where

$$c = \frac{D}{\frac{1 + \pi^2 D^4}{16A^2}} \left[1 + 0.15\left(\frac{\pi^2 D^4}{16A^2} - \frac{D}{2r}\right)\right] = 0.057,$$

$$r = \infty ,$$

$$K = \frac{F}{3 + 4\frac{F}{AU^2}} , \text{ and}$$

$$F = \int_0^U t^3 dU \ .$$

The terms t and U are derived by approximating the section's median line by a circular arc as shown in Figure 8. From Figure 8,

$$\rho \sin \alpha = R \sin \theta = \frac{\sqrt{3}}{2(8)} = 0.10825 \ ,$$

$$2\rho(1 - \cos \alpha) = R(1 - \cos \theta) = \frac{1}{16} = 0.0625 \ ,$$

$$\frac{1 - \cos \alpha}{\sin \alpha} = \frac{0.03125}{0.10325} = 0.2885 \ ,$$

and

$$0.2885 \sin \alpha + \cos \alpha = 1 \ .$$

Thus,

$$\alpha \approx 33 \text{ deg } (\sin \alpha = 0.5446 \text{ and } \cos \alpha = 0.8387)$$

and

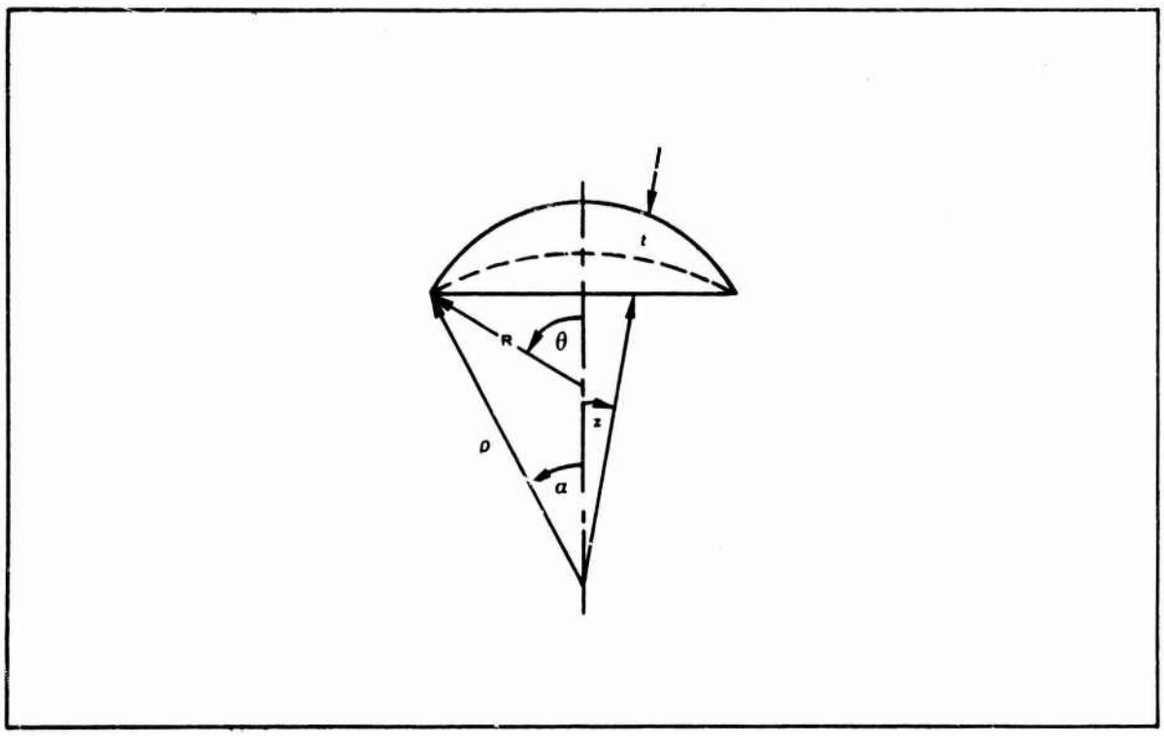

Figure 8. Section Thickness Median Line

$$\rho = \frac{0.10825}{0.5446} = 0.199 \text{ in.}$$

A check for the value of ρ is as follows:

$$(0.398)(0.1613) = 0.0644 \text{ versus } 0.0625 .$$

Then,

$$t = 2\rho\left(1 - \frac{\cos \alpha}{\cos z}\right) = 0.398 - \frac{1}{3 \cos z} ,$$

and

$$t^3 = 0.0631 - \frac{0.15813}{\cos z} + \frac{0.1329}{\cos^2 z} - \frac{1}{27 \cos^3 z} .$$

From Figure 8,

$$dU = \rho \, dz = 0.199 \, dz ;$$

therefore, $U = 0.23$ in., and $U^2 = 0.0529$. Substituting t^3 and dU into the equation for F yields

$$F = 2(0.199)\left[0.0631 \int_0^\alpha dz - 0.15813 \int_0^\alpha \frac{dz}{\cos z} + 0.1329 \int_0^\alpha \frac{dz}{\cos^2 z} - \frac{1}{27} \int_0^\alpha \frac{dz}{\cos^3 z}\right]$$

$$= 0.398\left[(0.0631)(0.577) - (0.15813)(0.6109) + (0.1329)(0.64941) - \left(\frac{1}{27}\right)\left(\frac{1}{2}\right)\left(0.6109 + \frac{0.64941}{0.8387}\right)\right]$$

$$= 2.39 \times 10^{-4} .$$

Also,

$$K = \frac{2.39 \times 10^{-4}}{3 + \frac{9.56 \times 10^{-4}}{(0.00959)(0.0529)}} = 4.9 \times 10^{-5} .$$

Finally, the torsional shear stress is:

$$s = \frac{(8.8)(0.0576)}{4.9} \times 10^5 = 10,350 \text{ psi}$$

The combined shear stress is,

$$f_s = f_{su} + s = 15,220 \text{ psi},$$

and

$$F_{su} = 55,000 \text{ psi (Reference 7)}.$$

Therefore,

$$\text{M.S.} = \frac{F_{su}}{(\text{F.S.})(f_s)} - 1 = \frac{55}{(2)(15.22)} - 1 = +0.80.$$

The torsional shear stress in the 0.090-in.-thick rectangular tab is given by (Reference 11),

$$s = \frac{3T}{wt^2} = \frac{(3)(17.6)}{\left(\frac{1}{2}\right)(0.090)^2} = 13,100 \text{ psi}.$$

Therefore,

$$\text{M.S.} = \frac{55}{(2)(13.1)} - 1 = +1.1.$$

c. Door Release Ring and Attachments

The door release ring (see Figure II-7) rotates through a 10-deg angle under the torque due to the two 25-lb tension springs. Assuming the spring force remains constant, the torque and the energy at the end of rotation are respectively:

$$T = (25)(8.625) = 216 \text{ in.-lb},$$

and

$$\text{K.E.} = T\theta = (216)\left(\frac{10\pi}{180}\right) = 37.8 \text{ in.-lb}.$$

The ring itself and the six AN-4 bolts are obviously more than adequate to resist this energy level.

d. Ram Air Inlets

Each of the four inlets (see Figure II-8) is essentially a builtup rectangular box of 0.090-in.-thick 1020 steel plate. The front of the box is open to admit the airflow that must change direction through two right angles and then flow through a slot in the rear of the box, thus inflating the BALLUTE. The exposed frontal area of each inlet is approximately

$$A_i = 4 \text{ in.} \times 2\text{-}1/2 \text{ in.} = 10 \text{ sq-in.}$$

For a stagnation pressure of q = 1050 psf, the applied force is

$$F_i = qA_i = \left(\frac{1050}{144}\right)(10) = 73 \text{ lb} .$$

After an inspection of Figures II-2 and II-3, the box is considered not critical under this loading condition.

The critical parts of the inlet are the stud (Figure II-3, Part -21) that retains the 25-lb spring (which deploys the inlet) along with the stud attachments. One end of the stud is threaded and welded to the central support tube (Figure II-3, Part -9) while a nut on the outer stud end terminates the movement of the inlet upon release of the spring. The 1-in.-wide tab that rides along the stud must deflect as a cantilevered beam to absorb the energy produced by the spring at the end of its travel.

The springs were tested and found to exhibit loads of 25 lb and 7 lb in the retracted and the extended positions, respectively. Assuming a linear spring over the 2-5/8-in. stroke, the spring load is

$$P_s = 25 - 6.85\delta_s .$$

The energy developed at the end of the stroke is

$$\text{K.E.} = \left[25 - (3.425)(2.625)\right](2.625) = 42 \text{ in.-lb} .$$

Consider the bent-up 0.090-in. tab as a cantilevered beam (see sketch below).

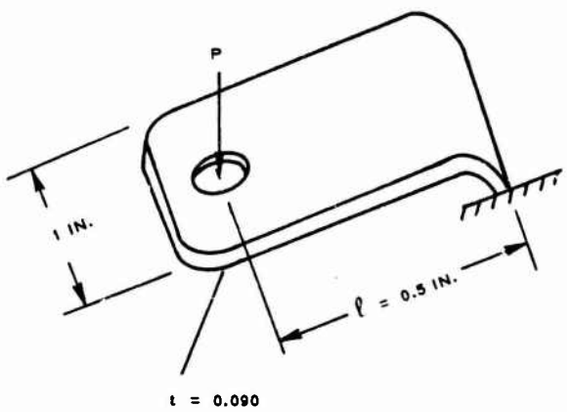

The bending deflection is

$$\delta_b = \frac{P\ell^3}{3EI} ,$$

while the shear deflection is,

$$\delta_s = \frac{P\ell}{AG} .$$

Now,

$$A = 0.090 \text{ sq in.},$$

$$E = 29 \times 10^6 \text{ psi},$$

$$I = \frac{(0.090)^3}{12} = 60.7 \times 10^{-6} \text{ in.}^4, \text{ and}$$

$$G = 11 \times 10^6 \text{ psi.}$$

Therefore,

$$\frac{\delta}{P} = \frac{\delta_b}{P} + \frac{\delta_s}{P}$$

$$= \frac{0.125}{(3)(29)(60.7)} + \frac{(0.5)(10^{-6})}{(0.09)(11)}$$

$$= 2.37 \times 10^{-5} + 5.05 \times 10^{-7}$$

$$= 24.205 \times 10^{-6} .$$

Energy also is absorbed by elongation of the stud (Figure II-3, Part -21). This elongation is

$$\frac{\delta_p}{P} = \frac{\ell_p}{AE}$$

$$= \frac{5}{\frac{\pi}{4}\left(\frac{3}{16}\right)^2 (30 \times 10^6)}$$

$$= \frac{(20)(256)(10^{-6})}{270\pi}$$

$$= 6.03 \times 10^{-6} .$$

Therefore, the total deflection is

$$\delta = (24.205 + 6.03)(10^{-6})\, P$$

$$= 30.235 \times 10^{-6} P .$$

By conservation of energy,

$$P\delta = \text{K.E.},$$

or

$$30.235 \times 10^{-6} P^2 = 42,$$

and

$$P = 10^3 \sqrt{\frac{42}{30.235}}$$

$$= 1180 \text{ lb}.$$

This is an excessive load that must be reduced by providing a shock absorber and/or allowing a greater deflection of the bent-up tab by considering plasticity.

First consider the addition of a washer cut from Tygon tubing between the tab and the nut on the rod. A ring of 60 durometer hardness and having the dimensions of Figure 9 was selected.

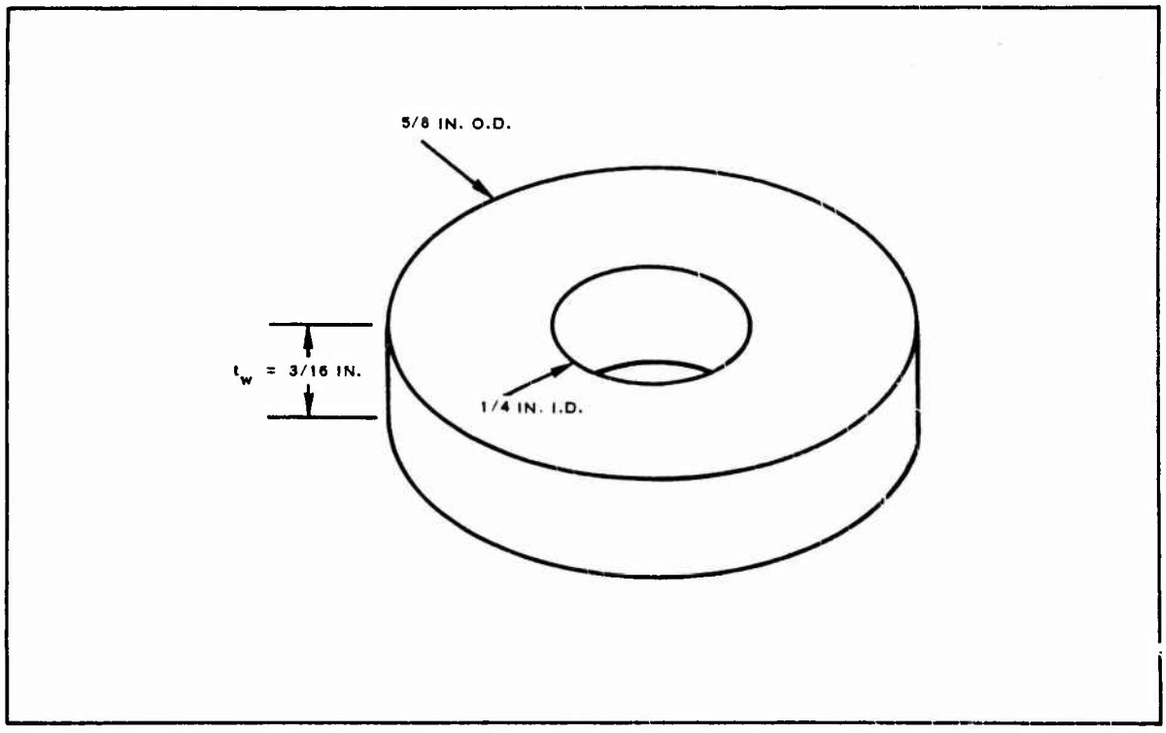

Figure 9. Dimensions of the Tygon Washer

Reference 12 gives an ultimate tensile strength and a breaking elongation of 2000 psi and 400 percent, respectively. The corresponding secant modulus of 500 psi agrees with that of 65 durometer rubber (see Figure 3-3, Reference 13). Since no compressive properties for Tygon are given in Reference 12, the properties of 65 durometer rubber from Reference 13 will be used.

The shape of a rubber piece has been found to significantly affect the compressive stiffness. Hence, a shape factor has been defined as

$$S = \frac{\text{one load area}}{\text{total free area}} .$$

Then for the washer:

$$S = \frac{\frac{\pi}{4}(d_o^2 - d_i^2)}{\pi t(d_o + d_i)} = \frac{\frac{25}{64} - \frac{1}{16}}{4\left(\frac{3}{16}\right)\left(\frac{5}{8} + \frac{1}{4}\right)} = \frac{1}{2} .$$

The compressive modulus of elasticity for this shape factor and for a limiting strain of 50 percent is determined from Figures 5-13 and 5-14 of Reference 13 as

$$E_c = \frac{1000}{0.5} = 2000 \text{ psi} .$$

The deflection of the washer then is given by

$$\delta_w = \frac{Pt_w}{E_c \frac{\pi}{4}(d_o^2 - d_i^2)} = \frac{\frac{3}{16}P}{(2000)\left(\frac{\pi}{4}\right)\left(\frac{25}{64} - \frac{1}{16}\right)}$$

$$= \frac{48P}{42,000\pi} = 3.63 \times 10^{-4} P$$

and the maximum 50 percent deflection is

$$\delta_{w_{max}} = \left(\frac{1}{2}\right)\left(\frac{3}{16}\right) = 0.0938 \text{ in.}$$

Adding this maximum deflection to the tab and stud deflections gives:

$$\delta_T = 30.235 \times 10^{-6} P + 0.0938 .$$

By conservation of energy,

$$P\delta_T = \text{K.E.} = 42 \text{ in.-lb}$$

and

$$30.235 \times 10^{-6} P^2 + 0.0938 P - 42 = 0 .$$

The load is found as follows:

$$P = -1550 \pm 500 \sqrt{9.6 + 5.56} = 395 \text{ lb} .$$

The corresponding flexural stress is:

$$f_b = \frac{6P\ell}{bt^2} = \frac{(6)(395)\ \frac{1}{2}}{(1)(0.0081)} = 146,200 \text{ psi} .$$

This excessive stress shows that the bent-up tab will undergo a plastic deformation to absorb the required energy. Although the tab will not fail, it will exhibit a permanent deflection. This deflection is estimated below.

The plastic moment for the rectangular cross section is:

$$M_p = \frac{F_{ty} bt^2}{4} .$$

Hence, the applied load that will form the plastic hinge at the root of the cantilever is:

$$P_p = \frac{M_p}{\ell} \frac{F_{ty} bt^2}{4\ell} .$$

The yield strength of the 1020 steel is F_{ty} = 30 ksi (Reference 7). Substituting this along with the proper dimensions gives:

$$P_p = \frac{(39 \times 10^3)(1)(8.1 \times 10^{-3})}{(4)(0.5)} = 158 \text{ lb} .$$

The elastic part of the deflection is given by substituting this load into the previous expressions:

$$\delta_e = \delta + \delta_w = (0.30235 + 3.63)(10^{-4})(158) = 0.062 \text{ in.}$$

Therefore, to absorb the energy of 42 in.-lb, the following additional plastic deflection is required:

$$\delta_p = \frac{\text{K.E.} - P_p \delta_e}{P_p} = \frac{42 - (158)(0.062)}{158} = 0.204 \text{ in.}$$

This is also the estimated permanent deflection.

e. Backplate Assembly

The tube and backplate assembly (see Figure II-3, Parts -13 and -103) consists of a circular flatplate welded to a tube that slides through a larger fixed tube during deployment. The assembly must absorb the kinetic energy developed at the end of the 10-in. travel. This energy is equal to the differential pressure force integrated over the travel. The pressure is determined by considering the pressure distributions over the aft end of the bomb. Figure 10 is a schematic description of the internal and external pressure forces acting during the initial inflation sequence. Reference 14 indicates that ambient pressure will exist internally and that a base pressure coefficient of

$$C_p = -0.01$$

and

$$S_{REF} = \frac{\pi}{4} d_{max}^2$$

will exist in the backplate. Total pressure was assumed to exist over the inlets. At the instant of backplate release, a differential force of -33.4 lb could move the plate aft a distance of 10 in. in 0.158 sec, neglecting friction. The actual time to travel 10 in. will be substantially longer. The rearward movement of the backplate reduces the internal pressure as the enclosed volume increases. Volume control is maintained through an

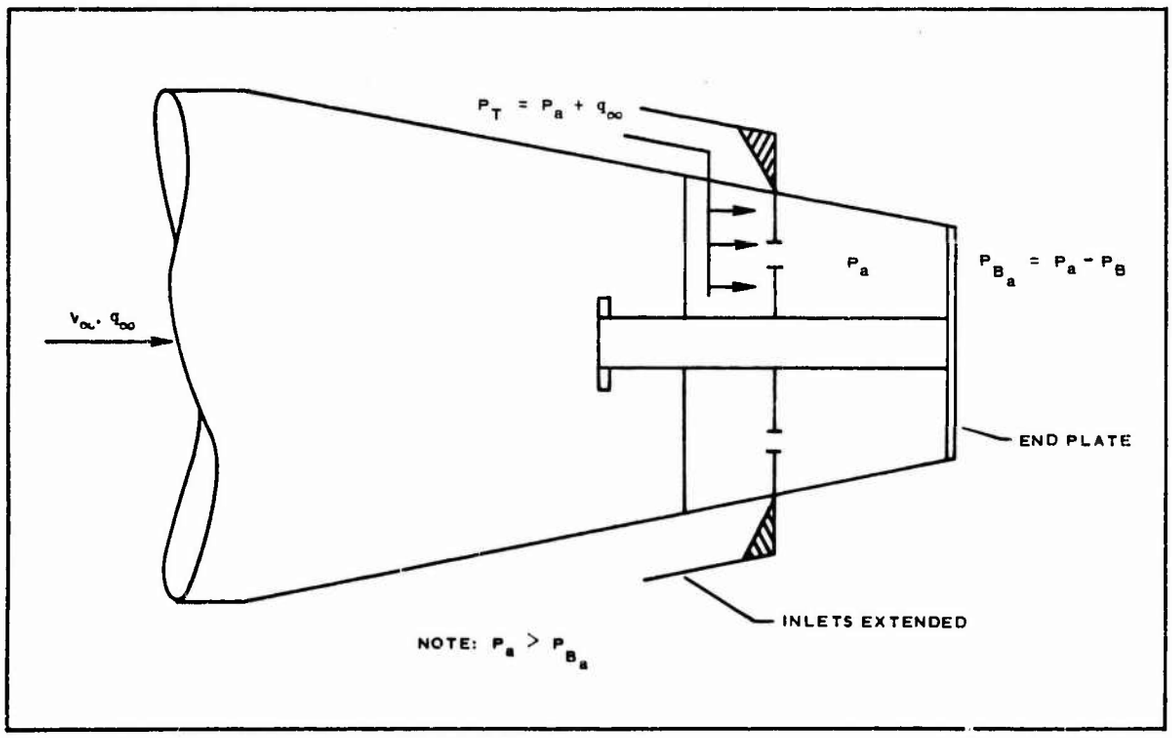

Figure 10. Diagram of Pressure Distribution during Inflation Sequence

orifice with 1.0 sq in. of area in each inlet such that the total BALLUTE volume will not be attained until 1/2 sec after inlet release (see Section VI). The 1/2-sec time interval for inflation is considered to be optimistic in lieu of the assumptions involved, flight attitudes other than a zero angle of attack will probably increase inflation time. Lower base pressure than indicated could increase the pressure differential across the backplate significantly. For design purpose a base pressure coefficient as high as $C_p = -0.06$ has been considered. The corresponding differential pressure force of 200 lb will be assumed constant, giving a final kinetic energy of 2000 in.-lb. This energy is absorbed by four mechanisms (see Figure 11).

1. Four spring steel straps are mounted inside the fixed tube (Part -9) and run the length of this tube. These straps provide a tight fit between the fixed tube on the sliding tube (Part -13) so that a frictional force is developed during the 10-in. travel.

2. The ends of the spring steel straps are extended past the end of the fixed tube and then are bent and returned (see Figure 11). The bents thus formed will "crush" upon impact with the stop (Part -15) and absorb some energy.

3. A hoop of the seal material (Part -23) is mounted in front of the stop. This is 30 durometer rubber that also can absorb some energy.

4. The eight AN-3 bolts that attach the stop to the sliding tube are subjected to single shear. These bolts also will absorb energy before failing.

First consider the eight AN-3 bolts. For 125-ksi heat-treated steel, the ultimate single shear strength of one No. 10 bolt is 2126 lb (Reference 7). An ultimate tensile elongation of 17 percent also is given in this reference. The ultimate deformation of the bolts in single shear must include shearing, bending, and bearing deformations of the bolts as well as the localized bearing deformation of the tube and stop. Reference 15 presents experimental shear-deformation data for high-strength steel bolts loaded to failure in double shear. These data give the ultimate tensile and the ultimate shear elongations as 19 percent and 25 percent, respectively. Therefore, a reasonable value of the ultimate shearing elongation of 22 percent will be used. The shank diameter of one bolt is 0.190 in.

The total strain energy that can be absorbed by the bolts is then:

$$U_B = (8)(2126)(0.22)(0.19) = 710 \text{ in.-lb} .$$

Next consider the rubber ring. The loaded area of the ring (see sketch) is:

$$A_\ell = \pi(5.5 + 0.25)\ \frac{1}{4} = 4.52 \text{ sq in.}$$

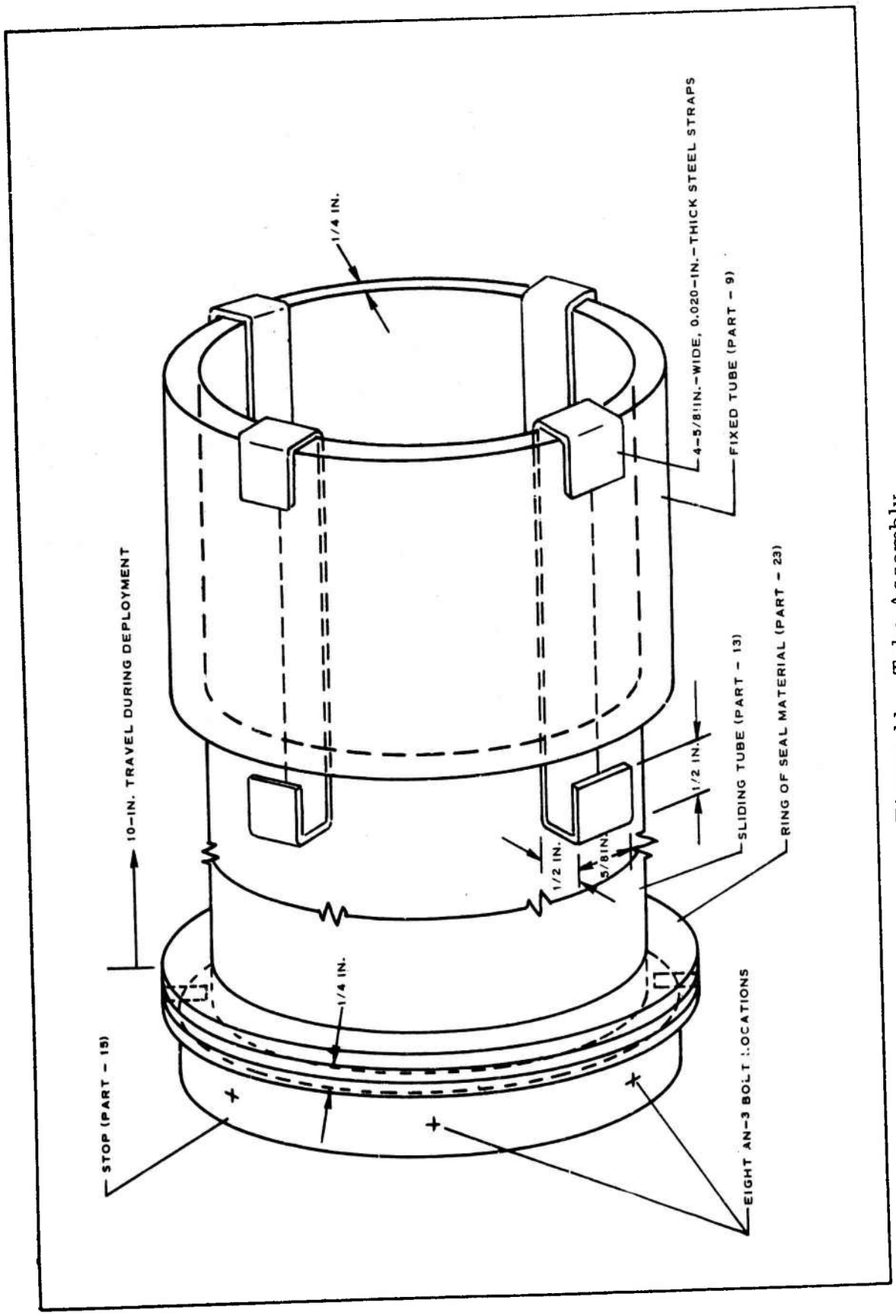

Figure 11. Tube Assembly

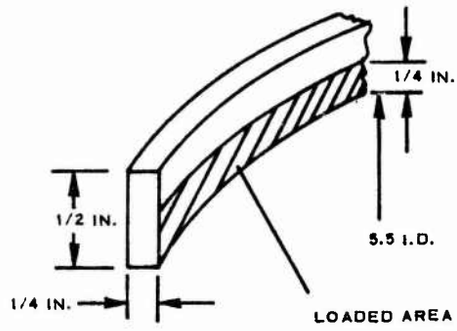

The total free area is:

$$A_f = \left(\frac{1}{4}\right)\pi(5.5 + 6.5) + 2\left(\frac{1}{4}\right)\pi(5.5 + 0.75)$$

$$= 9.45 + 9.82 = 19.27 \text{ sq in.}$$

Therefore, the shape factor is,

$$S = \frac{A_\ell}{A_f} = \frac{4.52}{19.27} = 0.235 .$$

The corresponding modulus at 50 percent compression is taken from Figure 5-10 of Reference 13 as

$$E_c = \frac{300}{0.5} = 600 \text{ psi} .$$

The deflection and the corresponding strain-energy of the ring are then:

$$\delta_r = \frac{Pt}{A_\ell E_c} = \frac{0.25P}{(4.52)(600)} = 9.2 \times 10^{-5} P .$$

For 50-percent deflection,

$$P = \frac{(0.5)\left(\frac{1}{4}\right)}{9.2} \times 10^5 = 1360 \text{ lb}$$

and

$$U_r = P\delta_r = 9.2 \times 10^{-5} P^2 = (9.2)(1.36)^2(10) = 170 \text{ in.-lb} .$$

Each of the steel strap bents is loaded and is considered to "crush" by the formation of a plastic hinge at Point b as shown in the following sketch.

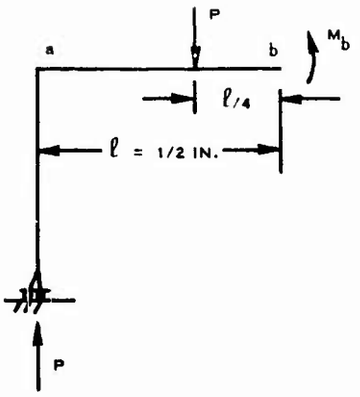

$$M_b = \frac{3P\ell}{4} = \frac{3}{8}P$$

and

$$M_a = 0 .$$

Equating the moment at Point b to the plastic moment and solving for the load, P_p, gives:

$$P_p = \frac{2}{3} F_{ty} bt^2 = \left(\frac{2}{3}\right)\left(\frac{5}{8}\right)(0.020)^2 F_{ty} = 1.665 \times 10^{-4} F_{ty} .$$

Assume the yield strength of spring steel is F_{ty} = 140 ksi. Then, P_p = 23.3 lb. The corresponding energy that may be conservatively absorbed by this mechanism is:

$$U_b = (4)\left(\frac{1}{2}\right)(23.3) = 46.6 \text{ in.-lb} .$$

The frictional force between the steel straps and the tube (Part -13) cannot be determined analytically. However, the results of the test described below does give some insight into the energy that may be absorbed by this mechanism.

The entire BALLUTE canister assembly was suspended by an eyebolt attached to the center of the backplate (Part -103). The release bar (Part -33) was released, allowing the canister to free fall over the 10 in. travel. Since the weight of the released mass was 133 lb, the kinetic energy developed was 1330 in.-lb as compared to the design in-flight deployment energy of 2000 in.-lb. The steel straps were present in this test. However, the rubber ring was omitted.

Assuming the previous energy capacities of the bolts, U_B, and the steel bents, U_b, are valid, the minimum energy developed by friction during this test had to be:

$$U_f = 1330 - 710 - 46.6 = 573 \text{ in.-lb} .$$

This corresponds to a friction force of 14.3 lb per strap.

Upon completion of this static drop test, the stop (Part -15) was removed and inspected along with the eight AN-3 bolts. There were no signs of permanent shearing or bearing deformations. On this basis, the above frictional force will be doubled. The resulting value, when added to the previous energy capacities, then will show that the system is adequate to absorb the design kinetic energy of 2000 in.-lb as follows:

Parameter	Value (in.-lb)
Frictional energy, U_f = (2)(4)(14.3)(10)	1144
Steel bent energy, U_b	47
Energy of rubber ring (at 50-percent deflection), U_r	170
Strain energy of bolts, U	710
Total, U	2071

f. BALLUTE Volume Control

The analytical approach used to determine the orifice size is based on a fluid flow analysis that ignores the pressure differential acting on the baseplate. The initial approach in determining inflation time was to assume that a column of air having free-stream properties would flow into all four inlets simultaneously at a zero angle of attack. Under this assumption, inflation would occur in 0.03 sec. This inflation time was considered unacceptable in lieu of the system structural requirements.

The approach used to circumvent this problem was to meter the flow into the BALLUTE so an inflation time of no less than 0.5 sec would occur at a zero angle of attack. To size an orifice for this inflation time interval, it was necessary to estimate the internal and external pressure distributions. Externally, it was assumed that free-stream total pressure was acting over the inlet openings. This approach is considered valid if the flow does not separate prior to reaching the inlets. Internal pressure was assumed to be ambient. By placing an orifice in the internal structure of the canister section (see Figure 11), it was possible to make some additional assumptions. On the aft side of the orifice, ambient pressure was assumed to exist. On the inlet side of the orifice, it was assumed that the flow would stagnate and that the stagnation pressure would be equivalent to that acting at the inlet openings; namely, free-stream total pressure:

$$P_p = P_a + \frac{1}{2} \rho_\infty V_\infty^2 .$$

Under the assumptions specified, it is possible to treat this problem using the Laval nozzle flow equation:

$$\frac{m}{A} = \sqrt{\frac{2\gamma}{\gamma - 1} P_o \rho_o \left(\frac{P}{P_o}\right)^{2/\gamma} \left[1 - \left(\frac{P}{P_o}\right)^{(\gamma - 1)/\gamma}\right]}.$$

Assuming an orifice efficiency of 65 percent and knowing the mass of air needed to inflate the BALLUTE in 0.5 sec, it was possible to size the orifice. After calculating the stagnation conditions, the Laval nozzle equation was evaluated with the result that for a zero angle of attack, four orifices each with an inlet area of approximately 1.0 sq in. would satisfactorily inflate the BALLUTE in 0.5 sec. Inflation time at angles of attack other than zero will exceed the minimum time of 0.5 sec since all inlets will not be exposed to the free-stream flow. This analysis is valid only under the assumptions specified and does not consider the movement of the end plate aft during the inflation sequence.

g. BALLUTE Shape and Strength

A necessary condition for stability of the BALLUTE's shape is that tensile stresses must exist everywhere over its surface. Since fabric has no compressive stiffness, wrinkling will occur that causes large deformations of the design shape. Therefore, the minimum stress areas of the design shape must be analyzed to prove that tensile stresses exist. In the problem at hand, the critical areas are at the forward and rear attachments of the BALLUTE to the rigid structure (Points 2 and 3 of Figure 12). The meridian stress at Point 2 is given by considering the static equilibrium of the membrane between Points 1 and 2 as shown in Figure 13, where the stress at Point 1 is first determined from statics of the free body of Figure 14.

The BALLUTE is considered as a body of revolution where the geometry of Figures 12 and 13 is based upon the profile shown in Figure II-5.

The pressure distribution of Figure 12 was estimated from the subsonic wind-tunnel test results if Reference 16. The magnitudes of these pressures were based on the specified design dynamic pressure of q = 1050 psf along with given base drag and frontal drag coefficients of 0.30 and 0.15, respectively. The pressure on the rear of the BALLUTE (to the tangency point of the two circular arcs) is considered constant. The pressure on the front of the BALLUTE is taken as a linear function with respect to the radial location so that

$$P_f = P_{fm} - (P_{fm} + P_r)\left[\frac{r - (R - r_o)}{r_t - (R - r_o)}\right] \qquad \text{for } (R - r_o) < r < r_t$$

$$= 5.13 - \left(\frac{7.32}{6.045}\right)(r - 8.75)$$

$$= 15.73 - 1.212\,r \text{ (see Figure 12)}.$$

The internal pressure is equal to the dynamic pressure as determined from the aerodynamic analysis of the ram-air inlets.

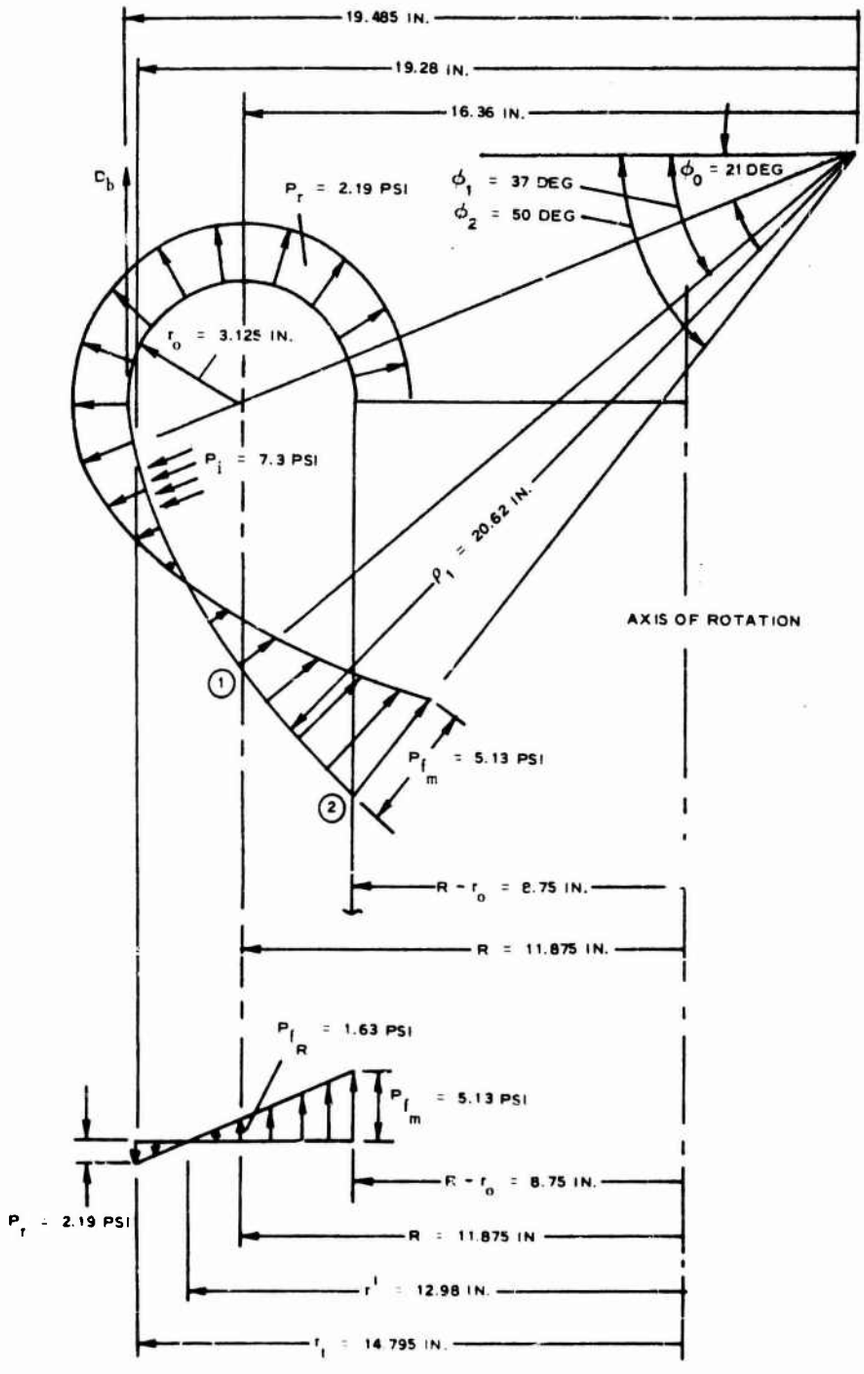

Figure 12. Half Meridian Profile of BALLUTE and Pressure Distribution

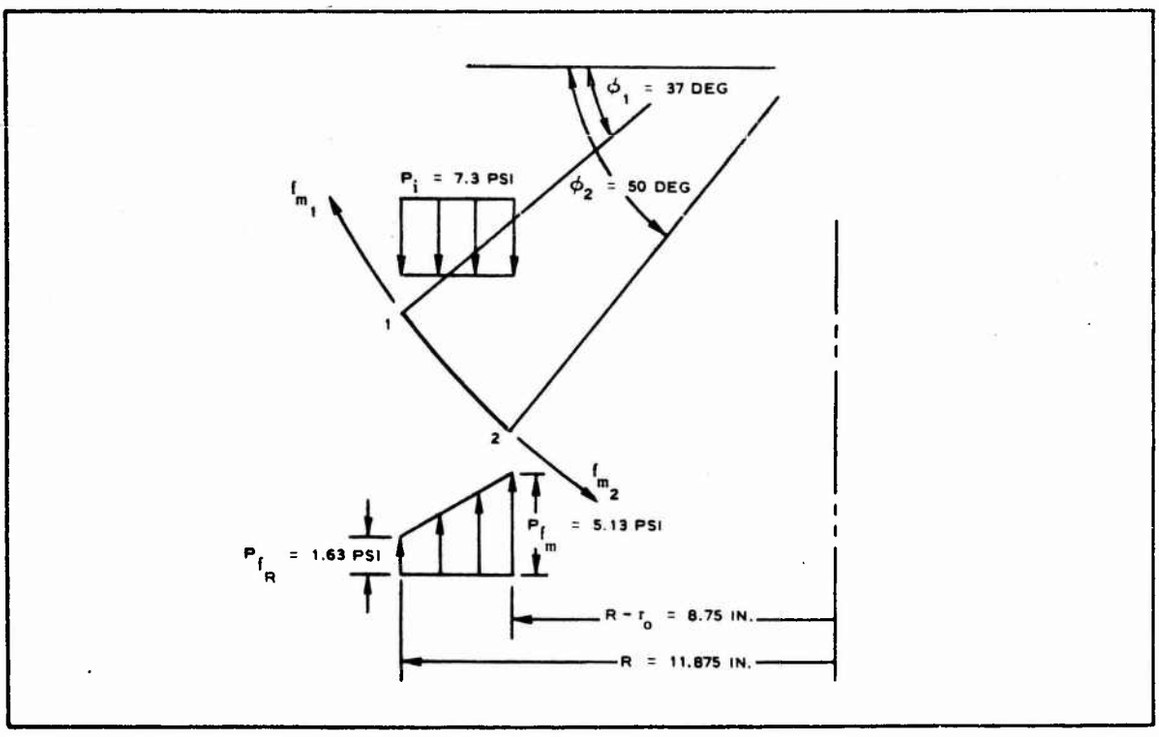

Figure 13. Statics for Meridian Stress at Point 2

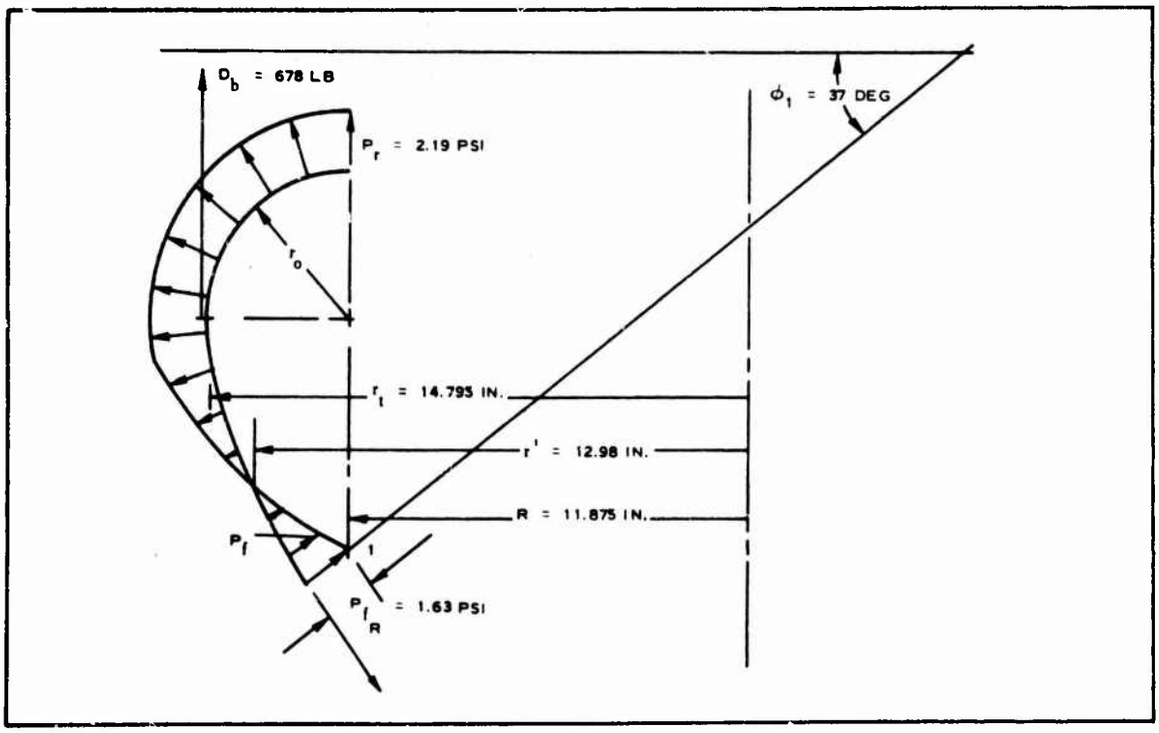

Figure 14. Statics for Meridian Stress at Point 1

In Figures 12 and 14, D_b represents the total aerodynamic drag on the burble fence that is applied around the maximum circumference of the BALLUTE. The projected area of each element of the burble fence is that of a half ellipse with major and minor diameters of 3 in. and 2.46 in., respectively (see Figure 16, shown later). Then for 32 elements with p = q, the burble fence drag is:

$$D_b = (32)qA = (32)(7.3)\left(\frac{\pi}{8}\right)(3)(2.46) = 678 \text{ lb} .$$

The meridian stress of Point 1 may now be determined from Figure 14 as follows:

$$2\pi R f_{m_1} \cos \phi_1 = \pi P_r (r_t^2 - R^2) + 2\pi \int_R^{r_t} P_f \, r dr + D_b$$

$$= 2.19\pi(r_t^2 - R^2) + 15.73\pi(r_t^2 - R^2) - \frac{2\pi}{3}(1.212)(r_t^3 - R^3) + 678$$

$$= (17.92)(78)\pi - \frac{2}{3}(1.212)(1550)\pi + 678$$

$$= 4400 - 3950 + 678$$

$$= 1128 \text{ lb} ,$$

$$f_{m_1} \cos \phi_1 = \frac{1128}{2\pi(11.875)} = 15.1 \text{ lb/in.}$$

and

$$f_{m_1} = \frac{15.1}{\cos 37 \text{ deg}} = \frac{15.1}{0.7986} = 18.9 \text{ lb/in.}$$

Next, consider the statics of Figure 13:

$$2\pi(R - r_o) f_{m_2} \cos \phi_2 = 2\pi R f_{m_1} \cos \phi_1 + 2\pi \int_{R-r_o}^{R} P_f \, r dr - \pi P_i \left[R^2 - (R - r_o)^2\right]$$

$$= 1128 + 15.73\pi(64.5) - \frac{2\pi}{3}(1.212)(1010) - 7.3\pi(64.5)$$

$$= 1128 + (8.43)(64.5)\pi - 2570$$

$$= 1128 + 1710 - 2570 = 268 \text{ lb} ,$$

$$f_{m_2} \cos \phi_2 = \frac{268}{2\pi(8.75)} = 4.87 \text{ lb/in.},$$

and

$$f_{m_2} = \frac{4.87}{\cos 50 \text{ deg}} = \frac{4.87}{0.643} = 7.6 \text{ lb/in.}$$

The meridian stress at Point 3 now is given by static equilibrium of the complete BALLUTE from Figure 12:

$$2\pi(R - r_o)f_{m_3} = 2\pi R f_{m_1} \cos \phi_1 + 2\pi \int_{R-r_o}^{R} P_f \, r\,dr + \pi P_r \left[R^2 - (R - r_o)^2\right] -$$

$$2\pi(R - r_o)f_{m_2} \cos \phi_2$$

$$= 1128 + 15.73\pi(64.5) - \frac{2\pi}{3}(1.212)(1010) + 2.19\pi(64.5) - 268$$

$$= 1128 + (17.92)(64.5)\pi - 2570 - 268$$

$$= 1128 + 3640 - 2570 - 268 = 1930 \text{ lb}.$$

$$f_{m_3} = \frac{1930}{2\pi(8.75)} = 35 \text{ lb/in.}$$

An independent check is next made using the previous drag coefficients:

$$2\pi(R - r_o)(f_{m_2} \cos \phi_2 + f_{m_3}) = q\pi\left[(R + r_o)^2 - (R - r_o)^2\right](C_{D_f} + C_{D_r}) + D_b$$

$$2\pi(8.75)(4.87 + 35) = 7.3\pi(148.5)(0.45) + 678 \text{ lb}$$

$$2200 = 2213.$$

Having shown that tensile meridian stresses exist at the critical locations, the next step is to prove that the corresponding minimum circumferential stresses are also tensile. The circumferential membrane stress is given by the well-known membrane equation (Reference 17).

$$\frac{f_m}{\rho_m} + \frac{f_c}{\rho_c} = p$$

or

$$f_c = \left(p - \frac{f_m}{\rho_m}\right)\rho_c .$$

At Point 1,

$$f_{c_1} = \left(P_i - P_{f_R} - \frac{f_{m_1}}{\rho_1}\right)\left(\frac{R}{\cos \phi_1}\right)$$

$$= \left(7.3 - 1.63 - \frac{18.9}{20.62}\right)\left(\frac{11.875}{0.7986}\right)$$

$$= 70.5 \text{ lb/in.}$$

At Point 2,

$$f_{c_2} = \left(p_i - p_{f_m} - \frac{f_{m_2}}{\rho_1}\right)\left(\frac{R - r_o}{\cos \phi_2}\right)$$

$$= \left(7.3 - 5.13 - \frac{7.6}{20.62}\right)\left(\frac{8.75}{0.643}\right)$$

$$= 24.5 \text{ lb/in.}$$

At Point 3,

$$f_{c_3} = -\left(P_i + P_r - \frac{f_{m_3}}{r_o}\right)(R - r_o)$$

$$= -\left(7.3 + 2.19 - \frac{35}{3.125}\right)(8.75)$$

$$= 14.9 \text{ lb/in.}$$

As expected (by inspection), the minimum circumferential stress as well as the minimum meridian stress occur at Point 2. Since these are tensile stresses, the design shape is stable.

It is interesting to note that the stresses at Point 3 agree with those given by the stresses in a pressurized torus (Reference 17, p 441):

$$f_m = \frac{pr_o}{2}\left(1 + \frac{R}{R - r_o}\right)$$

$$= (7.3 + 2.19)\left(\frac{3.125}{2}\right)\left(1 + \frac{11.875}{8.75}\right)$$

$$= (14.8)(2.37)$$

$$= 35 \text{ lb/in.}$$

and

$$f_c = \text{constant} = \frac{pr_o}{2}$$

$$= 14.8 \text{ lb/in.}$$

This shows that the stresses in the BALLUTE at locations aft of the point of attachment of the burble fence are unaffected by the burble fence loading and are equal to the stresses of a pressurized torus. Hence, in determining the maximum fabric stresses, only the equatorial location immediately in front of the burble fence need be checked. Then, at this location,

$$2\pi(R + r_o)f_{m_e} = 2\pi(R - r_o)f_{m_2} \cos \phi_2 + (p_i - qC_{D_f})\pi\left[(R + r_o)^2 - (R - r_o)^2\right] - D_b$$

$$= 268 + (1 - 0.15)(7.3)\pi(148.5) - 678$$

$$= 2490 \text{ lb},$$

$$f_{m_e} = \frac{2490}{2\pi(15)} = 26.4 \text{ lb/in.}$$

and

$$f_{c_e} = \left(p - \frac{f_{m_e}}{\rho_1}\right)\rho_2$$

$$= \left(7.3 + 2.19 - \frac{26.4}{20.62}\right)(15)$$

$$= 123 \text{ lb/in.}$$

This is the maximum stress in the BALLUTE when analyzed as a body of revolution. However, this BALLUTE is composed of eight gores of single curvature so that any section taken normal to the central axis is a regular octagon. A 9/16-in.-wide meridian strap of 1500-lb breaking strength is located on the centerline of each gore (see Figure II-6). As a result of this construction, the BALLUTE assumes a lobed or scalloped shape upon inflation. The meridional radii of curvature are assumed to be approximately equal to those of the above body of revolution. Hence, the previous calculated meridian stresses are considered valid. However, the principal circumferential radii of curvature of the lobed shape are obviously much less than those of the body of revolution. Since the spacing of the meridian straps is the widest at the equator, the lobe radius of curvature also is maximum at the equator, causing the maximum circumferential stress. The radius of curvature of each of the equatorial lobes is given from geometry by assuming that the straps hold the gore midpoint in place and that the flats simply assume a circular arc of the same length (see Figure 15).

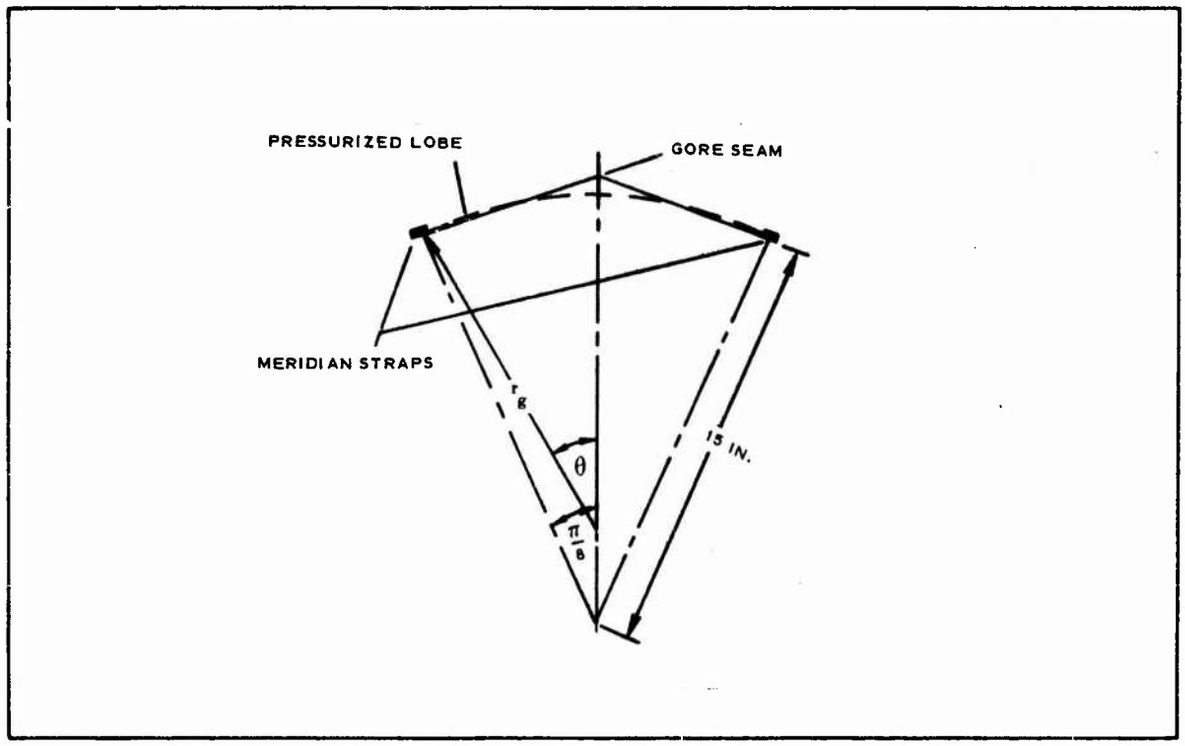

Figure 15. Fabricated and Pressurized Gore Geometry (Eight Gores)

Two equations of geometry yield the gore radius (r_g of Figure 15):

$$\theta r_g = 15 \tan \frac{\pi}{8} = 6.22 \text{ in.}$$

and

$$r_g \sin \theta = 15 \sin \frac{\pi}{8} = 5.75 \text{ in.}$$

Therefore,

$$\frac{\sin \theta}{\theta} = \frac{5.75}{6.22} = 0.923 , \qquad \theta = 39.5 \text{ deg}$$

and

$$r_g = \frac{6.22}{0.69} = 9 \text{ in.}$$

The corresponding maximum circumferential membrane stress is (refer to the previous calculation of f_{ce}):

$$f_{ce} = \left(\frac{9}{15}\right)(123) = 74 \text{ lb/in.}$$

The specified fabric has an ultimate tensile strength of 250 lb/in. so that the minimum factor of safety is:

$$F.S. = \frac{250}{74} = 3.4 .$$

A factor of safety equal to 3 is considered to be adequate for this application so that a margin of 13 percent exists.

In considering the meridian straps, it is conservatively assumed that they carry the entire aerodynamic drag force of 2200 lb. The maximum strap load then is given by placing this drag at the front attachment of the BALLUTE to the canister (Point 2 of Figure 12). Then by statics, the applied tension in each strap is:

$$T_m = \frac{2200}{8 \cos \phi_2} = \frac{2200}{(8)(0.643)} = 428 \text{ lb} ,$$

and

$$M.S. = \frac{T_{t_u}}{(F.S.)(T_m)} - 1 = \frac{1500}{(3)(428)} - 1 = +0.17 .$$

Consider one of the 32 elements that make up the burble fence. This is a conic section as shown in Figure 16. The stresses are due to an internal pressure that is equal to the dynamic pressure.

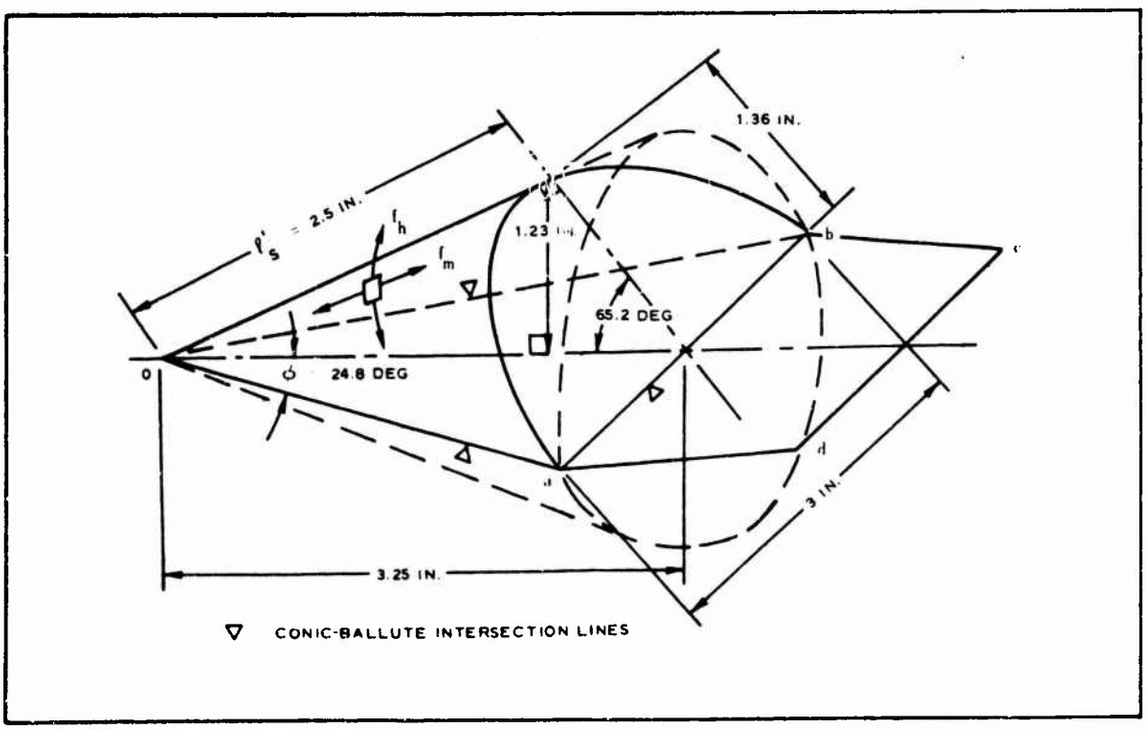

Figure 16. Geometry of One Element of Burble Fence

The principal membrane stresses are (Reference 17):

$$f_m = \frac{pr}{2 \cos \phi}$$

and

$$f_h = \frac{pr}{\cos \phi} .$$

These stresses are maximum at Points a and b of Figure 16. Then, for p = q = 1050 psf:

$$f_{h_{max}} = 2f_{m_{max}} = \frac{(1050)(1.5)}{(144)(0.908)} = (7.3)(1.65) = 12.1 \text{ lb/in.}$$

The ultimate tensile strength of the specified fabric is 250 lb/in. in the warp as well as in the fill directions. Therefore, a high margin of safety exists.

The conic element is cemented to the surface of the BALLUTE over the triangular area oab in Figure 16. A peeling condition then exists along the lines oa and ob. The applied peeling stress is equal to the principal hoop stress:

$$f_{p_{max}} = 12.1 \text{ lb/in.}$$

The peel strength of the cement has been determined from tests as

$$F_{p_u} = 7 \text{ lb/in.}$$

Although inadequate peel strength is indicated, the condition is local in the vicinity of Points a and b. Progression of any local peeling is believed to be significantly restrained by the effects of the doubled curvature of the cemented area odc that was assumed to be a plane surface in Figure 16. The test described below was conducted in order to substantiate the adequacy of the burble fence attachment.

The BALLUTE was inflated and an element of the burble fence was pressurized by sealing it off and attaching an air line to the front. A manometer was attached at Point o. Steady-state pressures of 2 to 4 psig were obtained with peak pressures of 10 psig. No evidence of peeling was observed. The burble fence-BALLUTE attachment is therefore considered to be structurally adequate.

SECTION V

RELIABILITY ESTIMATE

Using Paragraph 5.1.9 of MIL-STD-785 as a guide, a preliminary reliability prediction was estimated to be 0.9994. Table VII presents the mission or operating times that were assumed for the prediction.

TABLE VII. MISSION TIMES

Operational condition	Time
Preflight checkout to flight	1 hr
Flight on aircraft	1 hr
Release to detonation	40 sec

Further assumptions are listed below.

1. After ground checkout tests, the equipment is satisfactory. The reliability at time zero is 1.0.

2. The failure rate is constant (exponential failure distribution).

3. The environmental use factors for modifying the basic failure rates are 1.0 for preflight, 6.5 during flight on aircraft, and 1.0 for free fall.

4. The prediction excludes failures that could occur due to human errors, preflight checkout discrepancies, and aircraft carriage failures.

Table VIII presents the major functioning component/parts and their failure rates. The failure rates were obtained from FARADA and previous experience at Goodyear Aerospace on similar equipment. Such items as canister, fins, bulkheads, tubes, and baffles, which are constructed from steel and have an extremely large safety factor, were considered to have a negligible failure rate.

TABLE VIII. COMPONENT/PART FAILURE RATES*

Item	Quantity, Q	Failure rate per hour $\times 10^6, \lambda$	Time, T (hr)	$Q\lambda T$
Spring, tension	2	5.0	1	10.00
		32.5	1	65.00
Spring, compression	4	5.0	1	20.00
		32.5	1	130.00
Inlet door	4	22.0	1/90	1.00
Burble assembly BALLUTE, cement, etc.	1	15.0	1/90	0.16
Control pins	9	5.0	1	45.00
		32.5	1	292.50
Access covers	2	4.0	1	8.00
Miscellaneous hardware	1	20.0	1	20.00
				$\Sigma Q\lambda t$ = 591.7 failures per million hours

* Reliability = $e^{-591.7/10^6}$ = 0.99941.

SECTION VI

VIBRATION TEST

1. SUMMARY

One test unit M-118 bomb/BALLUTE system was subjected to a vibration test per Reference 18. The test unit was weighed and vibration parameters determined accordingly. Weight of the test unit was 168 lb, which indicated vibration at no less than 50 percent of the indicated level of 15 g's (Reference 18, Paragraph 4.0). Resonance frequencies were determined, and 30-min dwells at 8 g's were performed for no more than four resonance frequencies in each axis. The test unit then was subjected to sweep cycling, 5-2000-5 hertz (Hz), in 20-min periods at 8 g's to complete a total of three hours of vibration in each axis.

Vibration in two axes was completed successfully (axial and transverse). After five minutes of dwell in the 90-deg transverse axis at 68 Hz, one of the spring-loaded air scoops snapped open. A design fix was effected and resonance search, dwell, and sweep cycling in the 90-deg transverse axis was completely performed. Visual inspection subsequent to the test indicated no observable damage or deterioration.

2. TEST PROCEDURE

The test unit was weighed prior to vibration and the vibration parameter requirements were determined.

A test fixture was mounted on the vibration machine and the test unit mounted so that it would receive vibration in the longitudinal (axial) direction. Accelerometers were installed to permit monitoring in three locations: (1) on the vibration table adjacent to the fixture for monitoring the input, (2) on the aft surface of the test unit, and (3) in the center of one of the four air inlets (Figures 17 and 18).

The test unit was subjected to a resonance survey. As a result of the survey, 30-min resonance dwells were performed at the frequencies of 333 and 1734 Hz, followed by six 20-min sweep cycles of 5-2000-5 Hz at the required vibration levels.

The test unit and fixture were removed from the vibration machine and mounted on the slippery table plate oriented so that two opposite air inlets were in the plane of vibration and the test unit would receive vibration in the transverse axis. Accelerometers were installed to permit monitoring the input (drive), aft end cover, and one of the air scoops in the plane of vibration.

A resonance survey was performed. Resonance dwells of 30 min each were performed at the frequencies of 66, 166, 757, and 1807 Hz. Three 20-min sweep cycles of 5-2000-5 Hz were completed at the required vibration levels.

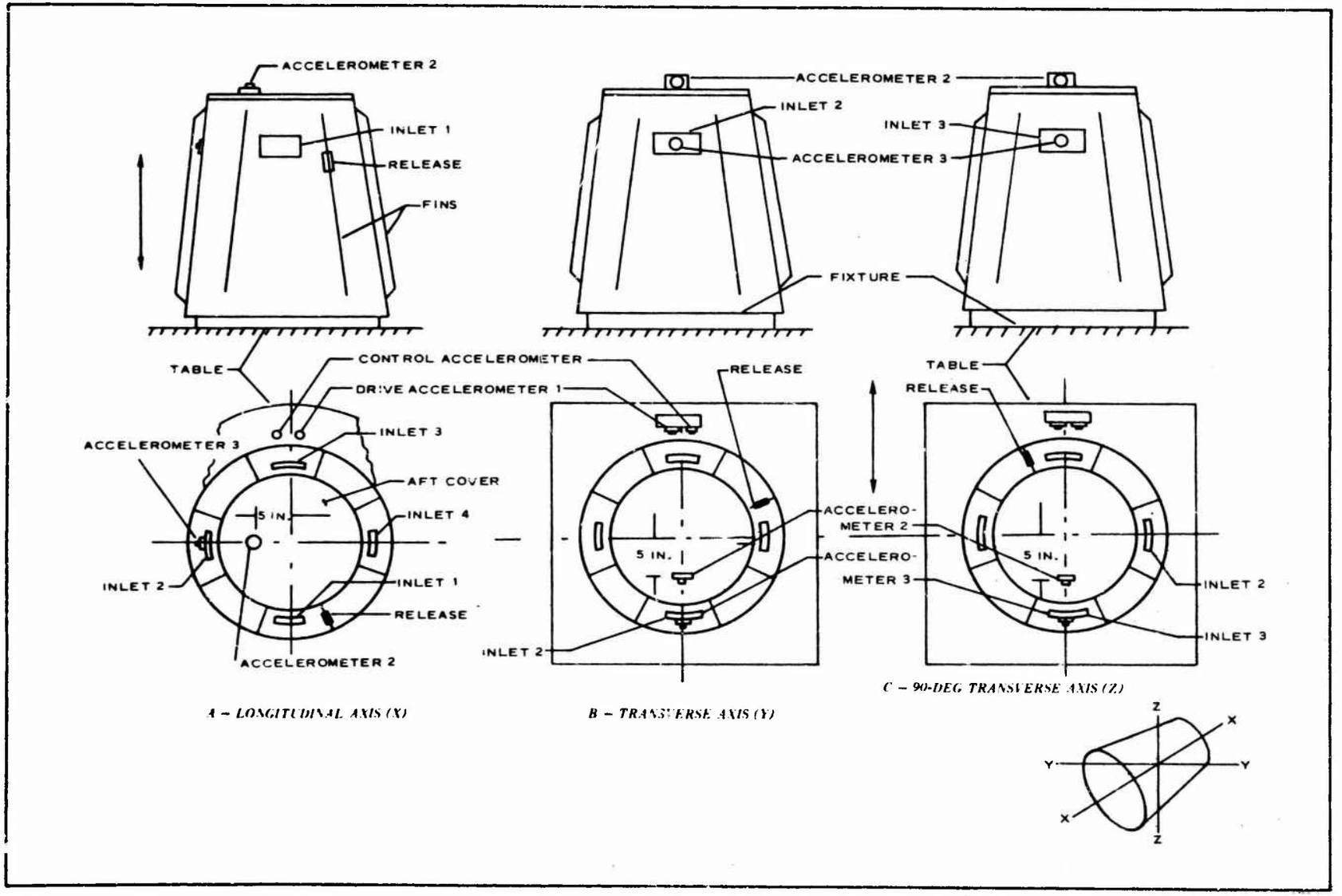

Figure 17. Canister Setup for Vibration Test

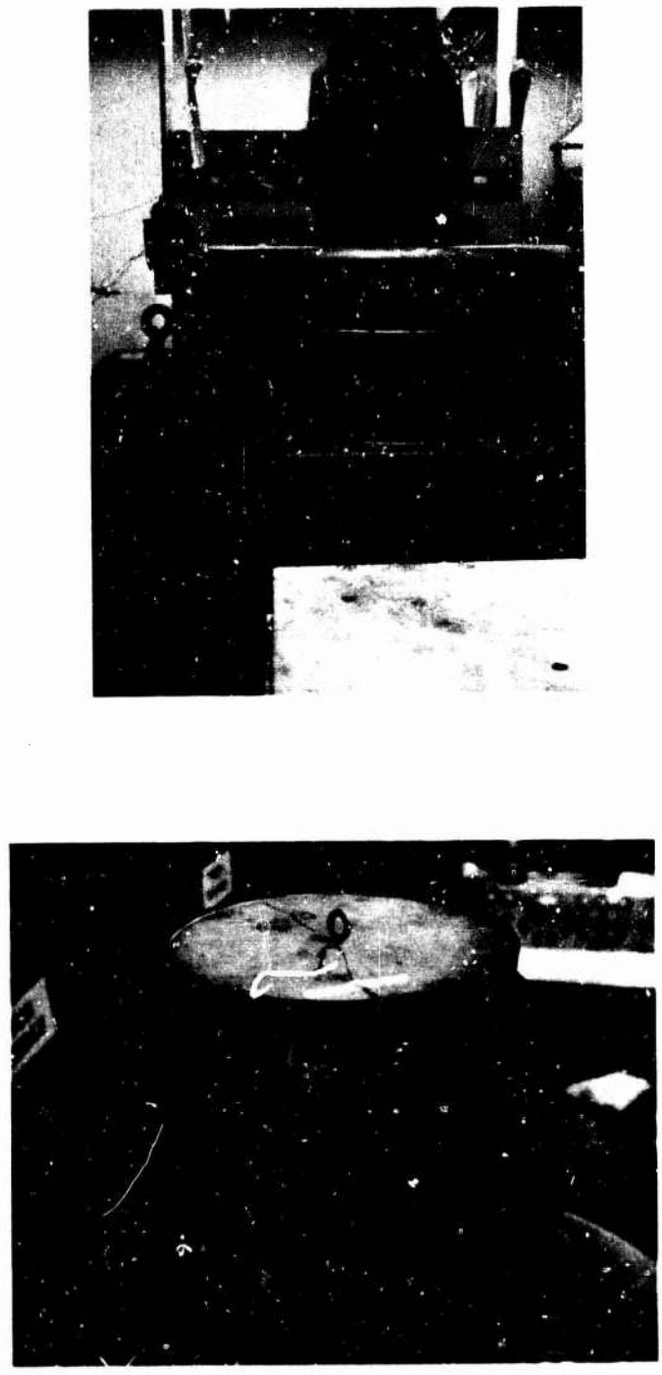

Figure 18. Test Setup on C-120 Vibration Machine for Vibration in Longitudinal (Axial) Axis

The test unit was rotated 90 deg on the fixture (which positioned the remaining two air scoops in the plane of vibration) so that vibration in the 90-deg transverse axis could be accomplished. Accelerometers were installed as in the transverse axis.

A resonance survey was performed. After five minutes into the resonance dwell at 68 Hz, a failure occurred, vibration was stopped, and the test unit removed from the table for examination and repair. Testing was resumed after repair by running the resonance survey again and performing 30-min resonance dwells at the frequencies of 71, 123, 912, and 1666 Hz. Three 20-min sweep cycles of 5-2000-5 Hz were performed.

A visual examination of the assembled test unit was performed subsequent to the completion of the vibration test.

3. TEST RESULTS

Examination of the test unit prior to vibration indicated that the most likely areas of resonance would appear on the aft cover and the air inlets. Resonance at the air inlets is due to the fact that none of the air inlets were totally secure, all being spring loaded and fitting loosely. High g levels due to shock (rattle) as well as resonance could be expected.

The resonance survey in the longitudinal axis indicated g levels in excess of a Q of 3 at 333 and 1734 Hz on the ram-air inlet, and at 66, 166, 757, and 1807 Hz in the transverse axis.

The resonance survey in the 90-deg transverse axis indicated resonances at 68, 166, 917, and 1427 Hz. After five minutes of dwell at 68 Hz with an 8-g input, one of the inlets (located 90 deg to the plane of vibration) released and opened. Vibration was stopped, engineering personnel were notified, and the test unit was removed from the vibration table for examination and repair.

Subsequent to repair, the test unit was installed on the vibration machine to receive vibration in the 90-deg transverse axis, and testing in this axis continued. The resonance survey was rerun and resonances at 71, 123, 912, and 1666 Hz were determined. Resonance dwells and sweep cycling were performed to complete the required total nine-hour vibration schedule.

There was no observable damage or deterioration of the assembled test unit at the completion of the vibration test.

SECTION VII

DESIGN

The system design for BALLUTE stabilization of the M-118 bomb culminated from the basic design requirements and those developed from the test and analyses described in the previous sections. The principal requirement was the aerodynamic shape and size for free flight of the bomb/BALLUTE determined from the small-scale wind-tunnel test and test analysis. In Figure 19, this overall bomb/BALLUTE configuration with the BALLUTE deployed is shown compared with the undeployed configuration and with the conventional shape of the M-118 bomb equipped with the M-135 fins. The complete system design, represented by the figures found in Appendix II, guided the fabrication of the prototype stabilization system, pictured in Figure 20.

The design figures also depict the mechanical features of BALLUTE deployment achieved by radial ejection of the four ram-air inlet doors and by axial release of the canister cover. These operations are accomplished by sequential tripping of cocked springs initiated by lanyard actuation at bomb release from the aircraft carriage. Details of the assembled deployment mechanism are shown in the canister photographs of the door release ring and the inlet door (see Figures 21 and 22).

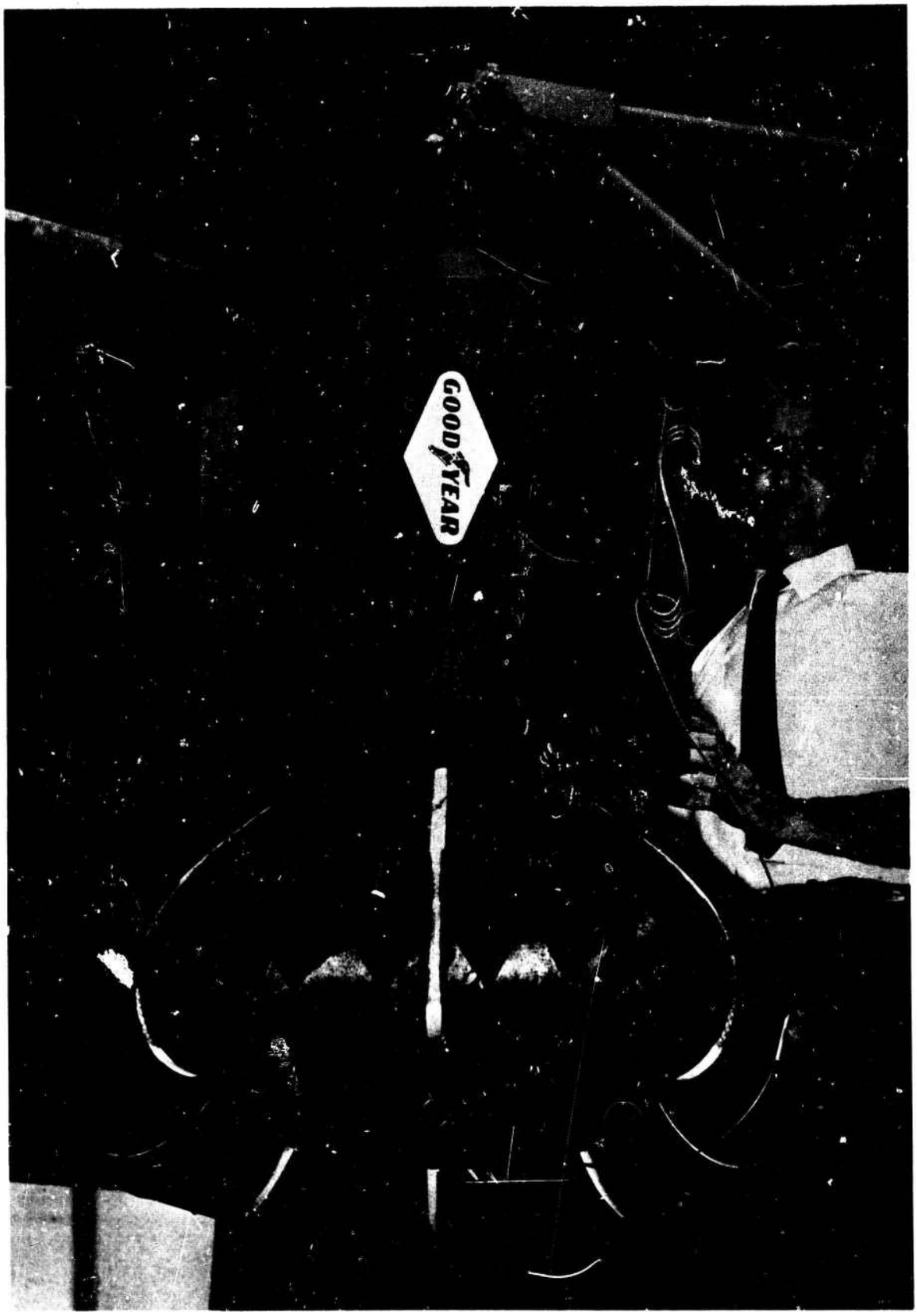

Figure 20. BALLUTE Stabilization System in Deployed Condition

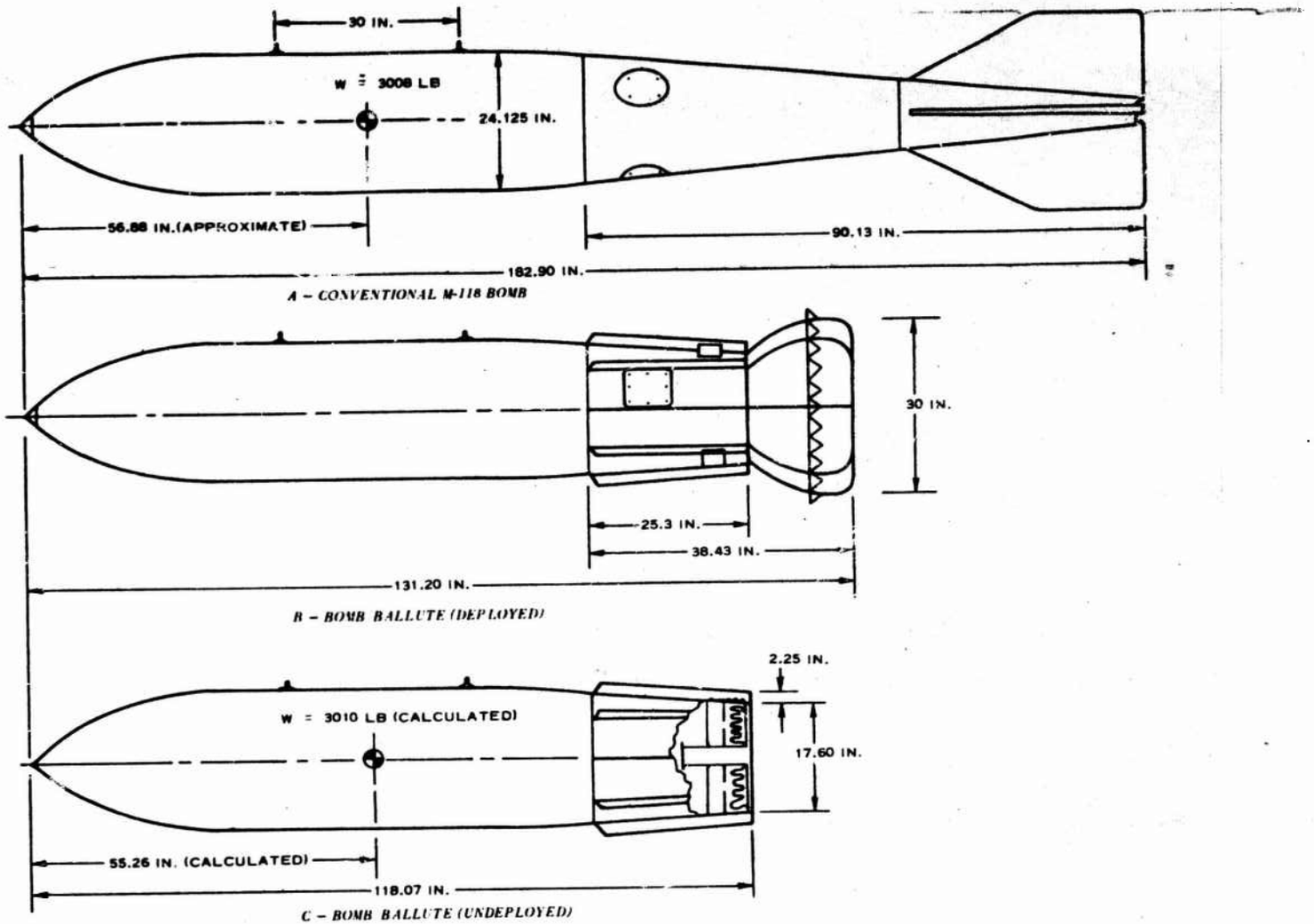

Figure 19. Comparison of M-118 Bomb Configurations

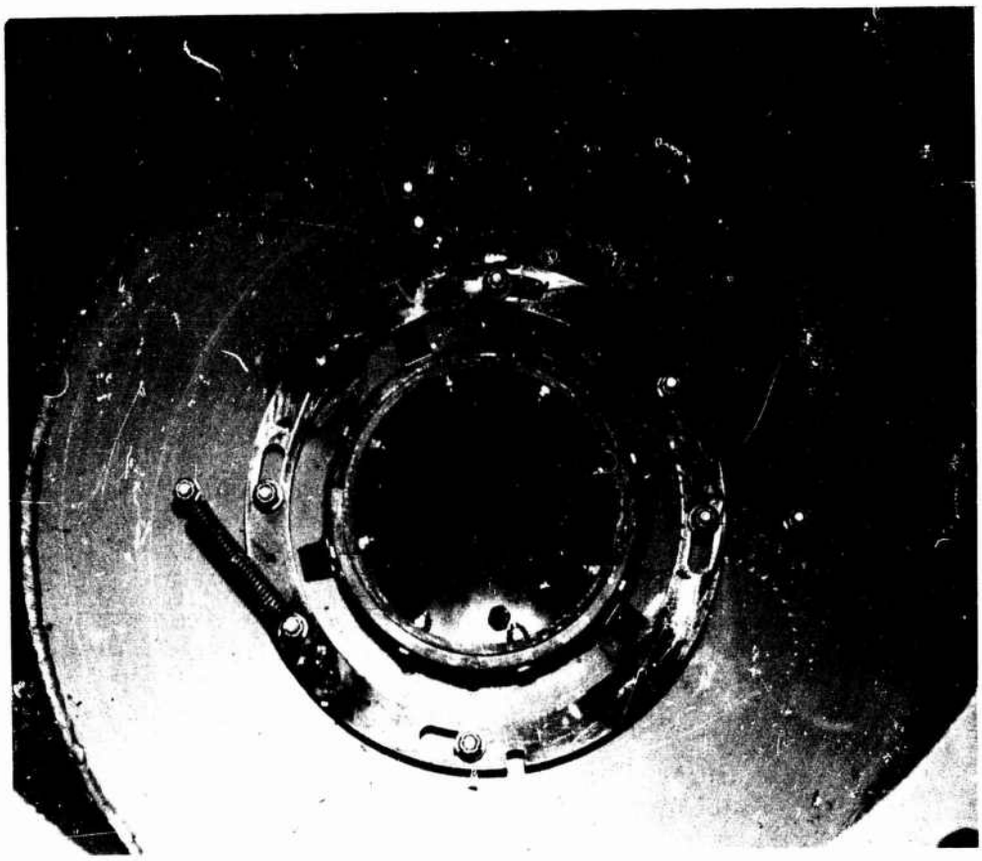

Figure 21. Door Release Ring (Actuated)

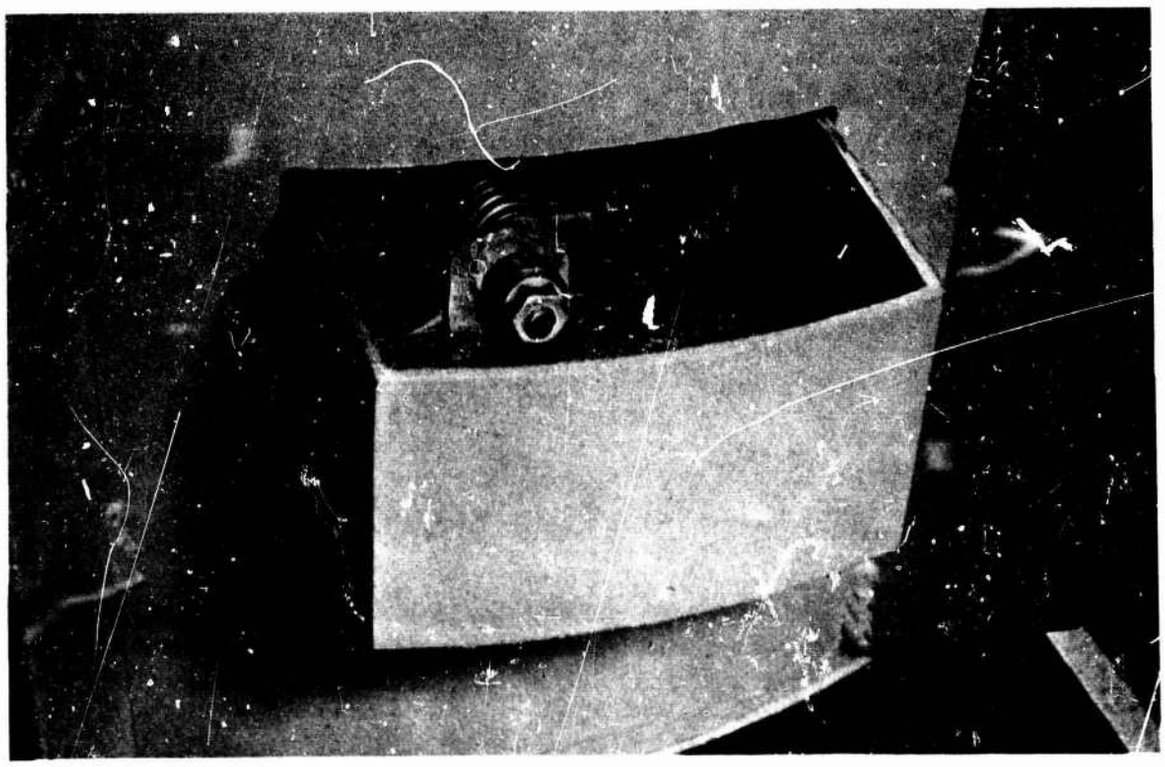

Figure 22. Air Inlet Door (Ejected)

SECTION VIII

CONCLUSIONS AND RECOMMENDATIONS

The concept of stabilizing the M-118 bomb with an attached BALLUTE in lieu of conventional fins was incorporated in five prototype units. The proposed units were designed to provide an inflated shape with sufficient drag for bomb/BALLUTE stability and system operation, yet remain compatible with planned uses of the M-118 bomb. The undeployed BALLUTE-packaged system also was vibration tested for validation as flight-testable hardware.

Accordingly, the recently delivered prototype units are recommended for flight test and evaluation of the concept.

APPENDIX I

OSCILLOGRAPHIC TRACES OF MODEL STABILITY

Recorded traces of 24 selected runs of the wind-tunnel test to determine dynamic stability for the choice of system configuration and size are contained in this appendix. The traces are shown on Pages 61 through 67.

(The reverse of this page is blank)

RUN 1

STANDARD M-118 BOMB
FINS (+ ORIENTATION),
SWEEP = 10 CM/SEC

RUN 2

STANDARD M-118 BOMB
FINS (× ORIENTATION),
SWEEP = 10 CM/SEC

RUN 4

STANDARD M-118 BOMB
FINS (+ ORIENTATION),
SWEEP = 6 CM/SEC

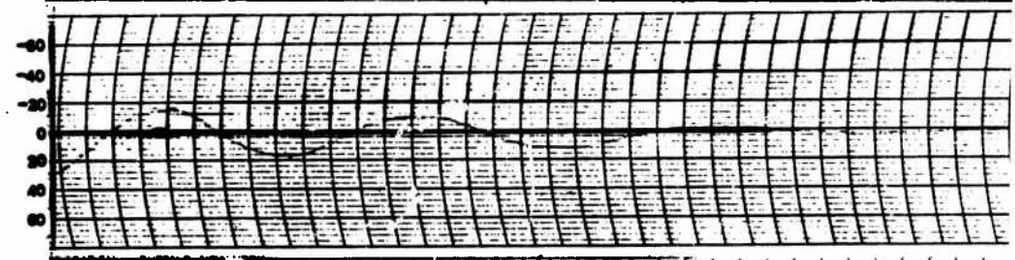

RUN 7

M-118 BOMB WITH ATTACHED
36-IN.-DIAMETER BALLUTE,
SWEEP = 10 CM/SEC

RUN 10

M-118 BOMB WITH ATTACHED
36-IN.-DIAMETER BALLUTE
PLUS 6-IN. BUBBLE FENCE,
SWEEP = 10 CM/SEC

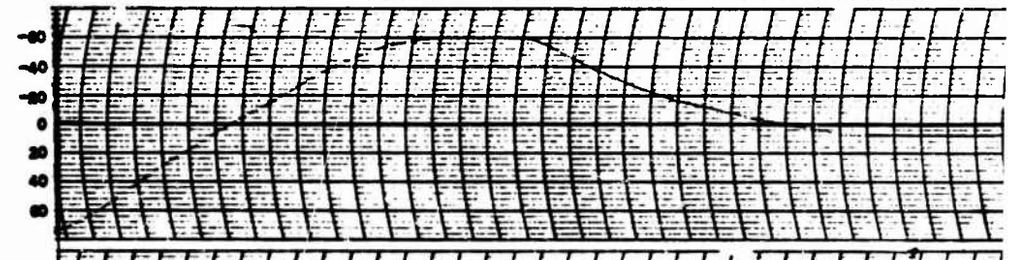

RUN 14

M-118 BOMB WITH ATTACHED
54-IN.-DIAMETER BALLUTE,
SWEEP = 10 CM/SEC

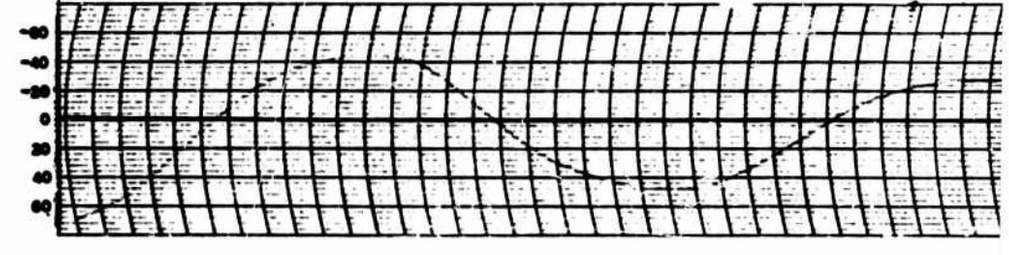

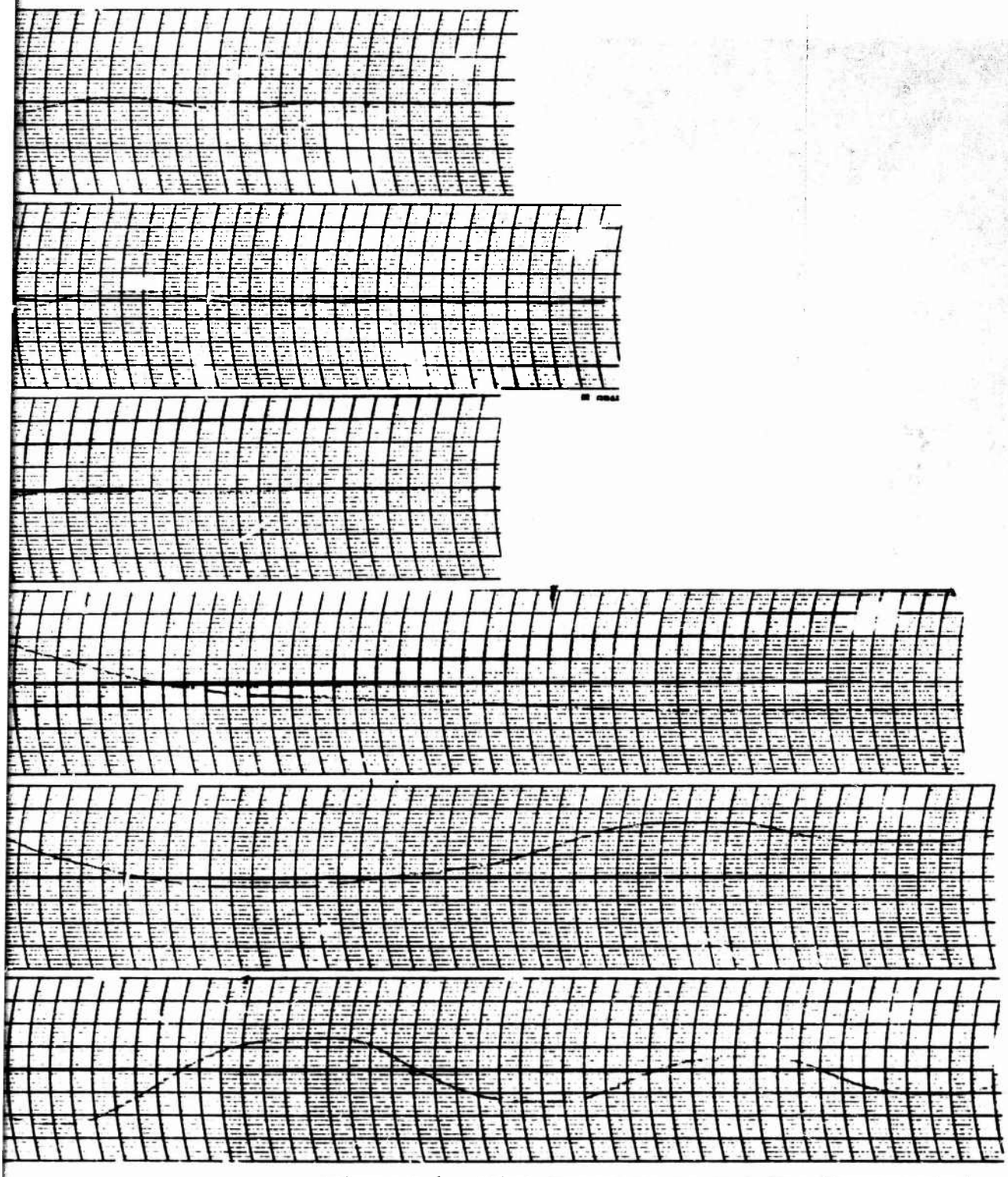

Figure I-1. Wind-Tunnel Model Stability Characteristics, Oscillograph Traces

(The reverse of this page is blank)

B

RUN 16

M-118 BOMB WITH ATTACHED 34-IN.-DIAMETER BALLUTE PLUS 6-IN. BURBLE FENCE, SWEEP = 10 CM/SEC

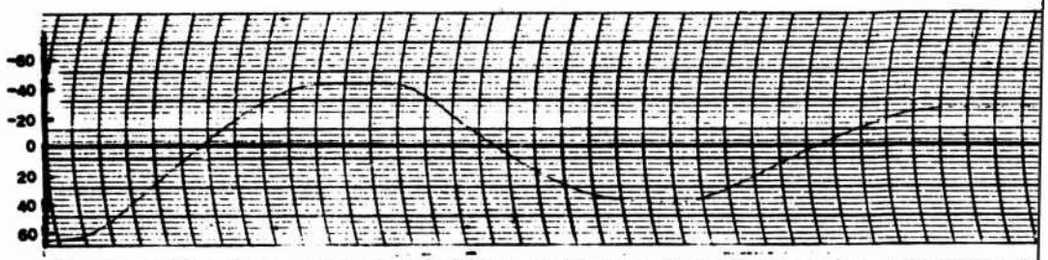

RUN 17

M-118 BOMB WITH ATTACHED 40-IN.-DIAMETER BALLUTE, SWEEP = 10 CM/SEC

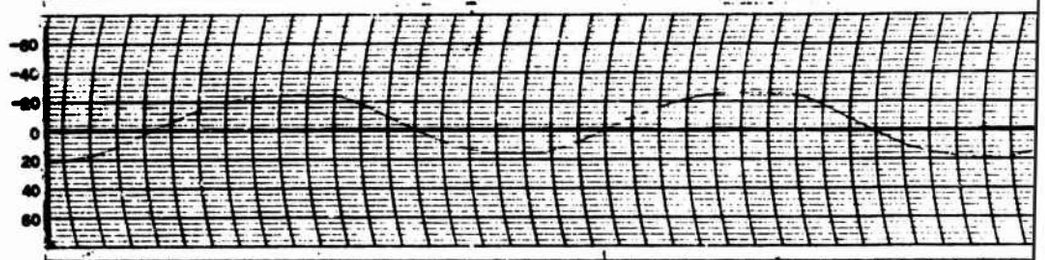

RUN 21

M-118 BOMB WITH ATTACHED 40-IN.-DIAMETER BALLUTE PLUS 6-IN. BURBLE FENCE, SWEEP = 10 CM/SEC

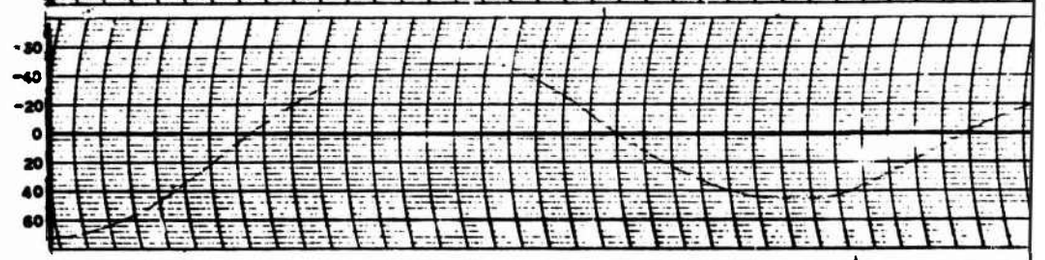

RUN 27

M-118 BOMB WITH ATTACHED 28-IN. DIAMETER BALLUTE PLUS 6-IN. BURBLE FENCE, TRIP WIRE ON NOSE, SWEEP = 10 CM/SEC

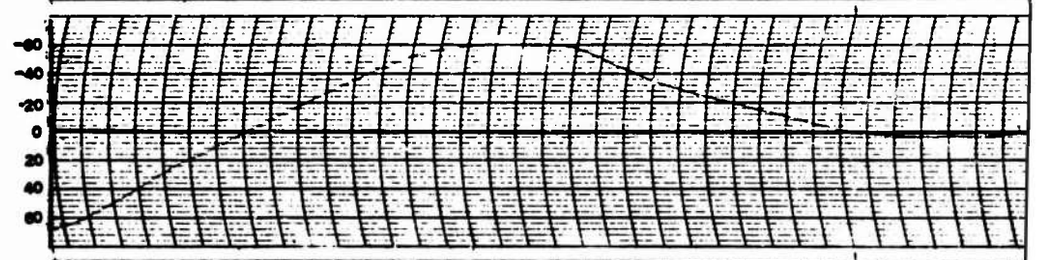

RUN 34

M-118 BOMB WITH ATTACHED 40-IN.-DIAMETER BALLUTE 4 LONGITUDINAL STRAKES ON CANISTER SECTION, SWEEP = 10 CM/SEC

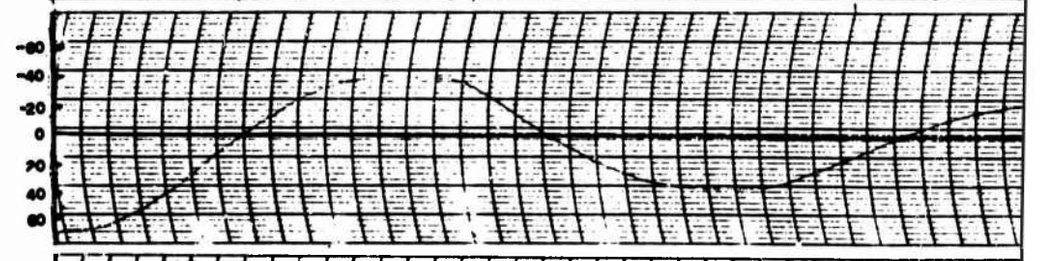

RUN 35

M-118 BOMB WITH CANISTER SECTION, SWEEP = 10 CM/SEC

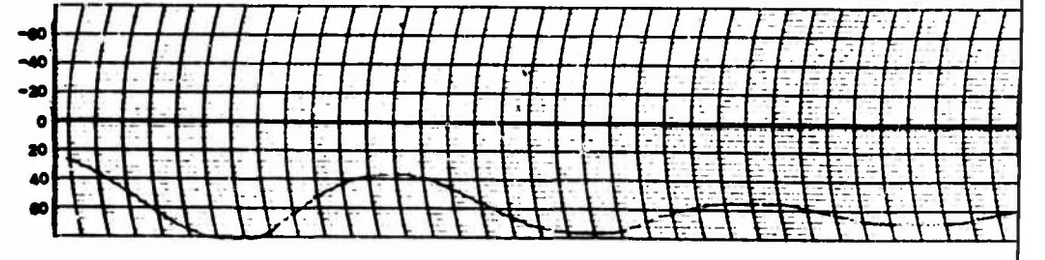

A

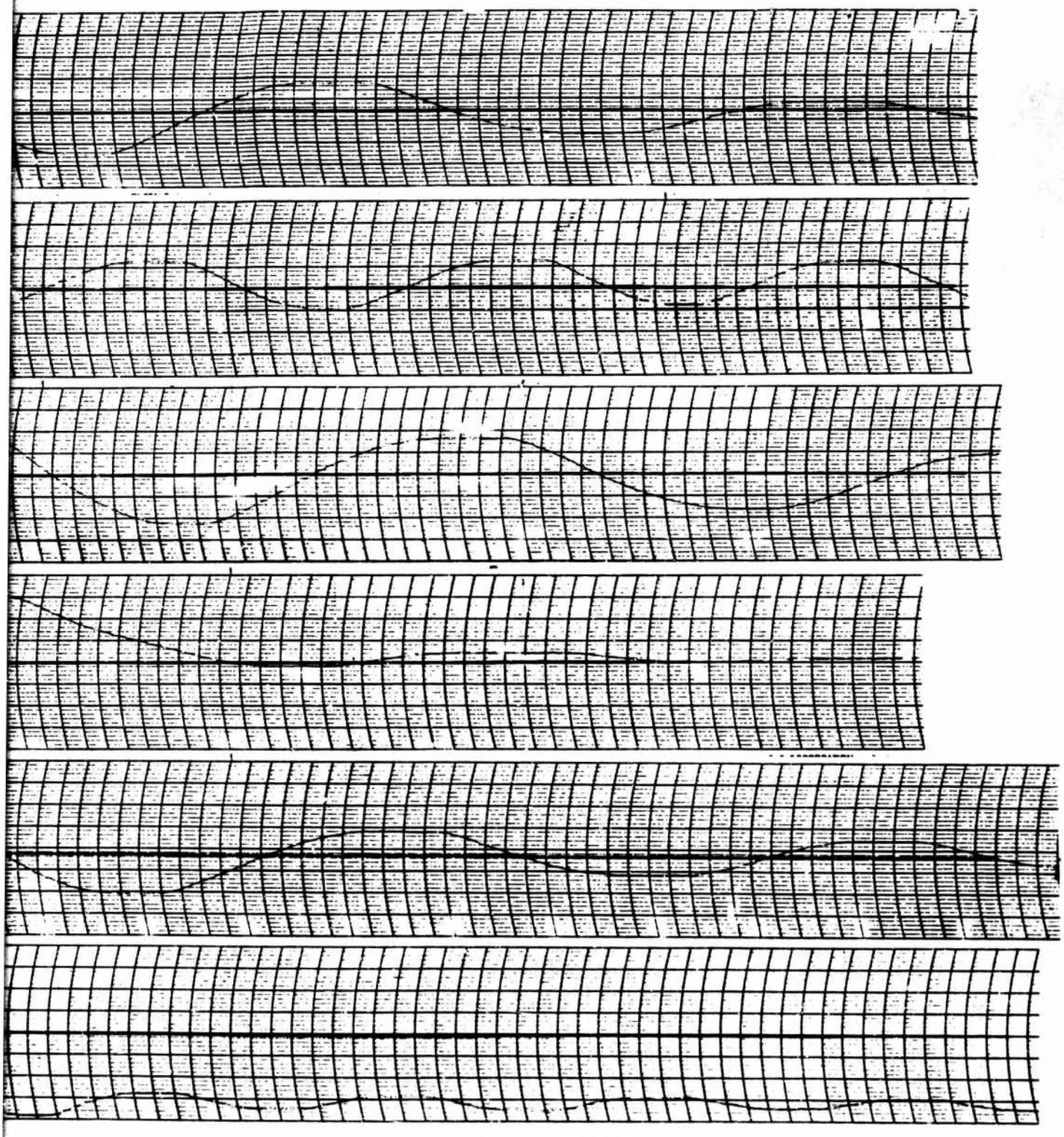

Figure I-1. Wind-Tunnel Model Stability Characteristics, Oscillograph Traces (Continued)

(The reverse of this page is blank)

B

RUN 36

M-118 BOMB WITH ATTACHED 24-IN.-DIAMETER CONICAL TUCKBACK BALLUTE, SWEEP = 5 CM/SEC, 4 STRAKES

RUN 39

M-118 BOMB WITH ATTACHED 28-IN.-DIAMETER BALLUTE INCLUDING 10 PERCENT BUBBLE FENCE, SWEEP = 5 CM/SEC, 4 STRAKES

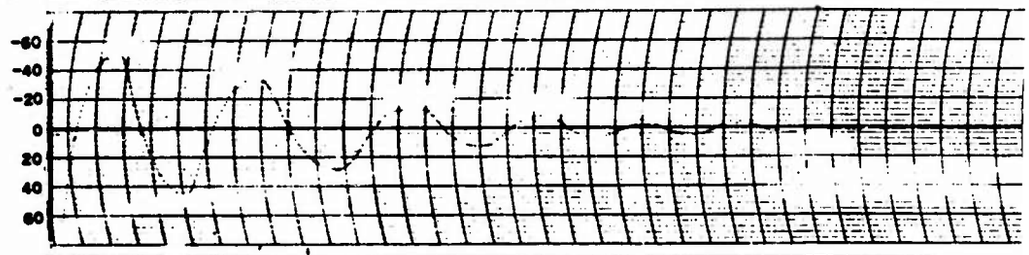

RUN 41

M-118 BOMB WITH ATTACHED 28-IN.-DIAMETER BALLUTE, SWEEP = 5 CM/SEC, 4 STRAKES

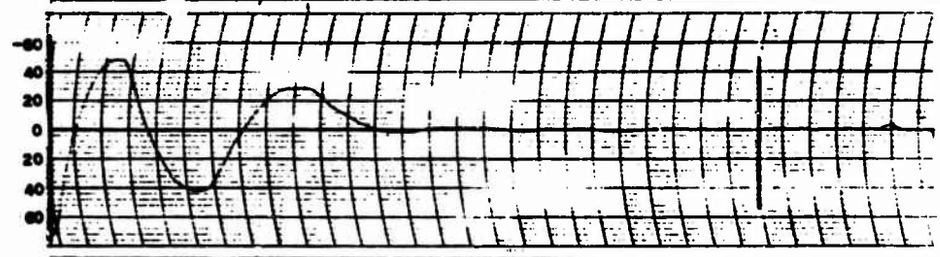

RUN 45

M-118 BOMB WITH ATTACHED 28-IN.-DIAMETER BALLUTE, SWEEP = 5 CM/SEC, 4 STRAKES

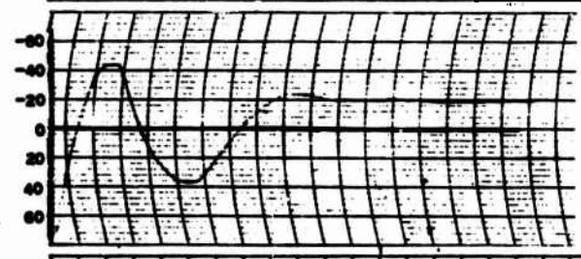

RUN 46

M-118 BOMB WITH ATTACHED 32-IN.-DIAMETER BALLUTE, SWEEP = 5 CM/SEC, 4 STRAKES

RUN 48

M-118 BOMB WITH ATTACHED 24-IN.-DIAMETER BALLUTE, SWEEP = 5 CM/SEC, 4 STRAKES

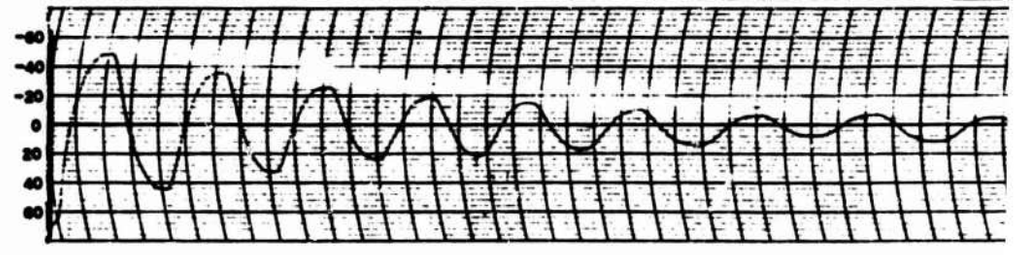

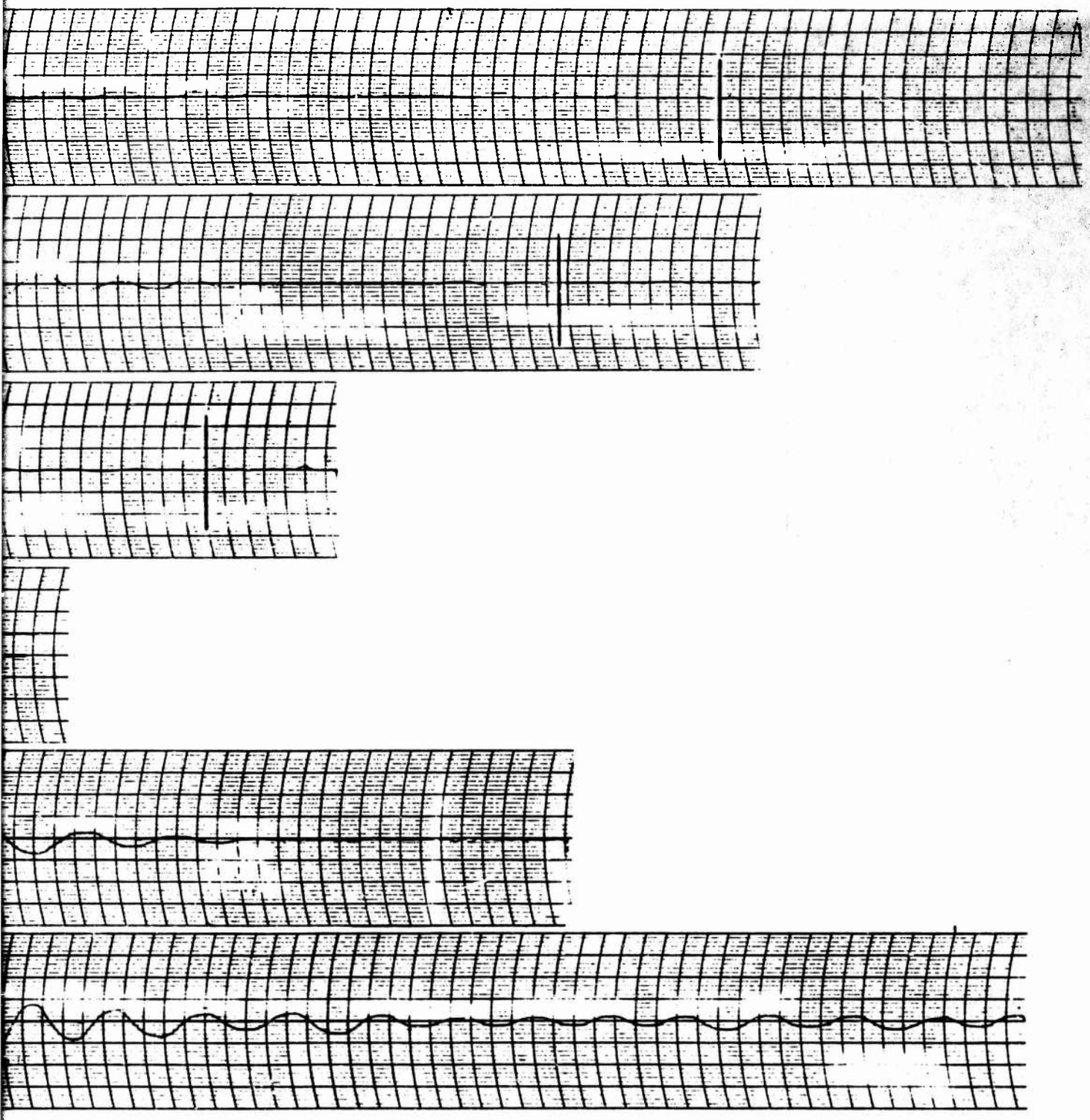

Figure I-1. Wind-Tunnel Model Stability Characteristics, Oscillograph Traces (Continued)

(The reverse of this page is blank)

RUN 48

M-118 BOMB WITH ATTACHED
34-IN.-DIAMETER BALLUTE,
SWEEP = 5 CM/SEC, 4 STRAKES

RUN 51

M-118 BOMB WITH ATTACHED
40-IN.-DIAMETER BALLUTE,
SWEEP = 5 CM/SEC, 4 STRAKES

RUN 53

M-118 BOMB WITH ATTACHED
20-IN.-DIAMETER BALLUTE,
SWEEP = 5 CM/SEC, 5 STRAKES

RUN 56

M-118 BOMB WITH ATTACHED
30-IN.-DIAMETER BALLUTE,
SWEEP = 5 CM/SEC, 8 STRAKES

RUN 58

M-118 BOMB WITH ATTACHED
30-IN.-DIAMETER BALLUTE,
2 PERCENT BURBLE FENCE,
SWEEP = 5 CM/SEC, 8 STRAKES

RUN 61

M-118 BOMB WITH ATTACHED
30-IN.-DIAMETER BALLUTE,
8 PERCENT BURBLE FENCE,
SWEEP = 5 CM/SEC, 8 STRAKES

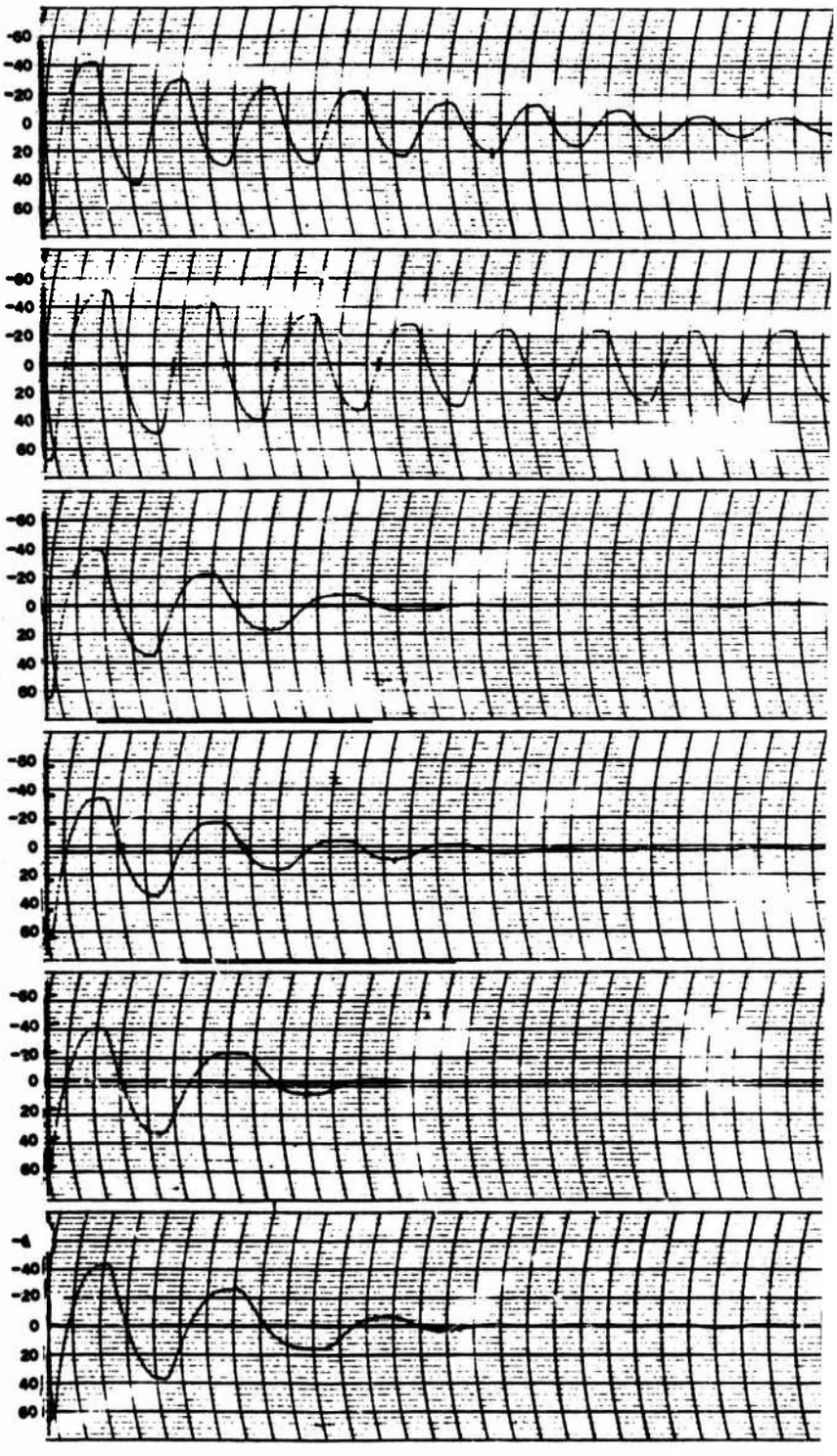

Figure I-1. Wind-Tunn
Oscillogra

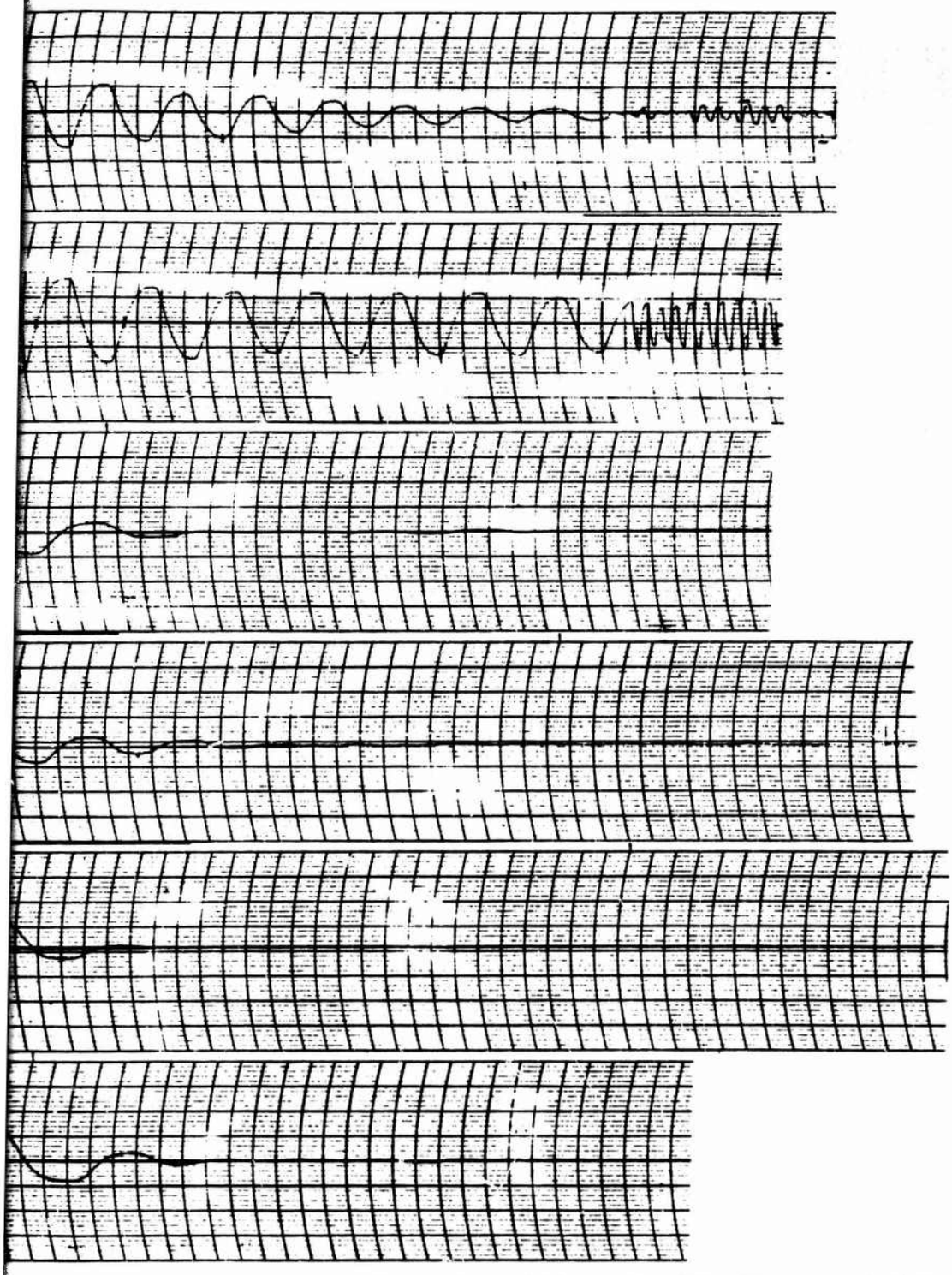

Figure I-1. Wind-Tunnel Model Stability Characteristics. Oscillograph Traces (Concluded)

(The reverse of this page is blank)

B

APPENDIX II

DESIGN FIGURES

Engineering data are contained in the following drawings to show the prototype stabilization system:

1. Decelerator assembly
2. Canister assembly (view looking aft and section view through centerline
3. Release mechanism
4. Assembly of BALLUTE
5. Gore pattern
6. Release ring
7. Air inlet door

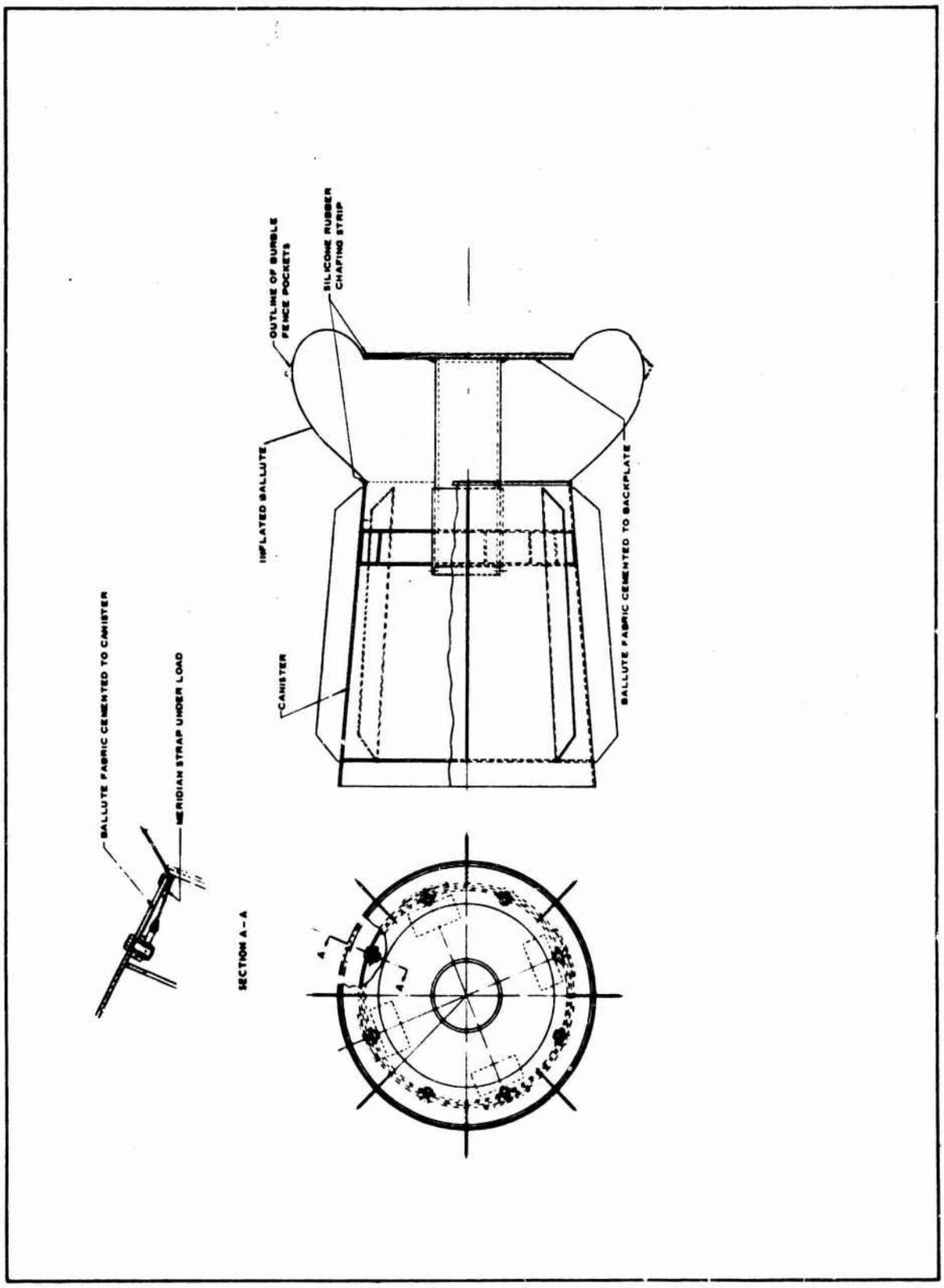

Figure II-1. M-118 Bomb Decelerator Assembly

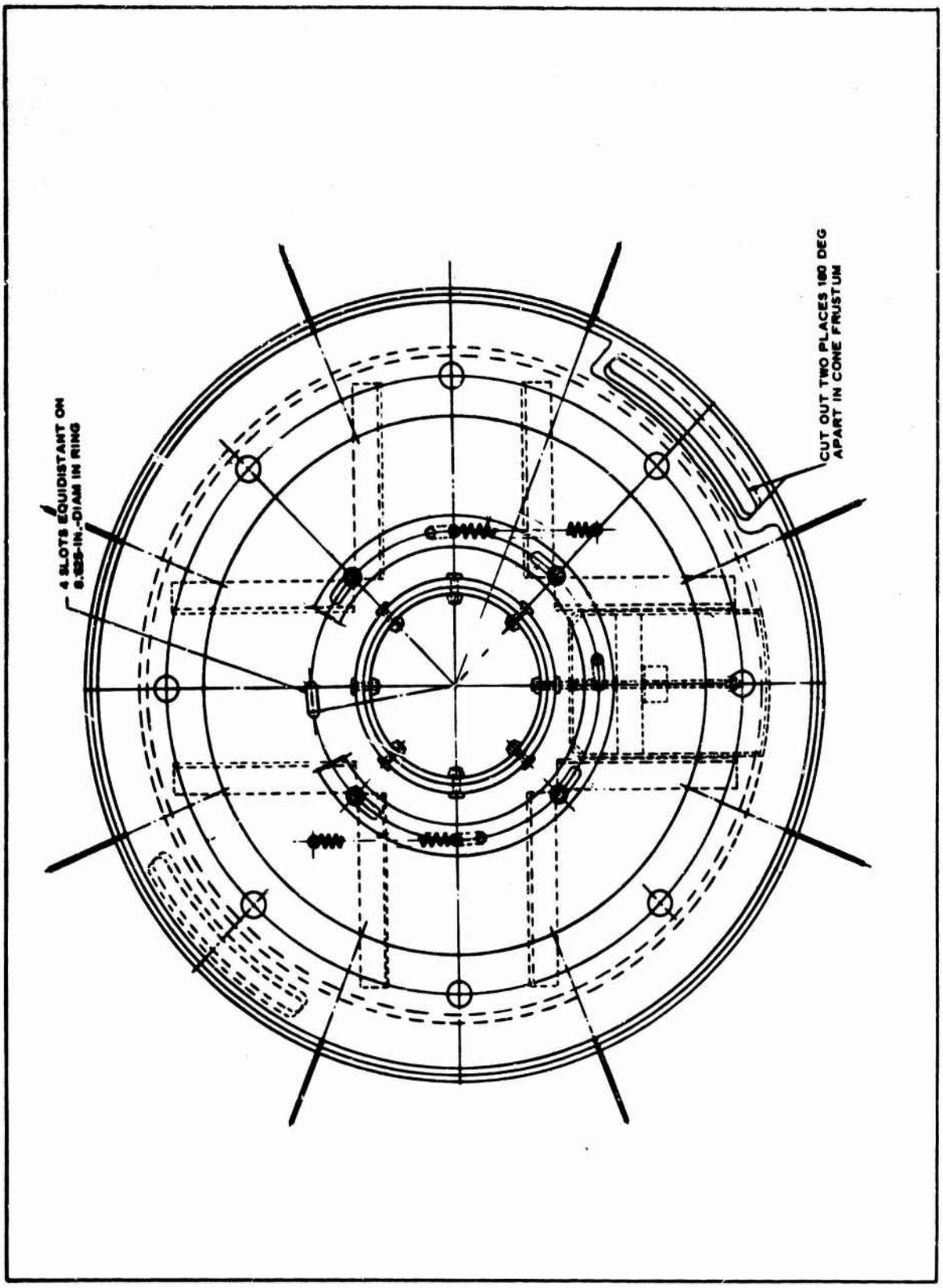

Figure II-2. M-118 Bomb Canister Assembly (View Looking Aft)

(The reverse of this page is blank)

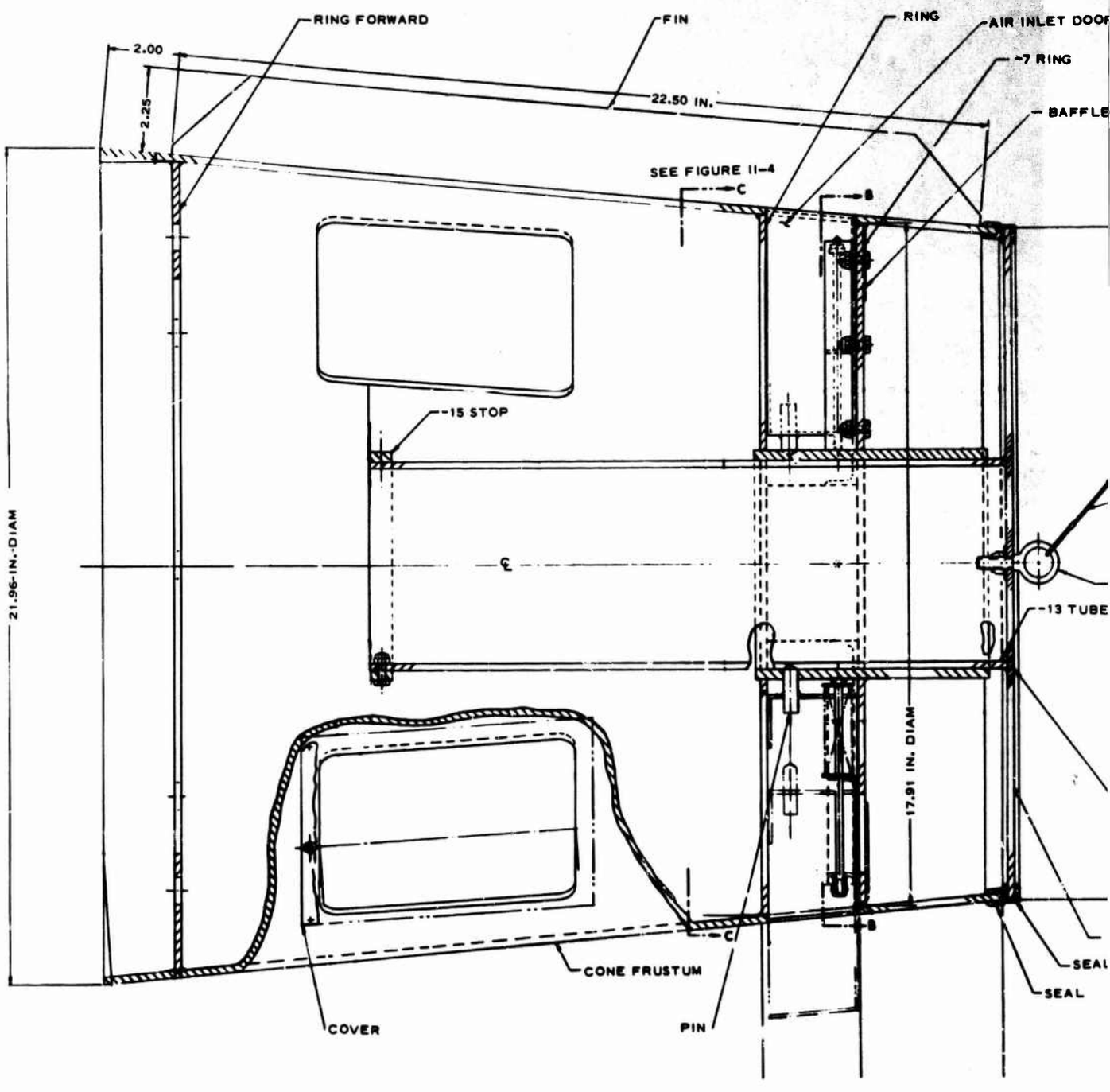
RING FORWARD
FIN
RING
AIR INLET DOOR
2.00
2.25
22.50 IN.
7 RING
BAFFLE
SEE FIGURE 11-4
C
B
15 STOP
21.96-IN.-DIAM
℄
13 TUBE
17.91 IN. DIAM
CONE FRUSTUM
SEAL
SEAL
COVER
PIN

A

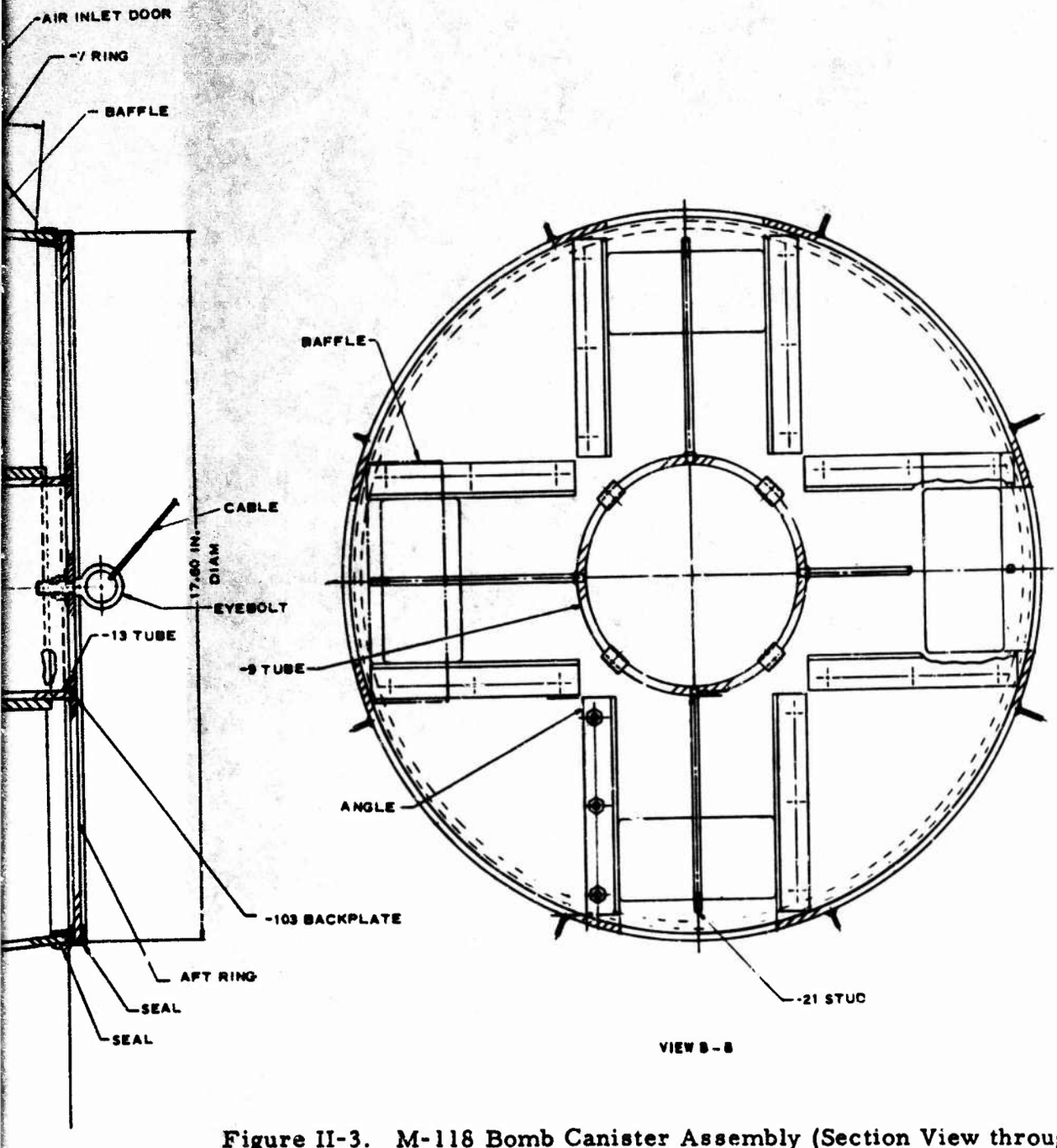

Figure II-3. M-118 Bomb Canister Assembly (Section View through Centerline)

(The reverse of this page is blank)

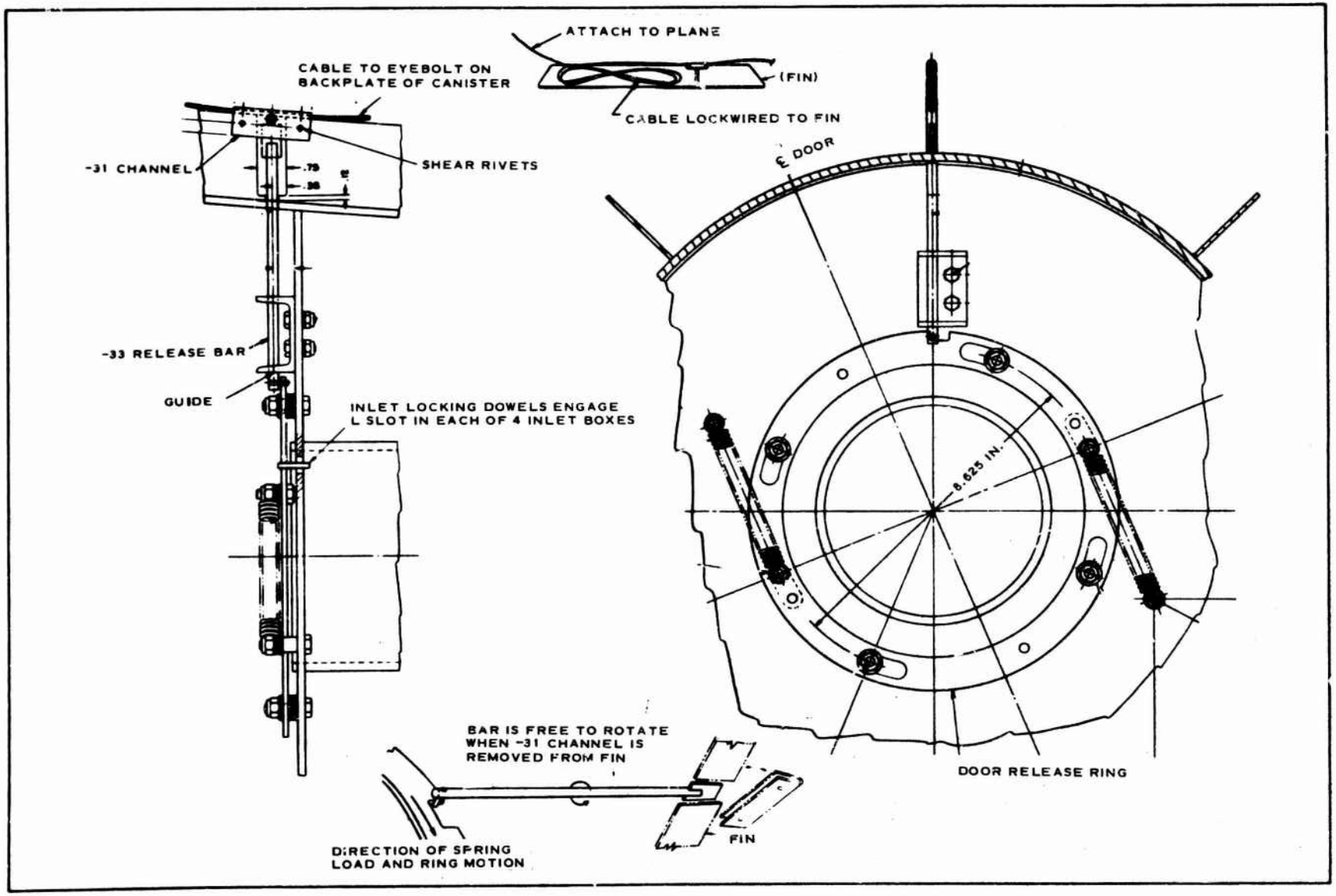

Figure II-4. Release Mechanism

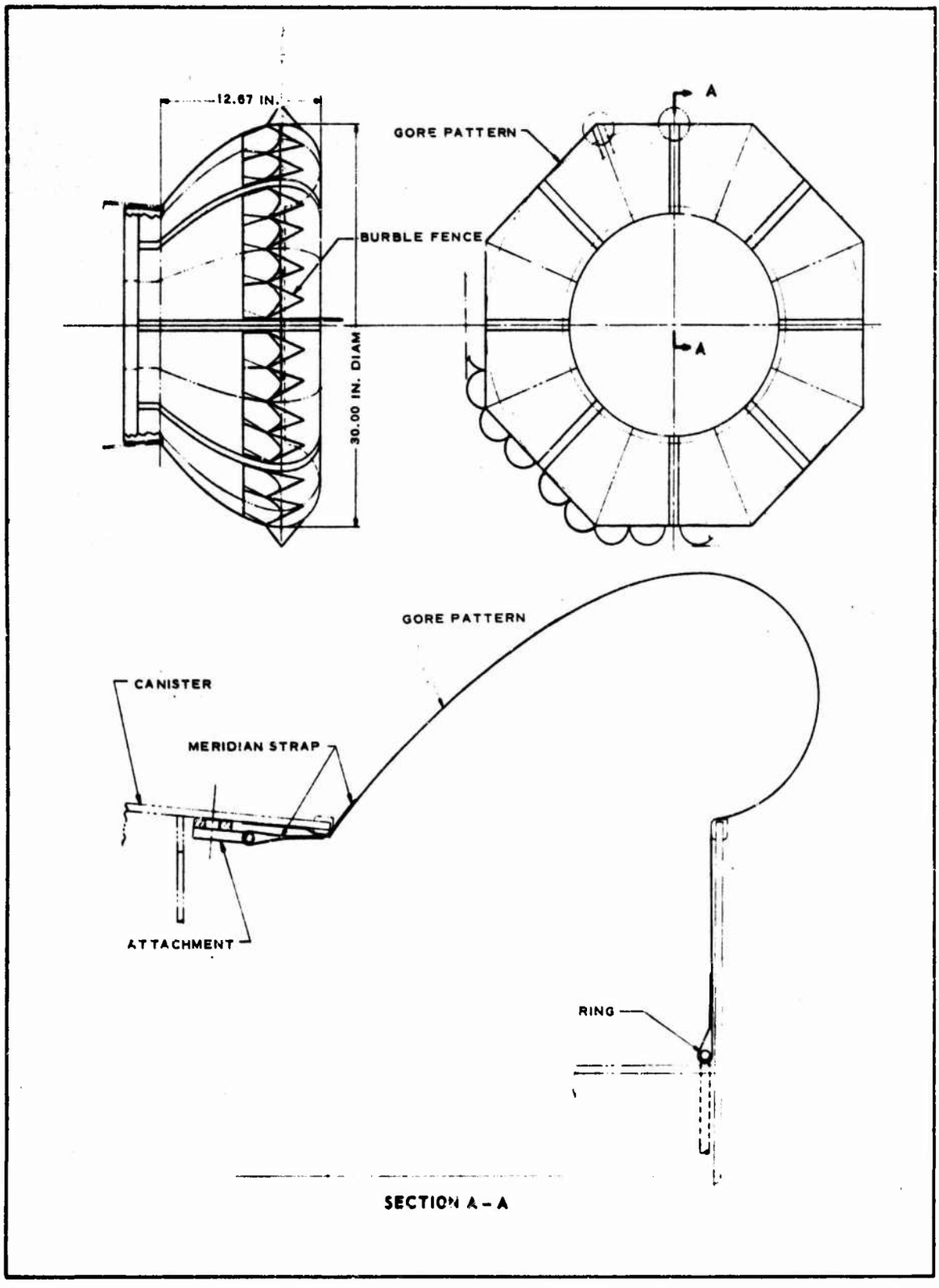

Figure II-5. Assembly of BALLUTE

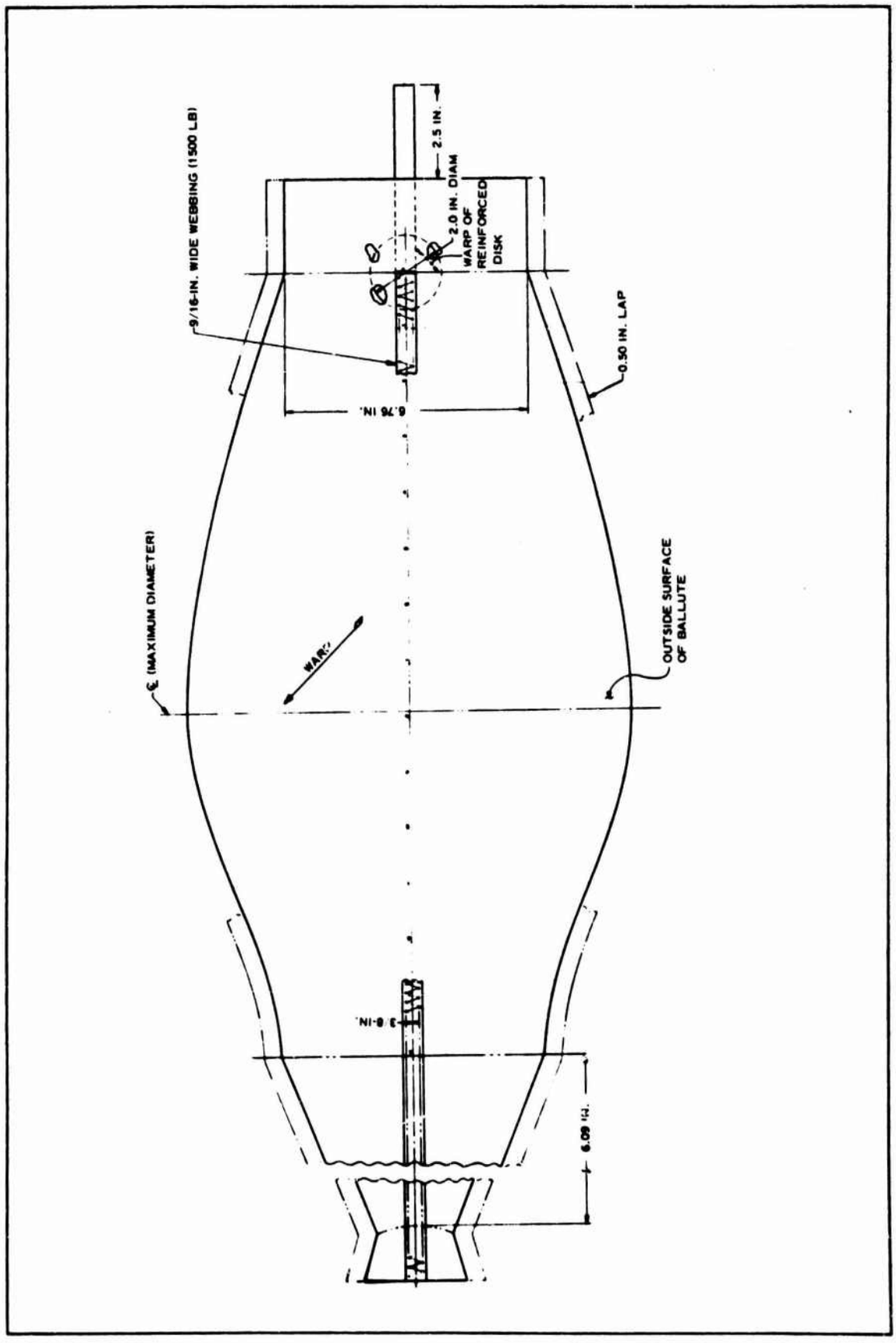

Figure II-6. Gore Pattern

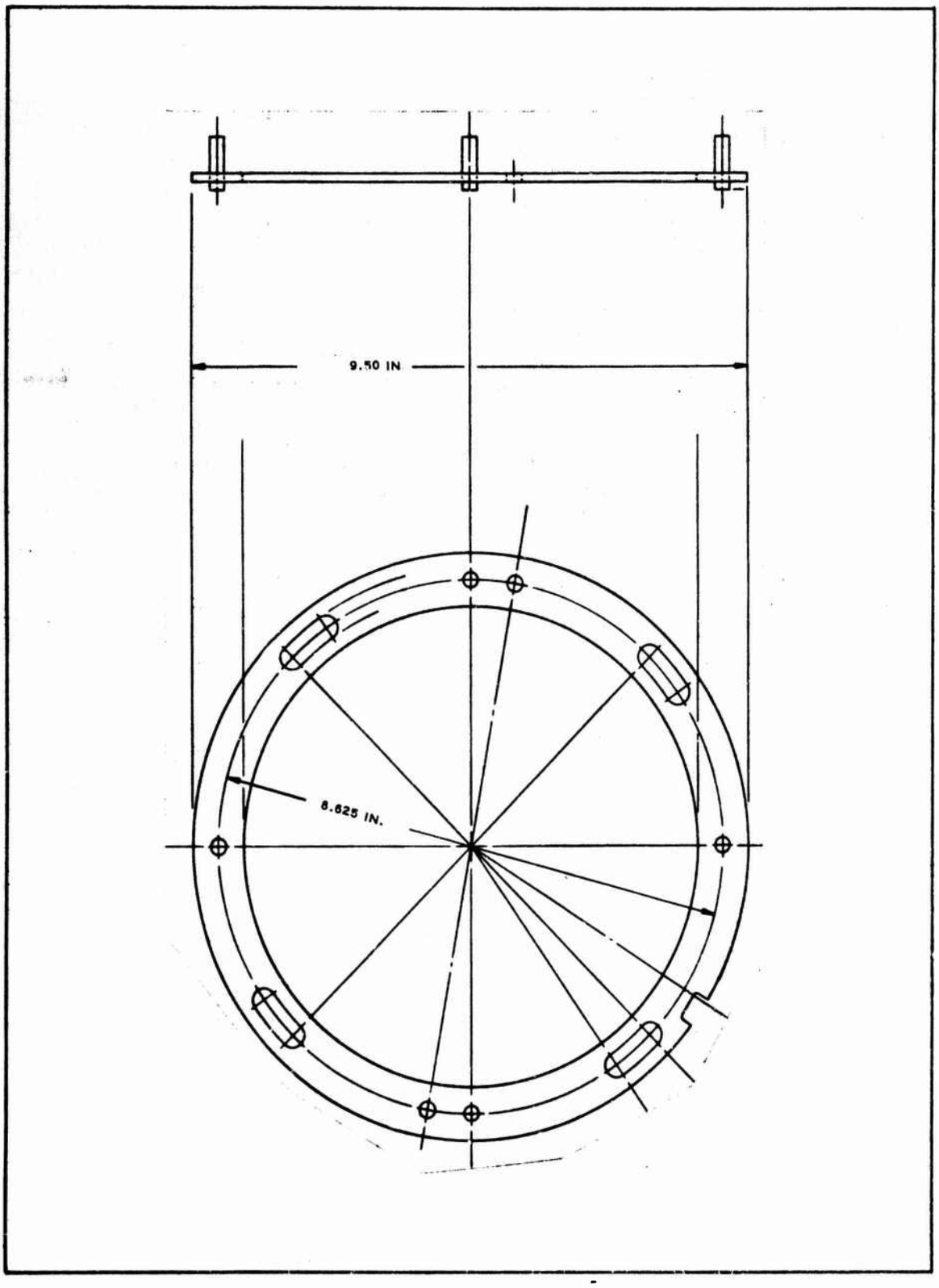

Figure II-7. Release Ring

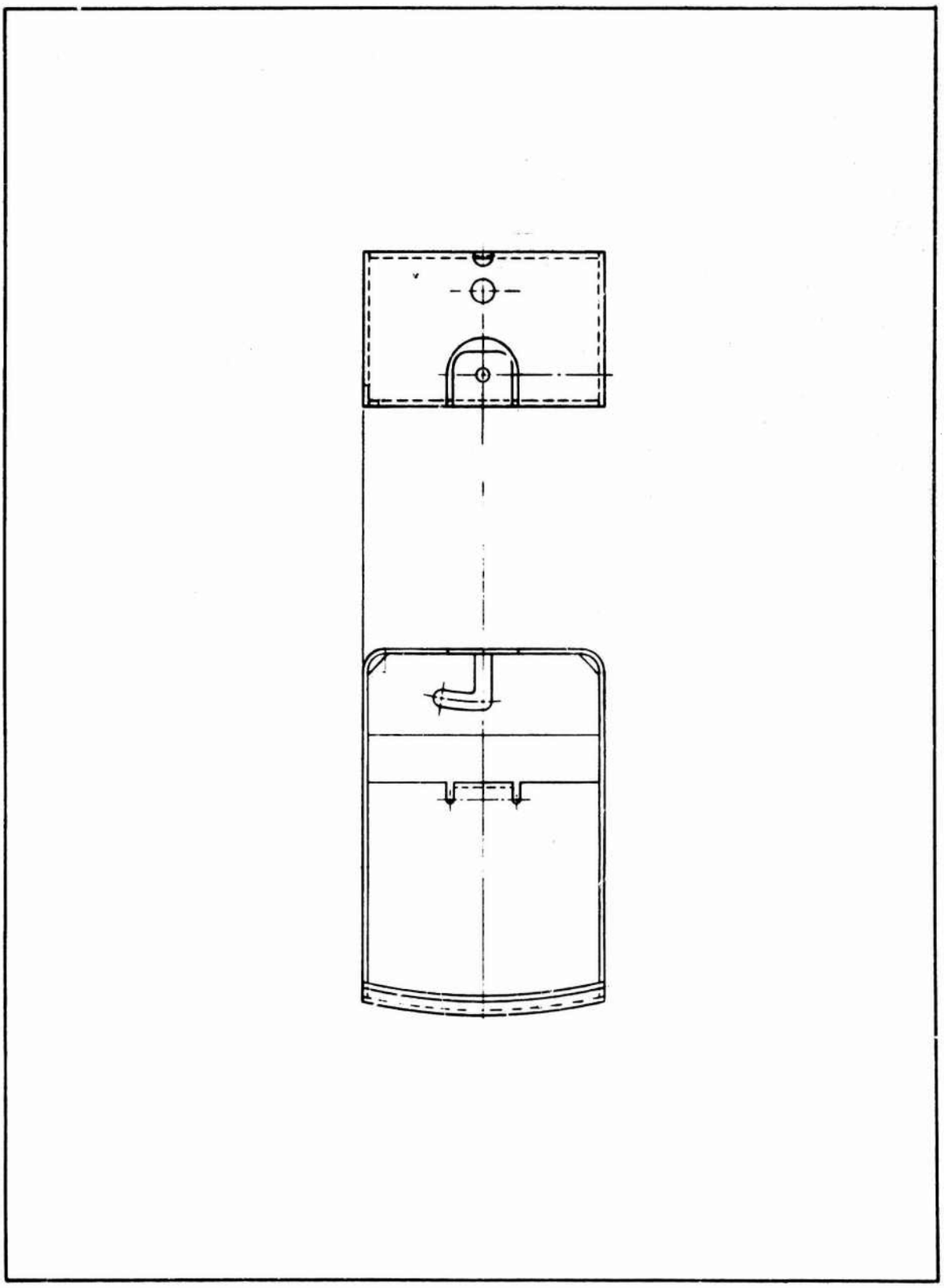

Figure II-8. Air Inlet Door

APPENDIX III

VIBRATION TEST RECORD

The information below is a summary record of the vibration test conducted on the M-118 bomb/BALLUTE container.

1. Start date - July 19, 1968

2. End date - July 22, 1968

3. Weight of test unit - 168 lb

4. Vibration schedule

5 to 14 Hz	0.100 in. double amplitude
14 to 23 Hz	1.0 g
23 to 65 Hz	0.036 in. double amplitude
65 to 2000 Hz	8.0 g

5. Visual inspection - after five minutes of vibration dwell at 8 g's in the 90-deg transverse axis, one air scoop released and opened. No damage or deterioration of the assembled test unit was observed at the conclusion of the test.

6. Resonance frequencies, dwell, and sweep time record - this record is shown below in Table III-I.

TABLE III-I. VIBRATION TEST RECORD

Resonance frequency (Hz)	Dwell (min)	Number of sweeps	Sweep time (min)	Total vibration time (min)	Indicated vibration level		
					Input (g)	Cover (g)	Scoop (g)
Longitudinal axis							
333	30	. . .	. . .	30	8	30	80
1734	30	. . .	. . .	30	8	25	60
Sweep	. . .	6	20	120	8	. . .	. . .
Transverse axis							
66	30	. . .	. . .	30	8	25	40
166	30	. . .	. . .	30	8	8	40
757	30	. . .	. . .	30	8	3	50
1807	30	. . .	. . .	30	8	2	40
Sweep	. . .	3	20	60	8	. . .	. . .

TABLE III-I. VIBRATION TEST RECORD (Continued)

Resonance frequency (Hz)	Dwell (min)	Number of sweeps	Sweep time (min)	Total vibration time (min)	Indicated vibration level		
					Input (g)	Cover (g)	Scoop (g)
90-deg transverse axis							
71	30	. . .	. . .	30	8	30	60
123	30	. . .	. . .	30	8	8	50
912	30	. . .	. . .	30	8	3	60
1666	30	. . .	. . .	30	8	2	50
Sweep	. . .	3	20	60	8	. . .	. . .

(The reverse of this page is blank)

REFERENCES

1. GER-8401: Goodyear Aircraft Wind Tunnel. Akron, Ohio, Goodyear Aerospace Corporation, 22 October 1957.

2. Tobak, M.; Reese, D. E., Jr.; and Beam, B. H.: Experimental Damping in Pitch of 45° Triangular Wings, NACA RM A50J26. Washington, D. C., NASA, 1 December 1960. (Declassified)

3. Schneider, L. J.; and Eirklein, K.: An IBM 360 Program for Predicting the Static Aerodynamic Characteristics of Low-Aspect-Ratio Configurations. GER-13630. Akron, Ohio, Goodyear Aerospace Corporation, December 1967.

4. Doyle, G. R., Jr.: 3 DOF Computer Program For Various Missile Systems. GER-13507. Akron, Ohio, Goodyear Aerospace Corporation, October 1967.

5. Bruhn, E. F.: Analysis and Design of Flight Vehicle Structures. Cincinnati, Ohio, Tri-State Offset Co., 1965.

6. MIL-A-8591D: Airborne Stores and Associated Suspension Equipment, General Design Criteria For. Washington, D. C., Naval Air Systems Command, 2 January 1968.

7. MIL-HDBK-5: Metallic Materials and Elements for Aerospace Vehicle Structures. Washington 25, D. C., Department of Defense, 8 February 1966.

8. Alcoa Structural Handbook. Pittsburgh Pa., Aluminum Company of America, 1965.

9. Lipson, C.; Noll, G. C.; and Clock, L. S.: Stress and Strength of Manufactured Parts. 1st ed. New York, N. Y., McGraw-Hill Book Company, Inc., 1950.

10. Roark, R. J.: Formulas for Stress and Strain. 3rd ed. New York, N. Y., McGraw-Hill Book Company, Inc., 1954.

11. Timoshenko, S.: Strength of Materials, Part II. 3rd ed. Princeton, N. J., D. Van Nostrand Company, Inc., June 1957.

12. U. S. Stoneware Catalog: Tygon Corrosion Resistant Gasketing. Bulletin G-531. Akron, Ohio, U. S. Stoneware, 1961.

13. Handbook of Molded and Extruded Rubber. 2nd ed. Akron, Ohio, The Goodyear Tire & Rubber Company, 1959.

14. Silhan, F. V.; Cubbage, J. M., Jr.: Drag of Conical and Circular-Arc Boatail Afterbodies at Mach Numbers from 0.6 to 1.3. NACA RM L56K22, Washington, D. C., NASA, January 1957.

15. Wallaert, J.J.; and Fisher, J.W.: "Shear Strength of High-Strength Bolts." J. Struct. Div. Am. Soc. Civ. Eng. June 1965; Vol 91, No. ST3, Part 1.

16. Shufelt, R.; and Wright, J.: BALLUTE Pressure Distribution Wind Tunnel Test. Memorandum No. T-6654, Akron, Ohio, Goodyear Aerospace Corporation, 6 June 1966.

17. Timoshenko, S.; and Woinowsky-Krieger, S.: Theory of Plates and Shells. 2nd ed. New York, N.Y., McGraw-Hill Book Company, Inc., 1959.

UNCLASSIFIED

Security Classification

DOCUMENT CONTROL DATA - R & D

(Security classification of title, body of abstract and indexing annotation must be entered when the overall report is classified)

1. ORIGINATING ACTIVITY (Corporate author) Goodyear Aerospace Corporation Akron, Ohio	2a. REPORT SECURITY CLASSIFICATION UNCLASSIFIED 2b. GROUP

3. REPORT TITLE

BALLUTE Stabilization System for M-118 Bomb

4. DESCRIPTIVE NOTES (Type of report and inclusive dates)

Final Report - 1 July 1968 through 31 December 1968

5. AUTHOR(S) (First name, middle initial, last name)

J. J. Graham

6. REPORT DATE	7a. TOTAL NO. OF PAGES	7b. NO. OF REFS
September 1968	86	17

8a. CONTRACT OR GRANT NO. F08635-68-C-0147 b. PROJECT NO. 1263 c. Task 1263-01 d.	9a. ORIGINATOR'S REPORT NUMBER(S) GER-13967 9b. OTHER REPORT NO(S) (Any other numbers that may be assigned this report) AFATL-TR-68-113

10. DISTRIBUTION STATEMENT

This document is subject to special export controls; each transmittal to foreign governments or foreign nationals may be made only with prior approval of the Air Force Armament Laboratory (ATZV), Eglin AFB, Florida 32542

11. SUPPLEMENTARY NOTES	12. SPONSORING MILITARY ACTIVITY
Available in DDC	Air Force Armament Laboratories Air Force Systems Command Eglin Air Force Base, Florida

13. ABSTRACT

A drag-stabilization system utilizing a ram-air inflatable BALLUTE was considered for compatible application to the operational M-118 bomb where use of the conventional M-135 fin assembly is physically prohibitive. Wind-tunnel tests of 1/10-scale models were conducted and the results were analyzed to determine a stable BALLUTE size and configuration. A positive operating mechanism was designed to ensure consistent deployment of ram-air scoops for initiating the BALLUTE inflation. Stress and reliability analyses were performed to support the design effort, and the first prototype was vibration tested to prepare the system hardware for Air Force flight testing. Several fabricated units were recommended for intended bomb drops to enable evaluation of the concept.

DD FORM 1 NOV 68 1473

UNCLASSIFIED

Security Classification

UNCLASSIFIED
Security Classification

14. KEY WORDS	LINK A		LINK B		LINK C	
	ROLE	WT	ROLE	WT	ROLE	WT
BALLUTE Stabilizer M-118 bomb Munitions stabilization system Attached inflatable BALLUTE						

UNCLASSIFIED
Security Classification